EVAN BENTLEY PERRY
Dissolved Krypton and Sulfur Hexafluoride Gases as Gas-Liquid Partitioning Tracers in Porous Media
(Under the direction of CHRISTOPHER SCOTT ROMANEK)

In this study the gas-liquid partitioning behaviors of the dissolved gas tracers, krypton and sulfur hexafluoride were examined. Although these dissolved gas groundwater tracers offer advantages over conventional tracers such as dissolved salts and dyes due to their innocuous nature, their utilization has been limited largely due to concerns about partitioning to trapped gas phases during transport.

Dissolved gases did not behave conservatively in column or field deployments in less than saturated conditions. However, the manner in which transport was retarded was predictable and occurred primarily as a function of the Henry's Law constant of the dissolved gas tracer. When used in conjunction with a conservative tracer such as tritium (^3H) the deviation from conservative behavior was used to predict the volume of unsaturated space in partially saturated porous media.

INDEX WORDS: Dissolved gases, Krypton, Sulfur hexafluoride, Groundwater, Gas-liquid partitioning, Henry's Law, Tritium

DISSOLVED KRYPTON AND SULFUR HEXAFLUORIDE GASES AS GAS-LIQUID PARTITIONING TRACERS IN POROUS MEDIA

by

EVAN BENTLEY PERRY

B.S. Furman University, 1997

A Thesis Submitted to the Graduate Faculty

of The University of Georgia in Partial Fulfillment

of the Requirements for the Degree

MASTER OF SCIENCE

ATHENS, GEORGIA

2001

DISSOLVED KRYPTON AND SULFUR HEXAFLUORIDE GASES AS GAS-LIQUID PARTITIONING TRACERS IN POROUS MEDIA

by

EVAN BENTLEY PERRY

Approved:

Major Professor: Christopher Romanek

Committee: John Dowd
David Wenner

Electronic Version Approved:

Gordhan L. Patel
Dean of the Graduate School
The University of Georgia
May 2001

ACKNOWLEDGMENTS

This research was funded by the education program of the Savannah River Ecology Laboratory. I would like to thank Christopher Romanek for his time and good advice and for providing me with the necessary resources to conduct this research. I am grateful to Vijay Vulava for introducing me to the world of laboratory column studies and providing me with a plethora of good information. Dave Dunn and Raymond Roseberry of the Savannah River Technology Center provided access to and thorough explanation of the Fourmile Creek groundwater-surface water site. I would also like to thank my committee members John Dowd and David Wenner for their input and advice. Randy Culp of the University of Georgia's Center for Applied Isotope Studies gave generous advice on the isolation and measurement of noble gases in water samples. There are too many people who helped me at the lab to name, but I feel especially indebted to Momin Uddin and B.T. Thomas for their suggestions and camaraderie and to Conchi and Alejandro, who through their tragedy reminded me what is important.

I am most grateful to Bethany for her love, patience, and support and to Haley for being a wild dog.

TABLE OF CONTENTS

Page

LIST OF TABLES

Page

LIST OF FIGURES

Page

CHAPTER 1
INTRODUCTION AND PREVIOUS WORK

1.1. *TRACER BACKGROUND*

A hydrogeologic tracer is form of matter or energy carried by groundwater that yields information about the direction of movement and/or velocity of water (Davis 1985). Tracer labeled water occupies a portion of a flow domain and is identifiable by various physicochemical characteristics such as color, density, and electrical conductivity, among other attributes. (Bear 1972). A hydrogeologic tracer may be classified based on its origin as: 1. naturally occurring, 2. deliberately introduced, or 3. unintentionally introduced into an aqueous system. Naturally occurring (ambient) tracers can include water (stable isotopes of hydrogen and oxygen) and its dissolved constituents (e.g. bromide [Br^-], chloride [Cl^-], dissolved gases), while introduced tracers include anions (particularly Br^- and Cl^-), weak acids, dyes, and biological materials. Unintentional tracers may include ^3H and ^{14}C from bomb tests, metals, chlorofluorocarbons, light non-aqueous phase liquids (LNAPLs), and dense non-aqueous phase liquids (DNAPLS).

All three classes of tracers have been used successfully for a variety of purposes. However, this study will primarily focus on tracers that are deliberately introduced. To obtain useful data from an introduced tracer, labeled water should not react with or adsorb to aquifer material. Such a tracer is said to be conservative and its transport will be governed by the unmodified one-dimensional convection-dispersion equation (CDE) (Jury et al.1991):

$$\frac{\partial C_l}{\partial t} = D\frac{\partial^2 C_l}{\partial z^2} - V\frac{\partial C_l}{\partial z} \qquad [1]$$

Table 1. Commonly used groundwater tracers. Compiled from Holbeck-Pelham et al. 2000.

Suspended Solids
- -Biological (bacteria, yeasts, spores, viruses)
- -Synthetic microspheres (silica colloids, polystyrene spheres, clay materials)

Dissolved Solids
- -Nonionic (sugars)
- -Weak acids (benzoic acids, toluic acids, salicylic acids, inorganic acids)
- -Cations (sodium, nickel, magnesium)
- -Anions (chloride, bromide, nitrate)
- -Rare Earth elements (europium)
- -Fluorescent dyes (uranine, rhodamines)

Organic Liquids
- -Low solubility solvents (LNAPLs, DNAPLs)
- -High solubility solvents (alcohols, methyl tertiary butyl ether)

Dissolved Gases
- -Noble gases (helium, neon, argon, krypton, xenon, radon)
- -Chlorofluorocarbons (freon-11, freon-12, freon-113)
- -Other gases (sulfur hexafluoride, oxygen, hydrogen)

Isotopes
- -Stable isotopes ($^{2}H/^{1}H$, $^{15}N/^{14}N$, $^{18}O/^{16}O$, $^{13}C/^{12}C$)
- -Radioactive isotopes (^{3}H, ^{14}C, ^{85}Kr)

where t = time, D = dispersion coefficient (length^2/time), C_l = longitudinal tracer concentration, V = the average pore water velocity (length/time), and z = the length of transport. With the exception of D and C_l, these parameters are physical properties of porous media and are independent of the solute. The dispersion coefficient is primarily a physical property of the media, but it also accounts for the effect of molecular diffusion, which varies among different solutes (Fetter 1993). When the movement of a solute is slower than that predicted by the CDE for a given a set of parameters, it is said to be retarded. An adjustment in the CDE must be made by adding a dimensionless retardation factor, R (Jury et al. 1991) to eq. 1:

$$R\frac{\partial C_l}{\partial t} = D\ \frac{\partial^2 C_l}{\partial z^2} - V\frac{\partial C_l}{\partial z} \qquad [2]$$

Although the adjustment to the CDE is simple mathematically, retardation greatly complicates tracer experiments because retardation may vary substantially as a function of the tracer and the medium through which it flows. It is generally thought that most porous media have a slight negative charge, so most positively charged tracers will be retarded (Jury et al. 1991). However, Seaman (1998) found that anions such as chloride and bromide do not behave conservatively in variably charged soils such as those found on the southeastern Coastal Plain of the United States. Additionally, it is known that dyes such as rhodamine-WT (RWT) have a slight charge so they too will be retarded in some porous media (Pang and Close 1999). Water enriched in the radioactive isotope of hydrogen, (^{3}H or tritium, substituting for a stable isotope of hydrogen, ^{1}H or ^{2}H, in the water molecule) is perhaps the best tracer for estimating groundwater flow parameters (Gaspar and Onescu 1972). However, due to health concerns, tritium is unlikely to be approved by licensing authorities for use as an introduced tracer in most applications. In laboratory column experiments, waters that contain a slight enrichment of tritium are useful as a benchmark to determine if other solutes are behaving conservatively. Tritium

has a half-life of ~ 12.46 years and is therefore not a conservative tracer, however a simple adjustment can be made to the CDE to account for this loss:

$$kC_l \frac{\partial C_l}{\partial t} = D\frac{\partial^2 C_l}{\partial z^2} - V\frac{\partial C_l}{\partial z} \quad [3]$$

where k = rate coefficient (time^{-1}) (Fetter 1993). For the purposes of this study, the time scale of experiments was less than 1 day, therefore the effects of radioactive decay on tritium concentrations were negligible and this adjustment to the CDE was not made.

Laboratory Studies

A laboratory column is a piece of tubing packed with a medium, typically aquifer materials such as quartz sand or soil, that is used to model the interaction of a solute with the solid in a tightly controlled setting. Tracer labeled water is passed through the column at a given rate for some time and the concentration of the tracer in the effluent is compared to the source concentration. A conservative tracer, such as water enriched in ^{3}H (called here tritiated water; note that ^{3}H is nonconservative in the strictest sense as defined above) or Br^-, is commonly used as a control for comparison to other tracers for which solid-solute interactions are strong, unknown or poorly constrained. The degree to which tracers deviate from a control is a measure of interactions with the aquifer material.

In addition to chemical interactions, column studies are conducted to determine physical properties of an aquifer material. The dispersion coefficient *(D)* is a parameter that describes the degree to which a tracer is redistributed during transport. Dispersion coefficient is primarily a mechanical property under conditions of significant advective flow. Under nearly stagnant conditions, molecular diffusion contributes significantly to *D* (Bear 1972). The value for *D* must be determined based on the transport of a conservative tracer because chemical interactions will mask physical effects on solute transport. Van

Genuchten (1981) used both conservative and reactive tracers simultaneously to discriminate physical and chemical effects in column experiments.

Field Studies

Tracer experiments are only practical for fairly small-scale field studies. With the exception of high velocity Karst systems, groundwater flow is too slow for a tracer to travel a significant distance over the life of many studies (Domenico and Schwartz 1990). In addition, over very large areas an introduced tracer may become too dilute for measurement. Domenico and Schwartz (1990) defined several useful ways of conducting field studies with tracers. The first is the natural gradient test. This simply involves introducing a tracer in a well and monitoring its movement down gradient. A major limitation of this test is the need for many wells down-gradient if more information than simple hydrologic connection is needed. Time may be an issue for slowly moving groundwater too. The second method is a single-well test, which is accomplished by injecting a slug of tracer labeled water into an aquifer delivered at a constant rate over some fixed interval of time. To further penetrate the formation the slug of tracer may be followed by tracer-free water delivered at the same, however this will cause a double diffusion front (dispersion occurs in two directions) and will complicate analysis. The well is then pumped in a similar fashion and the effluent is measured for tracer concentration. Longitudinal dispersion (D_L) and the sorption coefficient (K_d) can be estimated from these tests (Pickens et al. 1981). However, caution must be exercised when applying values to the entire aquifer due to scaling problems with dispersion and media heterogeneities over large areas. A third method is the two-well tracer test which is performed by injecting a tracer at a known rate into one well and simultaneously pumping a nearby well at the same rate. The effluent at the pumping well is then monitored for tracer breakthrough.

1.2. *DISSOLVED GAS TRACERS*

When choosing a groundwater tracer, conservative behavior is usually not the only criterion that must be met. The tracer should be present in a concentration well above ambient (preferably several orders of magnitude) and it should not modify the natural hydrologic properties of an aquifer system such as hydraulic conductivity and water density. Other considerations include toxicity, ease of detection, cost, and availability (Davis et al. 1985). In this study, the use of dissolved gases as an alternative to some of the more commonly used tracers, such as dyes and anions, will be examined. Previous studies have determined that under the appropriate conditions, dissolved gases meet all of these criteria.

Gas solubility is defined in terms of the mass of gas that can be dissolved in water for a particular overlying gas composition (Solomon et al. 1999). Solubility varies from very slight (hydrophobic gases) to very high (hydrophilic gases). Dissolved gas tracers such as CFCs, SF_6 and the noble gases are generally nonpolar and therefore hydrophobic. However, they are all slightly soluble to some degree and have the potential to be detectable in water. Equilibrium between the gaseous and aqueous phase is characterized by Henry's Law (K_H):

$$K_H = \frac{P_i}{C_w} \qquad [4]$$

where P_i = partial pressure of gas (atm) and C_w = concentration of the gas in water (moles L^{-1}). Often, it is more convenient to display Henry's Law as a dimensionless coefficient (ratio of air to aqueous concentration):

$$K'_H = \frac{C_a}{C_w} \qquad [5]$$

or

$$K'_H = \frac{K_H}{RT} \qquad [6]$$

where C_a = concentration of the gas in air, R = gas constant and T = temperature (in Kelvins; Schwartzenbach et al. 1993).

The rate at which equilibrium is reached is dependent on a variety of factors that are both independent (turbulence, diffusive layer thickness, etc.) and dependent (aqueous diffusion coefficient) on the tracer being considered. The aqueous diffusion coefficient is expressed in the units (length^2 time^{-1}) and is strongly a function of the molecular weight of the gas. Based on these properties, it is possible to have a highly insoluble gas such as SF_6 exsolve more slowly from water than a more soluble species such as Kr (Schwartzenbach et al. 1993). This flexibility allows dissolved gas tracers to meet the wide array of needs for a variety of laboratory and field applications.

There are three primary controls on the solubility of nonreactive gases in water: 1. temperature, 2. pressure, and 3. salinity (Colt 1984). Gas solubility is inversely proportional to temperature and salinity and proportional to pressure. For the purposes of groundwater tracing, water temperature is generally lower and hydrostatic pressure is higher in the aquifer than it is on Earth's surface so the conditions that injected dissolved gas tracers experience should not act to alter fluid composition once it enters the subsurface. Salinity effect is generally assumed negligible for most aquifers, however it may be important in studies of saltwater encroachment or where ionic salt tracers are used concurrently with dissolved gas tracers (Mazor 1991).

Selection of Dissolved Gas Tracers

The selection of a particular dissolved gas tracer for field or laboratory use is dependent on a variety of physical properties (see Table 2). Of particular interest is the difference between the natural background concentration of the aqueous species and maximum solubility. Gases with low background concentrations are attractive tracers because there can be six or more orders of magnitude difference between background concentration and maximum solubility (Wilson and Mackay 1993). Multiple dissolved

Table 2. Properties of various dissolved gas tracers.

Gas	Molecular Formula	Mol. Wt.	Dimensionless Henry's Law Constant at 25°C[a]	Liquid Density at 25°C (g/cm^3)[b]	Molar Volume (cm^3/mol) at 25°C (M.W./ρ)	Aqueous Diffusion Coefficient (cm^2/sec)[c]	Maximum* Solubility at 1 atm. and 25°C (mg/L)[e]	log K_{ow}[f]	Fractional volume in air (F_a) (dimensionless)[g]	Aqueous background concentration at 25°C* (mg/l)[e]
Water	H_2O	18.04	-	0.998 [w]	18.076	2.95E-05	-	-	-	-
Hydrogen	H_2	2.02	52.44	0.077 [x]	26.234	2.26E-05	1.57	0.45	5.00E-07	7.87E-07
Helium	He	4.00	107.63			7.22E-05[d]	1.52	0.28	5.24E-06	7.96E-06
Neon	Ne	20.17	90.89	1.251 [x]	16.123	3.19E-05	9.07	0.28	1.82E-05	1.65E-04
Nitrogen	N_2	28.02	62.92	0.87 [x]	32.207	1.95E-05	18.20	0.67	7.81E-01	14.21
Oxygen	O_2	32.00	31.46	1.306 [x]	24.502	2.37E-05	41.57	0.65	2.07E-01	8.60
Argon	Ar	39.95	29.21	1.417 [x]	28.193	2.15E-05	55.90	0.74	9.34E-03	0.52
Carbon Dioxide	CO_2	44.01	1.20	0.800 [y]	55.030	1.34E-05	1499.01	0.83	3.14E-04	0.47
Krypton	Kr	83.80	16.36	2.449 [x]	34.218	1.87E-05	209.36	0.89	1.14E-06	2.39E-04
Dichlorodifluoro-methane (CFC-12)	CCl_2F_2	120.90	17.67	1.486 [z]	81.359	1.01E-05	279.73	2.16	5.30E-10	1.48E-07
Xenon	Xe	131.30	9.51	2.978 [x]	44.090	1.56E-05	564.31	1.28	8.70E-08	4.91E-05
Trichlorofluoro-methane (CFC-11)	CCl_3F	137.35	4.39	1.494 [z]	91.934	9.28E-06	1279.76	2.51	*2.80E-10*	3.58E-07
Sulfur Hexafluoride	SF_6	146.06	170.42	1.445 [y]	101.085	8.68E-06	35.03	1.68	*3.00E-12*	1.05E-10
1,1,2-trichlorotri-fluoroethane (CFC-113)	CCl_3F_3	175.35	20.45	1.5635 [z]	112.152	8.06E-06	350.47	3.16	*8.00E-11*	2.80E-08

[a] Data taken from Sander (1996).

[b] Data taken from [w]Fetter (1994), [x]CRC Handbook of Chemistry and Physics (1994/1995), [y]Air products catalog (1999), [z]Spectrum Laboratoiries Inc. website (www.speclab.com).

[c] Based on correlation $D_w = 2.7*10^{-4}/(V)^{0.71}$, where D_w is the Aq. Molecular diffusion coefficient and V is the liquid molar volume, from Schwarzenbach et al. (1993).

[d] From Jardine et al. (1999).

[e] Calculated from $K_H = C_{air}/C_{water}$, where K_H is the dimensionless Henry's Law constant.

[f] Octanol-water partition coefficient estimated with SRC's WsKow computer program (chemical property estimation software).

[g] Data taken from CRC Handbook of Chemistry and Physics, Upstill-Goodard and Wilkins (1995), Szabo, et al. (1996). Italics indicate approximate value.

*Assumes negligible salinity and water that is in equilibrium with 1atm of ambient air.

gas tracers with different aqueous diffusion coefficients are useful when information about the influence of diffusive processes on solute transport is desired. Jardine et al. (1999) found that helium moved into dead pore space faster than neon due to a higher molecular diffusion coefficient. Fry et al. (1995) found that gases with relatively high Henry's Law coefficients partitioned into trapped gas pockets more effectively than gases with lower coefficients. Wilson and Mackay (1996) hypothesized that the octanol-water partitioning coefficient (K_{ow}) may serve as an approximation for the partitioning behavior of dissolved gases with organic matter, because of a positive correlation between K_{ow} and organic matter partitioning coefficient (K_{om}) for most aquifer materials.

Noble Gases

The stable noble gases (He, Ne, Ar, Kr, and Xe) are particularly attractive dissolved gas tracers. The nonreactive nature of noble gases is due to the fact that their outer shell electrons are complete (see Table 3). Solubility is an important consideration when choosing a noble gas tracer for a study. The polarizability and hence solubility of noble gases increase as a function of molecular weight. The noble gases of greater mass with large outer shells of electrons are more easily polarized and dissolved in water (Miller 1987). Although helium has a low solubility, its low cost and high molecular diffusion coefficient make it a viable option for some studies. Neon, while more expensive than helium, has a higher solubility and lower aqueous diffusion coefficient. Argon is an inexpensive and more soluble alternative to helium and neon, but the relatively high ambient concentration (~1% in air) limits its potential as a dissolved gas. Unfortunately, krypton and xenon are relatively expensive gases. However, if used in sufficiently small quantities, these gases may be viable tracer options for a number of reasons including:

1. low background concentration.
2. high solubility.

3. aqueous diffusion coefficients which are similar to most solutes.
   existence of many stable isotopes (six for Kr and nine for Xe) allows
4. for highly accurate identification with mass selective detection methods.
5. can be cryogenically separated from other gases.

Table 3. Electron shell configuration of the stable noble gases (Petrucci 1990).

Configuration	Number of shells
He $1s^2$	1
Ne [He] $2s^2$ $2p^6$	2
Ar [Ne] $3s^2$ $3p^6$	3
Kr [Ar] $3d^{10}$ $4s^2$ $4p^6$	4
Xe [Kr] $4d^{10}$ $5s^2$ $5p^6$	5

Other Types of Dissolved Gas Tracers

Like the noble gases, chlorofluorocarbons (CFCs) potentially work well as groundwater tracers, however they have been attributed to ozone depletion and their use is presently discouraged. Because CFCs are entirely synthetic and did not exist until the 20^{th} century, they are useful in determining if groundwater has been in contact with the atmosphere in the recent past (Cook et al. 1995). Fry et al. (1995) and Donaldson et al. (1996) used H_2 and O_2 as dissolved gas tracers. The problem with these gases is that they do not behave conservatively in a field setting because of abiotic and biologic interactions with aquifer materials. However, in sterile, fully saturated laboratory columns these gases were found to behave conservatively. Another gas that has been used in both atmospheric (Bench et al. 1978) and aqueous tracer applications (Wannikhof et al. 1985) is the synthetic gas SF_6, which was widely used until recently as an insulator for

electrical switches. Advantages of using SF_6 are similar to the noble gases, but unlike the noble gases, SF_6 has virtually no background concentration (~3 pptv; Butler et al. 1999). And unlike chlorofluorocarbons, SF_6 is widely available from gas distributors. Another non-CFC gas with potential use as a tracer is tetrafluoroethane (Holbeck-Pelham et al. 2000). This gas is also widely available and is commonly used as a lint and dust remover.

1.3. *PREVIOUS WORK*

Dissolved gases have been utilized as tracers in aqueous systems for at least six different purposes: 1. for mineral exploration (Dyck and Da Silva 1981), 2. to measure gas exchange in streams (Hibbs et al. 1998) and ocean ventilation (Wanninkhof et al. 1985), 3. to determine groundwater recharge temperature (Mazor 1991), 4. to age date groundwater (Dunkle et al. 1993), 5. as a seismic activity indicator (Sugisaki et al 1982), and 6. as a conventional groundwater tracer (Carter et al. 1959). Dyck and Da Silva (1981) placed ping-pong balls in lake sediments, allowed them to equilibrate and then analyzed them for helium content. Because helium occurs as a daughter product in the decay of uranium, high helium concentrations were interpreted as potential locations for uranium deposits. Hibbs et al. (1998) used SF_6 to determine transport parameters such as the gas-liquid mass transfer coefficient, dispersion coefficient, and mean residence times for stream water. Other gases used in stream tracer studies include propane, ethylene, and dichlorodifluoromethane (Freon-12). Wanninkhof et al. (1985) used SF_6 to determine gas exchange rates in an ocean-atmosphere gas exchange study. The authors cited the low background, low detection limit, and inert nature as the principle advantages for using SF_6 as a tracer. Mazor (1991) described a methodology to deduce groundwater recharge temperatures from noble gas concentrations assuming the salinity and elevation of recharge waters was known. Complications, such as the accumulation of argon from radioactive decay, can be eliminated with some knowledge of the isotopic composition of the argon source(s) that contributed to a groundwater signature. Dunkle et al. (1993) used

chlorofluorocarbons (CFCs) to date groundwater. Because CFCs are entirely anthropogenic, their presence in groundwater suggested contact with the atmosphere later than the 1930's or 1940's. Sugisaki et al. (1982) suggested that helium could be used as an indicator of active faulting. They hypothesized that faulting provided a conduit for the release of radiogenic helium to overlying waters.

Of most interest to this study is the use of dissolved gas tracers to better understand groundwater flow. Through the work of Carter et al. (1959), Sanford and Solomon (1998), Wilson and MacKay (1996), and Fry et al. (1995), it has been demonstrated that any nonreactive gas will behave as a conservative tracer under fully saturated conditions. The first application of dissolved gases as a potential groundwater tracer was conducted with helium. In both laboratory column work and in field studies, Carter et al. (1959) found that dissolved helium traveled at a slightly lower velocity than dissolved chloride anions. Unfortunately, it was many years before any follow-up work was conducted. Interest was renewed in the mid 1990's, when Wilson and Mackay (1993) demonstrated that with proper care, SF_6 behaved as a conservative tracer in fully saturated sandy media. Their work contradicted the work of Carter et al. (1959) in that they found that the dissolved gas tracer behaved identically to the conservative tracer Br^-. Wilson and Mackay (1993) were the first to show that under completely saturated conditions the transport of a dissolved gas is essentially no different than any other non-reactive solute. Gupta et al. (1994) continued the work of Carter on helium as a groundwater tracer in field and column work. Their results supported the findings of Wilson and Mackay (1993) in that under fully saturated conditions helium behaved similarly to the conservative tracer, Cl^-. They also presented data that demonstrated the retardation of helium in partially saturated media.

Fry et al. (1995) were the first to thoroughly examine the gas-liquid partitioning behavior of gas tracers. They suggested that retardation of gas tracers was caused by partitioning of gas into trapped air pockets and proposed the following relationship:

$$R = 1 + H'\left(\frac{\theta_g}{\theta_w}\right) \quad [7]$$

where R = retardation factor, H' = dimensionless Henry's Law coefficient, θ_g = volume of trapped gas present in column and θ_w = volumetric water content. Given that different gases have a wide range of Henry's Law coefficients, it was shown that tracers partitioned to different extents when used contemporaneously in partially saturated media. Fry et al. (1995) also demonstrated a strong positive relationship between the volume of trapped gas in a medium and retardation of the dissolved gas tracer. They concluded that eq. 7 was generally valid for calculating retardation at ≥ 95% saturation, but below this value calculated values of R underestimated the timing of the observed breakthrough of the tracer. In a follow-up paper, Fry et al. (1996) conducted laboratory studies using a two dimensional model to examine oxygen transport in a setting that was more similar to field conditions. They showed that dissolved oxygen available for *in situ* bioremediation can be reduced greatly by a small percentage (< 2%) of unsaturated pore space.

Wilson and Mackay (1996) investigated the potential use of SF_6 as a groundwater tracer further by examining diffusivity in media under fully saturated conditions and liquid-solid partitioning in the presence of organic carbon. They found that SF_6 eluted prior to Br^- in media devoid of organics and attributed this to Br^- having a smaller hydrated radius than SF_6. The smaller size of Br^- permitted it to move into minute, intragranular crevices that were unavailable to SF_6. They also hypothesized that because SF_6 has a significant octanol-water partition coefficient ($K_{ow}^{\circ} \approx 13.8$), it should obey the following relationship:

$$R = 1 + \frac{\rho_b}{\theta} K_d \quad [8]$$

where R = retardation coefficient, ρ_b = soil bulk density, θ = porosity and K_d = distribution coefficient. Further,

$$K_d = f_{oc} \bullet K_{oc} \quad [9]$$

where f_{oc} = fraction of organic carbon and K_{oc} = organic carbon partition coefficient

Finally,

$$\log K_{oc} = a(\log K_{ow}) + b \qquad [10]$$

where a and b are empirically-derived fitting parameters. Assuming a value of $f_{oc} \approx 0.025$ for an experimental porous media, Wilson and Mackay suggested SF_6 should be retarded by a factor of ~1.1. However, the experimental breakthrough curves for SF_6 showed no retardation relative to Br^-. They concluded that K_{ow} alone was insufficient to predict sorption of SF_6 onto geologic media.

Sanford et al. (1996) presented laboratory and field data from tracer tests using the noble gases helium and neon. In laboratory columns conducted with fractured shale saprolite as the porous media, helium was retarded relative to bromide under fully saturated conditions. They hypothesized that the difference in breakthrough was attributed to He preferentially diffusing into matrix components unavailable to Br^- based on the relative aqueous diffusion coefficients ($7.22 \times 10^{-5} cm^2/sec$ and 2.01×10^{-5} cm^2/sec at 25°C, respectively). Sanford et al. (1996) also performed a natural gradient field tracer test with He, Ne and Br^-. Just as in the laboratory column experiments, a slight retardation of He (and Ne) was noted and attributed to matrix diffusion.

Donaldson et al. (1996) closely examined the mass transfer of Br^- and dissolved oxygen between water-filled and gas-filled void space. While the breakthrough curves for Br^- were bell-shaped, the curves for O_2 were highly asymmetrical. The asymmetry of the breakthrough curves was an indication that instantaneous equilibrium between the oxygen and air pockets was not reached. They successfully fit the breakthrough curves to a kinetic model (van Genuchten 1981) and concluded that in the presence of trapped gas pockets oxygen transport was limited by mass transfer processes. From the mathematical model, they calculated the volume of trapped gas and the mass transfer coefficients for O_2 in their experiments.

1.4. *GOALS OF THIS STUDY*

This study was conducted to determine the behavior of two dissolved gases, Kr and SF_6, in saturated and partially saturated media in both laboratory and field settings. These two gases were selected because they exhibit significantly different partitioning behavior in the presence of trapped air pockets (see Table 2). In the laboratory experiments, Ottawa sand (~ 98 % quartz) was used as the medium to ensure that potential partitioning occurred strictly due to the presence of trapped gas and not sorption onto the other phases (e.g. organic matter). The nonequilibrium partitioning of dissolved gas tracer into air pockets was examined by varying the average linear velocity of the injected tracer solution.

Field tests were conducted to determine if trapped air pockets in partially saturated media can be detected or quantified in water table aquifers. This research required the development of novel sampling techniques, and delivery and recovery protocols under field conditions. The influence of salinity gradients on dissolved gases was also examined to determine if dissolved gases and salts could be used simultaneously as conservative tracers.

CHAPTER 2
MATERIALS AND METHODS

2.1. *DISSOLVING GAS IN WATER*

The volatile nature of dissolved gas tracers requires the user to develop novel techniques for dosing water and collecting samples compared to methods used for conventional groundwater tracers. However, the partitioning behavior of gases is consistent and predictable. If proper care is taken with injection, sampling, storage, and analysis, accurate and precise measurements of dissolved gases in water can be made.

Gaseous krypton (Kr) and sulfur hexafluoride (SF_6) were dissolved in natural surface water that was collected from Fourmile Creek on the Savannah River Site (SRS; Fig. 1). Tracer gases were passed through the creek water using a recirculating pump to recycle the gas of interest through a water column. The Four Mile Creek water used contained an elevated tritium concentration compared to natural water and therefore provided an intrinsic conservative tracer. Air tight fittings were mounted on a removable lid that was securely fastened to a container half-filled with water (Fig. 2). The inlet of the pump was connected by tubing to the headspace of the container and the outlet was connected to a frit submerged in the water so that a circuit between the water and headspace was formed. A third opening in the lid was used to discharge the gaseous tracer into the container. Tracer gas was introduced into the headspace until a positive pressure of 20-30 psi was reached and the cap was then loosened. This procedure was repeated several times to ensure that air in the headspace was replaced with tracer gas. The carboy was then isolated and the pump was turned on for ~1 hr to ensure steady state conditions between the water and headspace.

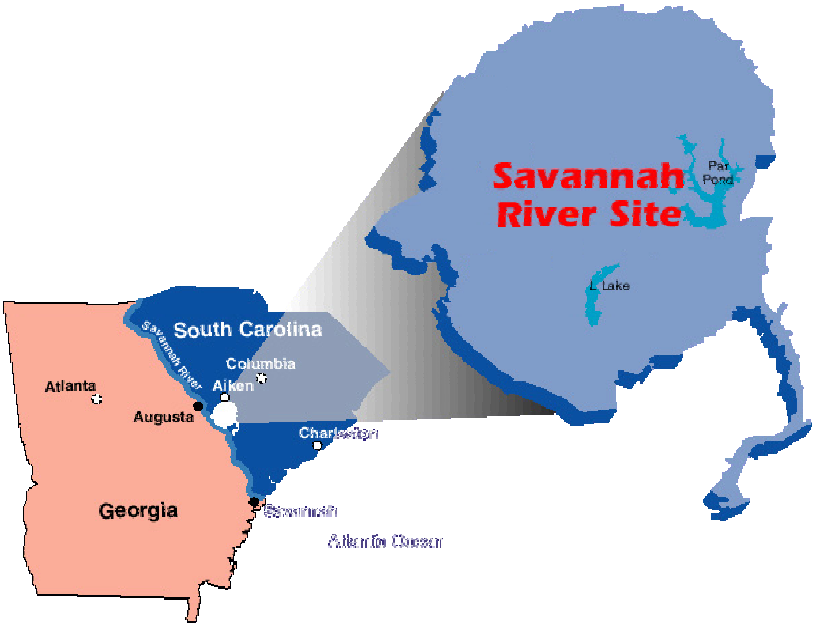

Figure 1a. Map showing location of Savannah River Site (SRS).

Figure 1b. Map showing location of Four Mile Creek well site where field experiments were conducted.

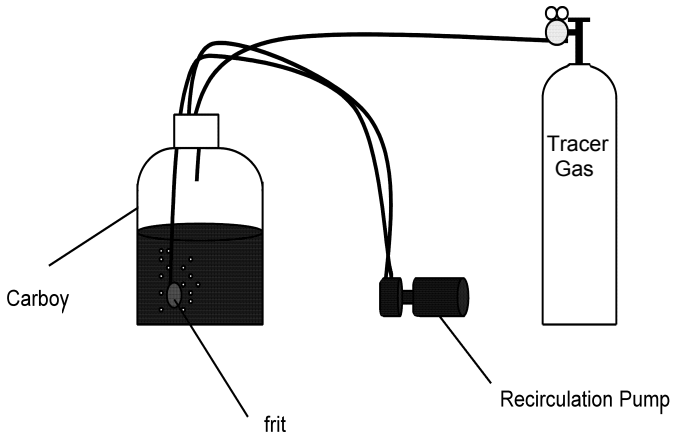

Figure 2. Schematic of water charging system. Air in the carboy headspace was flushed with tracer gas prior to the recirculation of gas through the system

In most cases, it was necessary to charge the solution with both SF_6 and Kr. While water can be charged with a mixture of the tracer gases or individually charged solutions can be mixed to produce a solution containing multiple tracers, this was not necessary for the experiments performed in this study. Due to the low ambient concentration of SF_6 in air and the low analytical detection limits possible for this gas, the solution was always charged first with pure SF_6 and then Kr. Even after flushing Kr through a SF_6 charged solution, the dissolved SF_6 concentration (~ 1 ppm) was typically six orders of magnitude above natural background (see Table 2).

The concentration of dissolved Kr (~ 160 ppm) did not reach theoretical maximum solubility at 25°C (~ 209 ppm) with the procedure described here. One possible reason for this was that the headspace above an SF_6-charged solution probably contained a significant proportion of SF_6 as Kr was circulated through the carboy. Bubbling an open container of water with pure Kr for a period of several hours likely would have achieved complete saturation, however the high cost of Kr warranted a method that conserved the amount of Kr used. Additionally, continual sparging of the solution with Kr would eventually displace all SF_6 in solution.

2.2. *STANDARD PREPARATION*

Four gas mixtures of SF_6 and Kr (Table 4) were prepared for calibration of samples analyzed on the GC-ECD and GC-MS systems. In order to prepare the standards, it was necessary to use a vacuum line and three pressure gauges (Fig. 3) that accurately measured pressure from ~ 1 mtorr to ~100 psi (positive pressure). SF_6 was introduced into lecture bottles at a low pressure followed by Kr at a higher pressure to ensure that mass always flowed into a lecture bottle. Two lecture bottles (A and B shown in Fig. 3) were attached to the vacuum line along with an additional bottle (C) attached at the vent. All three bottles (volume ~ 0.86 L) were evacuated to less than 4 mtorr pressure. Pure Kr or SF_6 was introduced by attaching a tank of the pure gas to the gas connection valve on the line. SF_6 was admitted into the line and lecture bottles A and B to a pressure of 5.9 ± 0.1 torr. Bottles A and B were closed, the line was isolated and then evacuated. Next, 200 torr of Kr was expanded into the line and the third evacuated lecture bottle C. The line was then isolated and the valves on lecture bottles A and B were slowly opened simultaneously, resulting in a final pressure of ~59 torr within the entire line. Bottles A and B were closed, the line was evacuated a third time and then connected to a N_2 cylinder with a regulator set to ~ 100 psi. The bottles were then "topped off" to 100 psi total pressure. The resulting gas mixture in lecture bottles A and B contained ~ 0.1 % SF_6 and ~1% Kr in a N_2 balance. The standards were mixed by shaking, and were diluted with N_2 by factors of ten to yield less concentrated mixtures. This procedure involved reducing the pressure in a bottle to ~590 torr and then repressurizing it to 100 psi with N_2, and resulted in standard mixtures having a composition of 1,000 ppm Kr /100 ppm SF_6. Additional bottles were then diluted by factors of ten to produce a suite of standards having a wide range of compositions (Table 4).

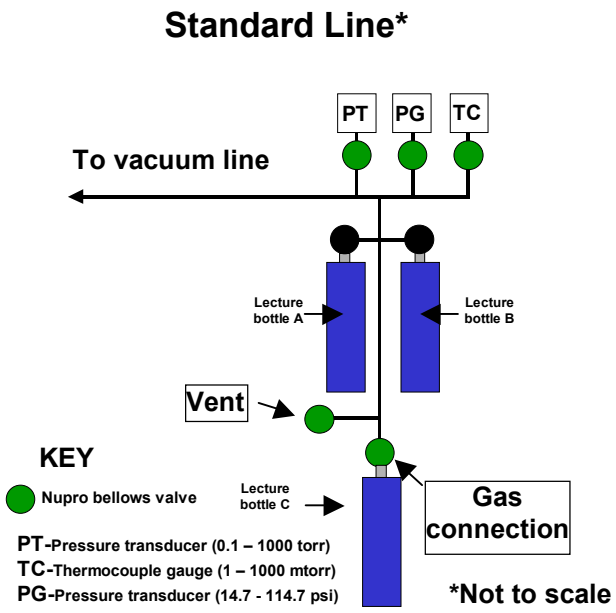

Figure 3a. Schematic of standard preparation setup.

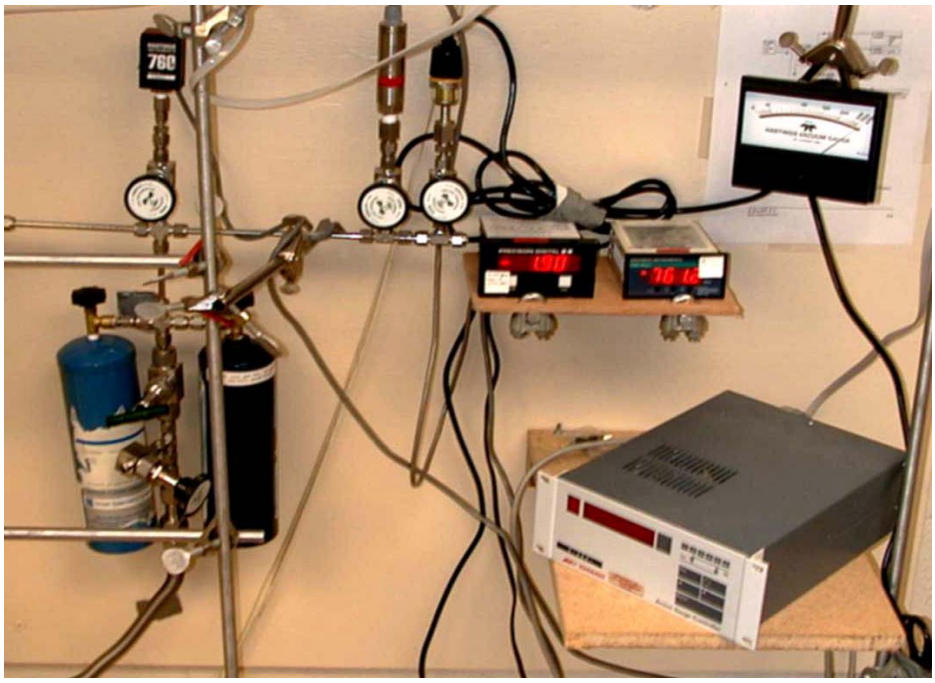

Figure 3b. Photograph of standard preparation setup.

Table 4. Concentrations of Kr and SF_6 gas standards used in this study.

1. 10,000 ppm Kr /1,000 ppm, SF_6
2. 1,000 ppm Kr /100 ppm SF_6
3. 100 ppm Kr /10 ppm SF_6
4. 10 ppm Kr /1 ppm SF_6

2.3. *CHROMOTOGRAPHY*

Four milliliter samples of solution were collected in ~12.2 mL headspace vials (sealed with septa and crimp) for dissolved gas analysis. Because the initial headspace (~8.2 mL) consisted only of air, dissolved Kr and SF_6 strongly partitioned to the gas phase. Gas was allowed to equilibrate between the gas and liquid phase prior to analysis. To promote mass exchange, samples were vigorously shaken for ~30 sec prior to analysis (Thene and Gulliver 1990). The headspace was then subsampled using a gas-tight syringe. Due to the different physical properties of SF_6 and Kr, different chromatographic techniques were employed to measure the concentration of dissolved SF_6 and Kr in a sample.

Chromatographic separation of Kr from air and other noble gases was problematic because most GC columns do not separate noble gases from air very well (Jones 1996). The National Council of the Paper Industry for Air and Stream Improvement (NCASL 1991) devised a GC method of separating noble gases from air with a molecular sieve 5A 40/60 mesh column and measuring Kr/Ar concentrations with a thermal conductivity detector (TCD). However, low detection limits and gas specificity are compromised by this technique. Consequently, Jones (1996) modified this method using a quadrapole mass selective detector (MSD) to quantify Kr concentration after extracting all dissolved gases and purifying Kr using a vacuum extraction line.

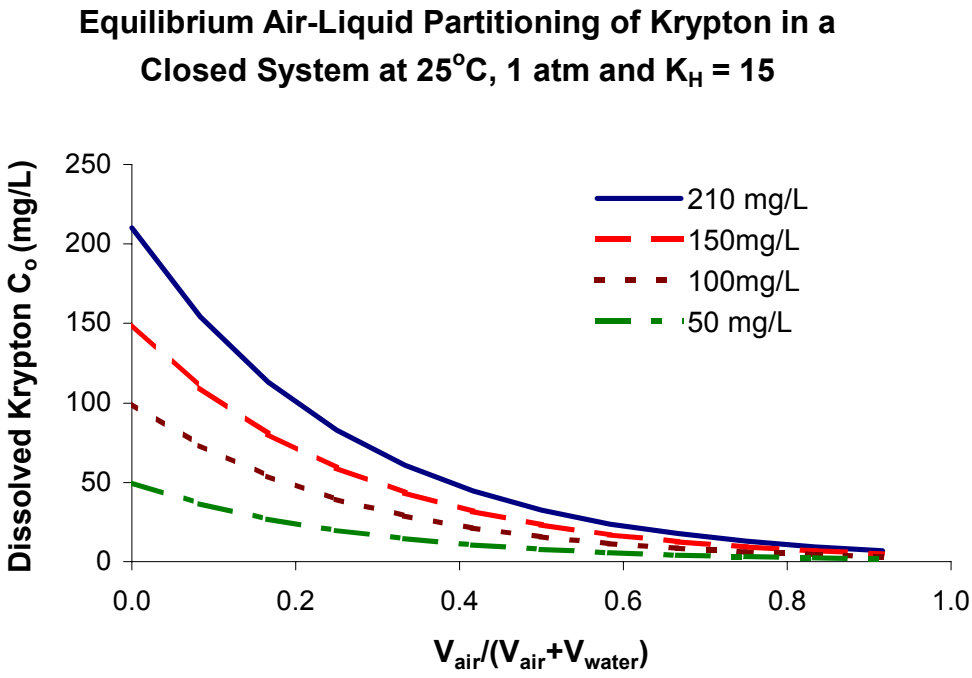

Figure 4. Equilibrium partitioning of Kr from the aqueous phase to the gas phase in a closed system. In this study, $V_{air}/(V_{air}+V_{water})$ was ~ 0.68 (4 mL water samples with ~ 8.2 mL of headspace) for all samples analyzed.

In this study, a low detection limit for Kr, such as that in most natural waters (~239 ppt), was not required because input concentrations of dissolved Kr were relatively high (in ppm range) and tracer dilution was not significant during the course of an experiment. In addition, sample preparation on an extraction line is a time consuming procedure so a method was developed where samples were analyzed more quickly.

The equilibrium partitioning of a water sample containing significant dissolved Kr with even a relatively small volume of air is significant. The 4 mL water samples of this study lost most (~ 96 %) of the Kr initially present in the liquid to the headspace (~ 8.2 mL) once equilibrium was reached (Fig. 4). In order to calculate the original dissolved Kr concentration, the mass of the Kr in the headspace was quantified relative to standards and the mass of Kr remaining in solution was back calculated by applying Henry's Law. These two masses were then summed and divided by the volume of fluid to yield an

original (C_o) dissolved Kr concentration for a sample. The partitioning of SF_6 to headspace at equilibrium is nearly complete because of a high Henry's Law coefficient (~ 170 at STP) so the sensitivity of an analysis to the volume ratio of gas-liquid is not as great as it is for Kr.

For Kr, a 10 µL sample of equilibrated vial headspace was sampled using a gas-tight syringe and injected directly into a Hewlett-Packard© 5890 GC equipped with a 5970 Mass Selective Detector (MSD). A Supelco Carboxen© 1010 PLOT column was used for noble gas separation. This column was designed for the separation of noble gases and effectively separated Ar and Kr by ~1 minute when the GC was set in isothermal mode at 155°C (Fig. 5). Hewlett-Packard© Chemstation© software was used to program the GC-MS (see APPENDIX A). Maximum instrument sensitivity was achieved by setting the MSD in selected ion monitoring mode, where the masses of the six stable isotopes of Kr (^{78}Kr, ^{80}Kr, ^{82}Kr, ^{83}Kr, ^{84}Kr, ^{86}Kr) were analyzed. Additionally, three stable isotopes of Ar (^{36}Ar, ^{38}Ar, ^{40}Ar) were analyzed as an internal standard. This Ar originated from air (~ 0.93%) that was trapped in the vial when it was sealed after collection of a sample. The peak area of Kr was normalized to Ar to facilitate comparisons between samples. A detection limit for Kr of ~ 375 ppb for water samples was achieved using this method, the lower limit could be reduced if larger water samples were collected in the headspace vials to increase the equilibrium headspace concentration (see Fig. 4). The detection limit (~ 375 ppb) provided a working range of greater than four orders of magnitude, which was adequate for the purposes of this study.

For SF_6, somewhat different analytical instrumentation was required. Headspace vials were analyzed using a HP 7694 headspace sampler interfaced to a HP 5870 GC. Chromatographic separation of SF_6 was accomplished using a DB-5 capillary column. The nonreactive nature of SF_6 allowed for the rapid elution of SF_6 from the column (~0.9min.). An electron capture detector (ECD) with a ^{63}Ni source was used to measure the concentration of SF_6 in a sample. The ECD provided the best sensitivity for

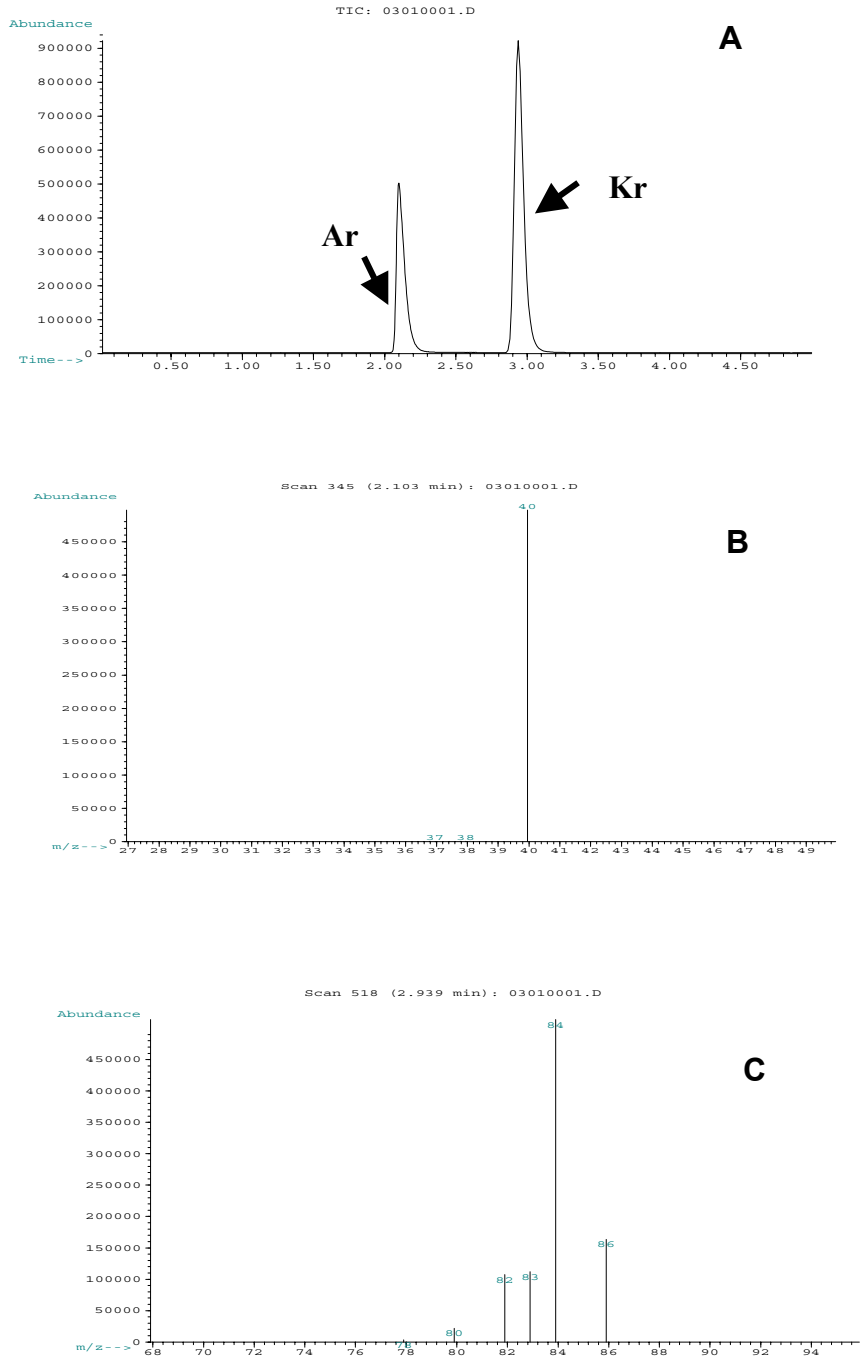

Figure 5. Typical total ion chromatograph for argon and krypton (A). Extracted ion chromatographs for argon (B) and krypton (C) at peak elution times of ~2.1 minutes and 2.9 minutes respectively.

halogenated compounds, such as SF_6 (Miller 1987). However, the response of the detector was typically non-linear over a dynamic range of four orders of magnitude (as noted by Wanninkhof et al. 1990), and the detector was saturated when the concentration of SF_6 exceeded ~ 1 ppm (Miller 1987). In order to avoid these problems, the concentration of dissolved SF_6 used in tracer experiments was kept within the working range of the instrument for the sampling methods employed. This method yielded a detection limit of ~ 250 ppt for SF_6.

2.4. *CALIBRATION*

Krypton calibration curves were constructed by subsampling headspace vials (12.2 mL; sealed and crimped) that contained known amounts of pure Kr gas or standard mixture and air. As such, the vials all contained Ar (~15.53 mg/L) in approximately the same concentration as the headspace of equilibrated water samples collected during experiments. For water samples that contained no Ar initially, a small amount of Ar potentially partitioned back into solution, but because the equilibrium concentration of Ar in water (with air at 25°C and 1 atm) is ~0.52 mg/L, the liquid phase was not a significant sink for Ar. Krypton peak areas were normalized to Ar peak areas to reduce uncertainty associated with sampling and thereby improve precision (Fig. 6). Original water concentrations were calculated by: 1. determining equilibrium vial headspace concentration based on the calibration curve, 2. applying Henry's Law to determine the water concentration, 3. multiplying the concentration by volume to determine sample mass, 4. adding the mass of Kr in air and water, and 5. dividing the total mass by the volume of the water sample (Fig. 6).

Sulfur hexafluoride calibration curves were constructed by subsampling headspace vials containing known amounts of pure SF_6 or standard mixtures (Fig. 7). The detector provided a nonlinear response that was described by a second order polynomial regression. In this case, Ar could not be analyzed because of the detector, and the

calibration curve was based solely on the mass of SF_6 injected by syringe. Due to the high $K_H^{'}$ value of SF_6 (~ 170 at STP) only a negligible mass of gas remained in water in the vials at equilibrium. This mass was ignored and the mass of SF_6 present in the headspace of water samples was divided by the water sample volume for determination of water concentration.

In some laboratory and field experiments, bromide was used as an ionic tracer. Dissolved Br^- concentrations were measured using a bromide specific ion electrode. The probe was calibrated in the lab with standard KBr solutions before each use. The curve was found to be linear over several orders of magnitude with a detection limit of ~10 mg/L, however the probe response was greatly diminished at low (10^2 ppm) and high (10^4 ppm) concentrations (Fig. 8).

Tritium analysis was performed on a Packard 2550 TR/AB liquid scintillation analyzer. This instrument provided a linear response over a wide range of concentrations. Tritium analysis was typically performed on 4 mL water samples stored in 25 mL plastic scintillation vials. Field samples were filtered before analysis to improve sample clarity. Ten milliliters of scintillation cocktail were added to each scintillation vial. After gently shaking samples to mix the cocktail, they were placed in the autosampler for analysis. Absolute concentrations were not required for experiments in this study; therefore a working range of standards was made by dilution of a single sample of Four Mile Creek water with deionized water (Fig. 9). The scintillation counter provided a linear response over the range of activities measured in this study.

2.5. *EXPERIMENTAL MATERIALS*

Laboratory Column Experiments

The column set up used in all experiments (Fig. 10) was chosen to minimize complexity and potential for unaccountable loss of dissolved gas tracers. A 2.5 cm ID by 30 cm long glass tube (Kontes©) with tightly sealing (Telflon©) end pieces was used for

the experiments. The porous medium was 20-30 mesh Ottawa sand. This medium (> 98% well rounded quartz grains) was chosen to keep the system as simple as possible. The medium was washed to remove residue from the surface of grains. The sand was dried and poured into the column so that the grains were tightly packed. Gas-charged and deionized water were stored in gas impermeable sampling bags or a Pyrex© bottle and pumped into the packed column using a constant-flow piston type pump (SciLog©). All tubing was 1/8" O.D. (1/16" I.D.) stainless steel, as plastic was avoided to prevent sorption of gases (Wilson and Mackay 1996). Solution was pumped through the column and collected with a rotating fraction collector. All tubing connections, except at the pump head and tubing end pieces, were brass or stainless steel fittings (Swagelok©). A bypass was added to the column so that the tracer could be sampled in the same manner that experimental samples were collected.

Field Experiments

Field experiments were conducted at a well field located just below the headwaters of Four Mile Creek on the Savannah River DOE Site (SRS) (see Figs. 1, 12). This portion of Four Mile Creek contains uncontaminated, riparian wetlands. Dunn et al. (1998) chose this site as a location to study the natural interactions between groundwater and surface water to gain a better understanding of the relevant processes that occur in riparian wetlands. An array of multilevel wells was constructed across the floodplain and stream so that groundwater and surface water samples could be collected from various depths (up to ~ 12 feet). The wells were installed by vibracoring to minimize the disturbance to the wetland sediments (Dunn et al. 1998). The wells were made of 4" O.D. PVC tubing with up to three independent 4" screened intervals. The screens were surrounded with filter pack and were isolated from each other with bentonite seals. Each screened interval was connected to the surface by 3/8" I.D. tubing (see Fig. 13).

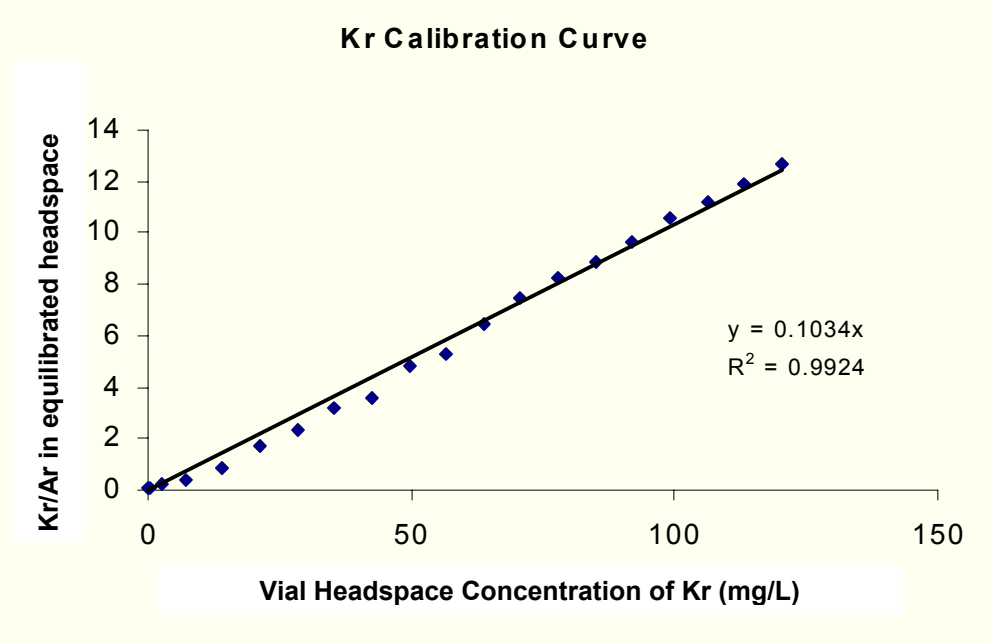

Figure 6a. Calibration curve for Krypton from pure Kr or standard mixtures injected into sealed headspace vials containing ambient air. A 10 µL subsample was introduced into the GC-MS.

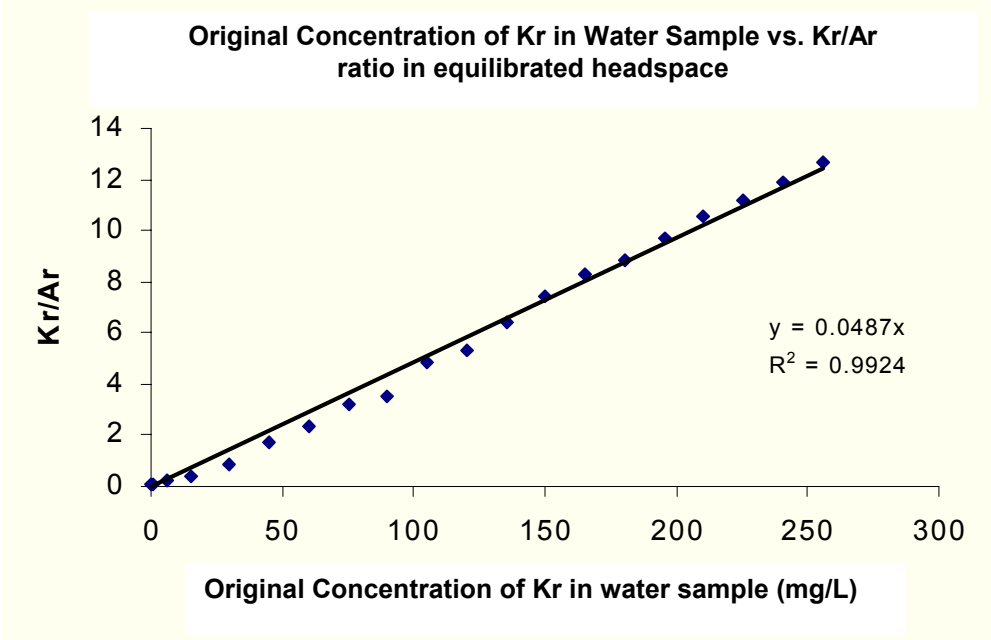

Figure 6b. Predictive curve for estimating the original water concentration of a sample based on the equilibrated headspace concentration. This assumes $K_H^{'} \approx 15$ at 1 atm pressure and 25°C.

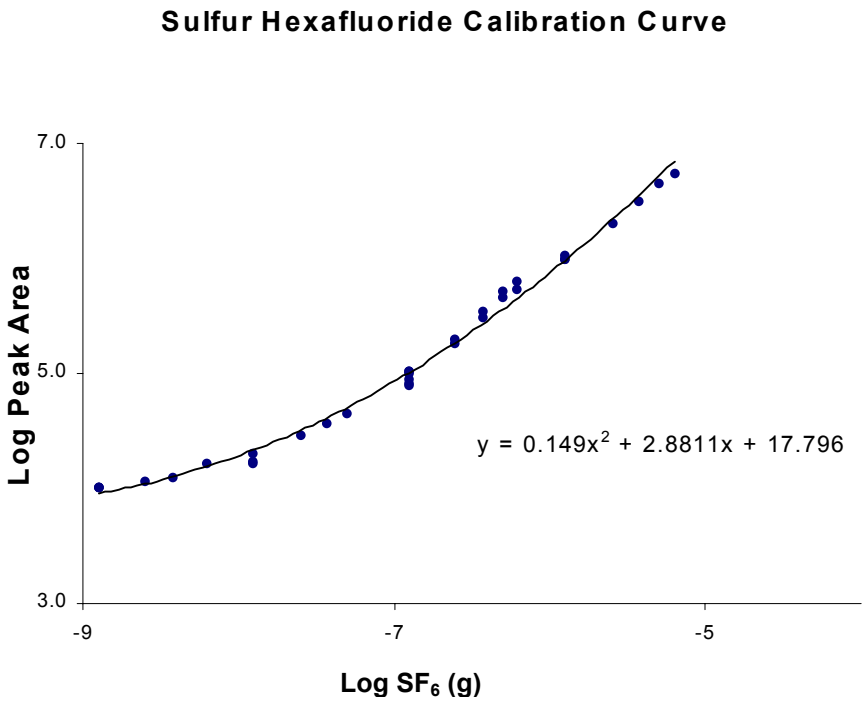

Figure 7. Calibration curve for SF_6 using a GC-ECD. Known volumes of pure SF_6 or standard mixtures were injected into air filled vials with a syringe, then subsampled by the headspace analyzer, and injected into the GC.

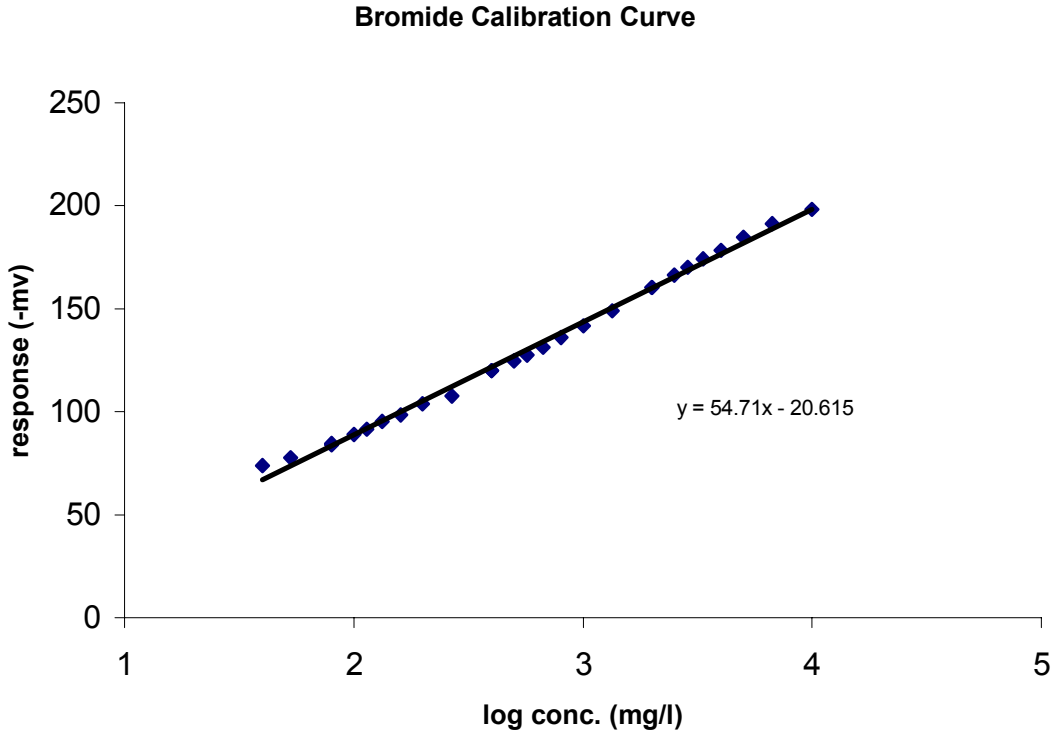

Figure 8. Calibration curve for bromide probe.

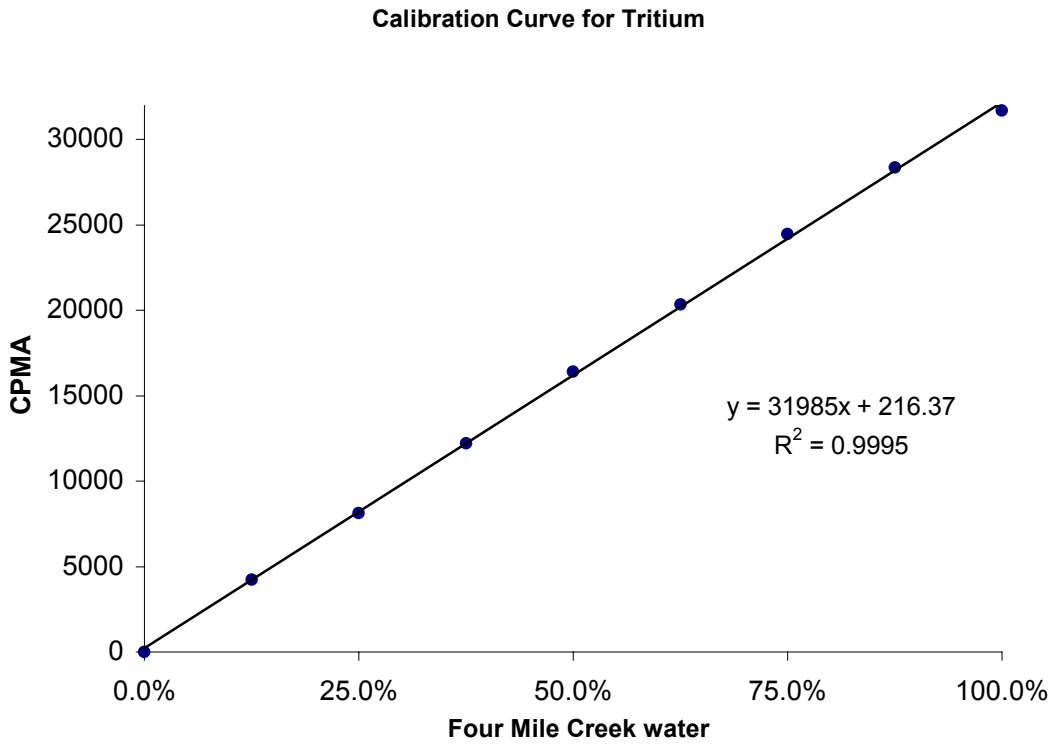

Figure 9. Calibration curve for diluted samples of tritiated tracer water.

Wells were typically screened in sandy horizons because they were believed to have higher hydraulic conductivity than the adjacent clay- and silt-rich horizons. The well log for Well 274 describes the typical lithology of the well field (Fig. 14). Some horizons were of variable thickness or were missing at the various well sites, but the lithologies generally ranged from clean sand to sand/silt, and kaolinitic clay lenses, with an organic rich layer less than 0.5 feet thick covering the surface of the floodplain.

2.6. *EXPERIMENTAL METHODS*

Laboratory Column Experiments

Several steps were necessary to conduct a column experiment. First, the sand packed column was weighed (with tubing and valves on both ends). The column was then flushed in vertical position from below with pure CO_2 gas at a slow flow rate for ~ 30 minutes. The valves were then closed and the column was attached to the pump. The lower 3-way valve connected to the pump was opened to the bypass to flush air out of the tubing. The lower valve was opened to the column (the upper valve remained closed) and deionized water was forced into the column from below at a high flow rate (~10 mL/min). As the column filled, the highly soluble CO_2 ($K_H^{'} \approx 1.2$) dissolved facilitating the complete saturation of the column. Periodically, pressure in the column was relieved by briefly cracking the upper valve of the column. Once the column was full of water, both valves were opened and water was circulated through the system for ~ 1 hour. The column matrix was then closely inspected for air pockets. If none were seen, the column was assumed saturated. The column was then isolated from the pump by closing the upper and lower valves, it was detached from the system and reweighed. The pore volume was calculated by subtracting the weight of the dry sand-filled column from the weight of the column after filling it with water. A small amount of water was present in the tubing connecting the valves to the column; this volume was estimated based on the internal volume of the tubing and the deadspace of the valves. The contribution from these sources was minimal (~ 1.5%) compared to the weight of the column, and this value was subtracted from calculations pore volume size.

Experiments were conducted by injecting tracer solution containing dissolved Kr, SF_6, and ^3H_2O at a constant flow rate and collecting column effluent with the fraction collector. The effluent was collected in a headspace vial dropwise until a volume of 4 mL was reached (1 – 4 min) at which time the vial was sealed with a crimp and septa.

An important assumption made in sampling was that gas loss by diffusion from a headspace vial was not significant over the few minutes needed to collect a sample. To test this assumption, fourteen 12 mL headspace vials were completely filled with Kr charged water and left unsealed. At a periodic time interval, a 4 mL aliquot of water was subsampled from a vial, transferred into an empty vial and crimped sealed. After equilibration with the headspace, the subsamples were analyzed for Kr concentration. Krypton concentration was plotted as a function of time and fit with an exponential regression (Fig. 10). The Pearson correlation coefficient (R^2) of ~0.77 was significant at $\alpha = 0.01$ for n=15 (Triola 1995). For sample collection times of less than 5 minutes, the loss of dissolved Kr from an open vial was less than 2%. Jones (1996) conducted a similar experiment, but with a 50 gallon open barrel containing 30 gallons of water with an initial Kr concentration of ~33.5 mg/L. He found that the loss of Kr occurred more slowly than in the experiment with headspace vials, but this is to be expected because of the much lower surface area to volume ratio of the open barrel.

In this study, it was noticed that samples that were circulated through stainless steel tubing and collected as drops in vials lost ~ 20% of their dissolved gas concentration relative to the input solution. This effect was compensated for by collecting drops of input solution circulated through a tubing bypass and collected in open vials. This collection was performed prior to and after each column experiment at the same flow rate that the experiment was conducted. The concentration of Kr in these vials was taken as the C_o for a column experiment rather than the actual concentration of input solution in the sample bag or bottle. It was assumed that because Kr loss by diffusion was not significant in the time necessary for sample collection (< 5 min), it would not be significant for SF_6 either. Despite the fact that the degree of disequilibrium for SF_6 between liquid and ambient air was greater than for Kr, SF_6 should degas more slowly. The process of degassing under stagnant conditions is diffusion limited. The transport of gas in solution is based on the relationship:

$$t_d = \frac{L^2}{2D^{\circ}_{aq}} \quad [11]$$

where: t_d = characteristic transport time (sec), L^2 = distance (cm^2), and D°_{aq} = aqueous diffusion coefficient (cm^2/sec; Schwartzenbach et al. 1993). The diffusion coefficient for SF_6 (8.68e-6 cm^2/sec) is over two times less than that of Kr (1.87e-5 cm^2/sec) so degassing effects should also be less.

Gas-filled void space was created in columns following the method of Fry et al. (1995). A preweighed fully saturated column was drained of a small amount of water by first opening the upper valve and then the lower valve attached to the column. This water was collected and weighed, as was the column after draining. After reattaching the column to the system, water was allowed to circulate through the system for an additional hour. The column was detached once again and reweighed. The difference in mass (g) between the fully saturated column and the mass after recirculation was considered to be the volume of air space (mL) in the column assuming 1 g of distilled water occupies a volume of ~ 1 mL.

A slight increase in weight was noticed between the first and second weighing of the partially unsaturated column, suggesting that a period of stabilization of void space was required prior to the execution of an experiment under partially saturated conditions.

To assess variation of in measurement, triplicates of C_o were collected and analyzed for ^3H, Kr, and SF_6 in each experiment. From these samples a coefficient of variation (CV) was calculated for each tracer by dividing the standard deviation of the C_o values by the average. The CV values were multiplied by 100 and expressed as a percentage (Figs. 16 – 28).

Field Experiments

Six small volume push-pull experiments were conducted where a ~5 L slug of tracer solution was injected into the green (lowest) level of Well 274, or red (upper)

screened intervals of Well 335 and 356. The tracer slug was prepared using Four Mile Creek water that was charged with Kr, SF_6 and/or Br^-. The slug was introduced by a peristaltic pump at a rate of ~0.6-1.0 L/min. The total time required to deliver the slug was ~ 5 min.

Within a minute of injecting the tracer slug, the pump was reversed and water was removed from the screened interval. The water pumped out was collected in carboys and disposed of downstream to prevent reintroducing tagged water to the system. A 40 mL sample was collected every 5 minutes and analyzed for bromide (where appropriate) in the field with a bromide specific electrode. For SF_6 and Kr analysis, 4 mL subsamples were transferred by pipette to 12 mL headspace vials and crimp-sealed immediately.

For the experiments conducted on Well 274, the yellow level (middle screened interval) was sampled to determine if there was any upward movement of tracer. The middle (yellow) level was continuously pumped at a rate of ~0.1 L/min (except 01/06/00 experiment), which was an order of magnitude slower than the lowest (green) level. Sampling in this fashion precluded the induced upward flow of water. In the 01/06/00 experiment, the pump attached to the middle (yellow) screened level was engaged only long enough to collect a 40 mL sample. The small volume push-pull experiments were conducted for ~2 hrs. 30 min. and resulted in ~ 150 L of water being removed from the lower (green) screened interval and ~15 L from the middle (yellow) interval.

Water levels were measured intermittently during reconnaissance experiments using a water level meter tape. It was determined that pumping at 1.0 L/min for ~ one hour produced a drawdown of only ~ 0.2" for Well 274.

Two additional field tests were conducted in the upper (red) screened interval of Well 335 and lower (green) screened interval of Well 274. A ~ 20 L slug of tracer solution (tritium, SF_6 and Kr) was injected followed by ~ 30 L of non-labeled Four Mile Creek water to push the tracer slug further into the formation. The pump was then

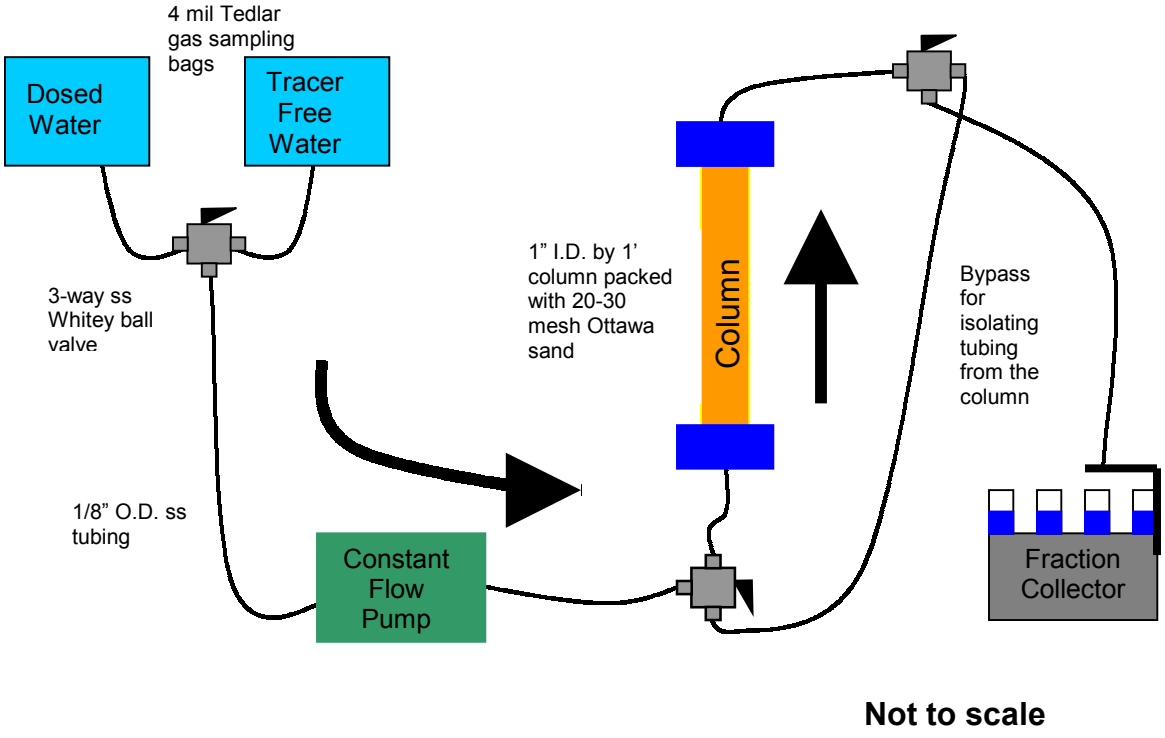

Figure 10a. Schematic of column setup.

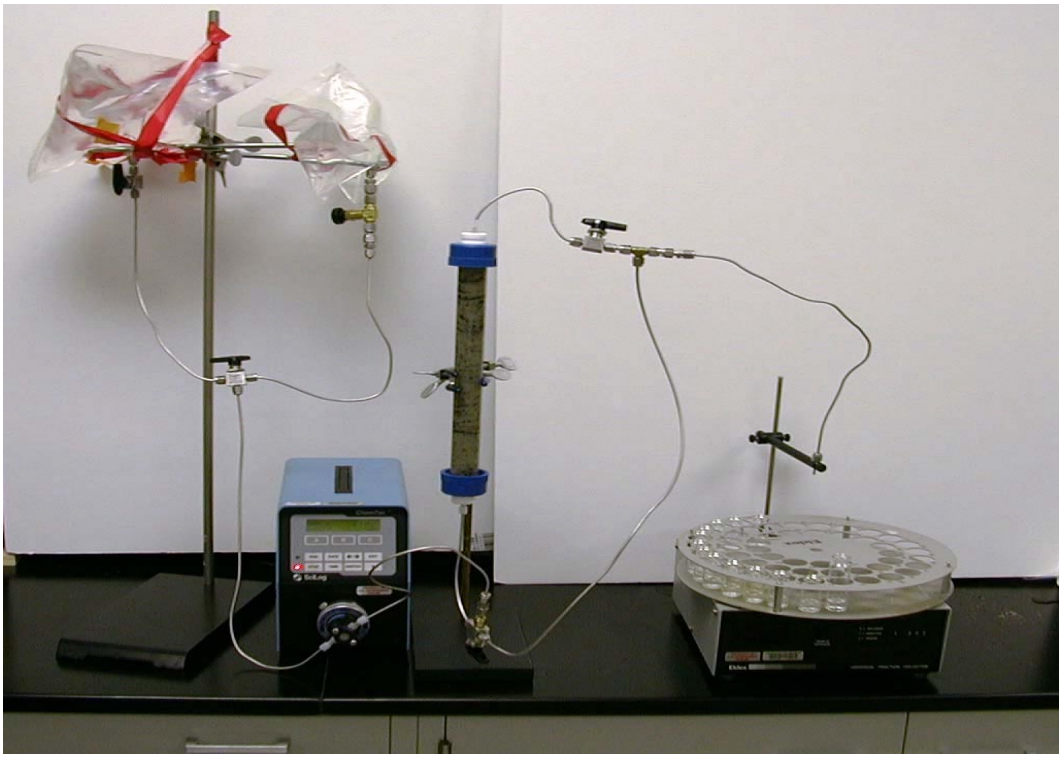

Figure 10b. Photograph of typical column setup.

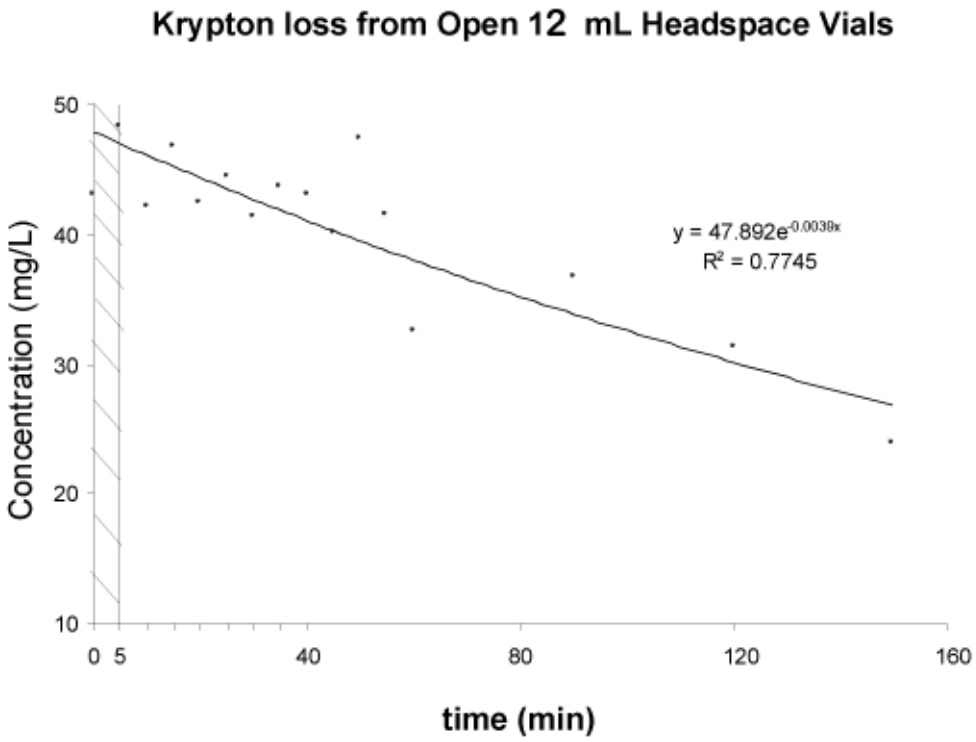

Figure 11. Loss of Kr by diffusion from 12 mL headspace vials.

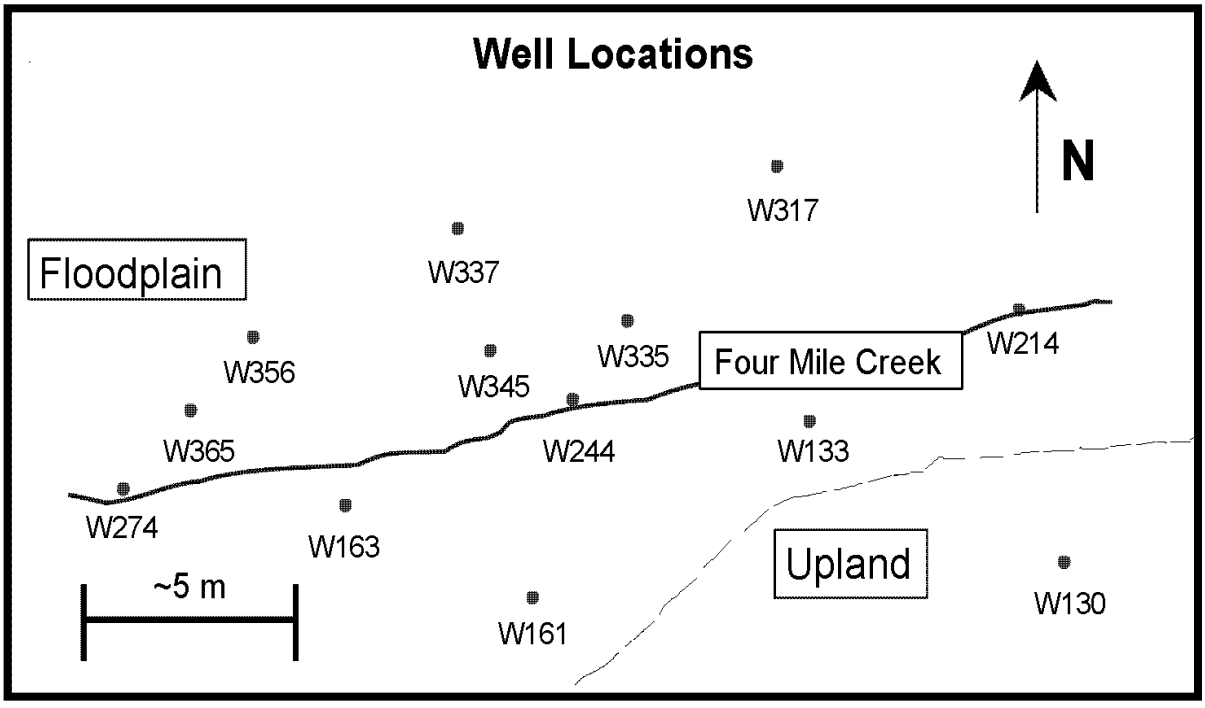

Figure 12. General layout of groundwater-surface water well sites on the Four Mile Creek floodplain.

Well 274

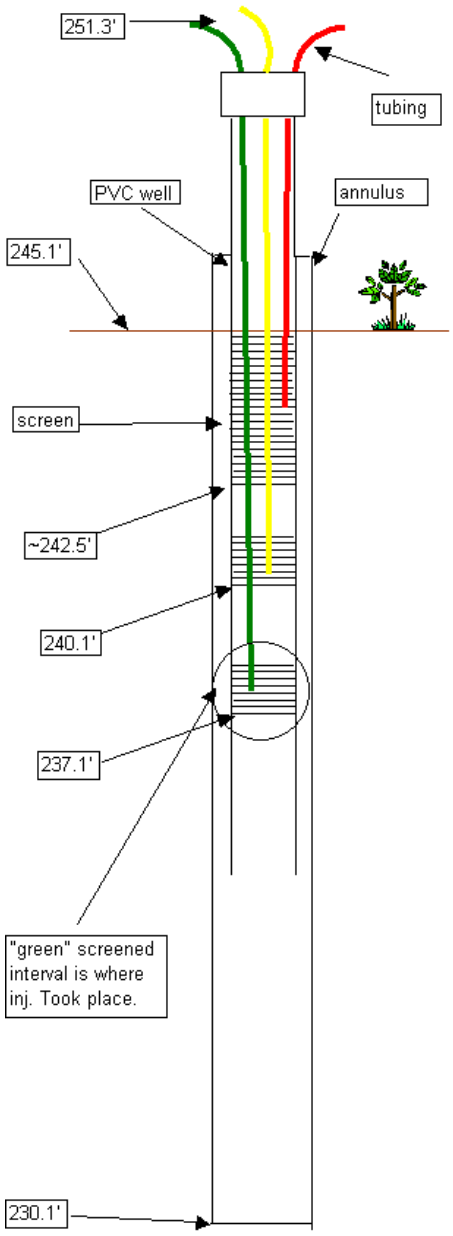

Figure 13. Schematic of typical multilevel well (Well 274). Screened intervals contain color coded tubing: green = lower, yellow = intermediate, and red = upper.

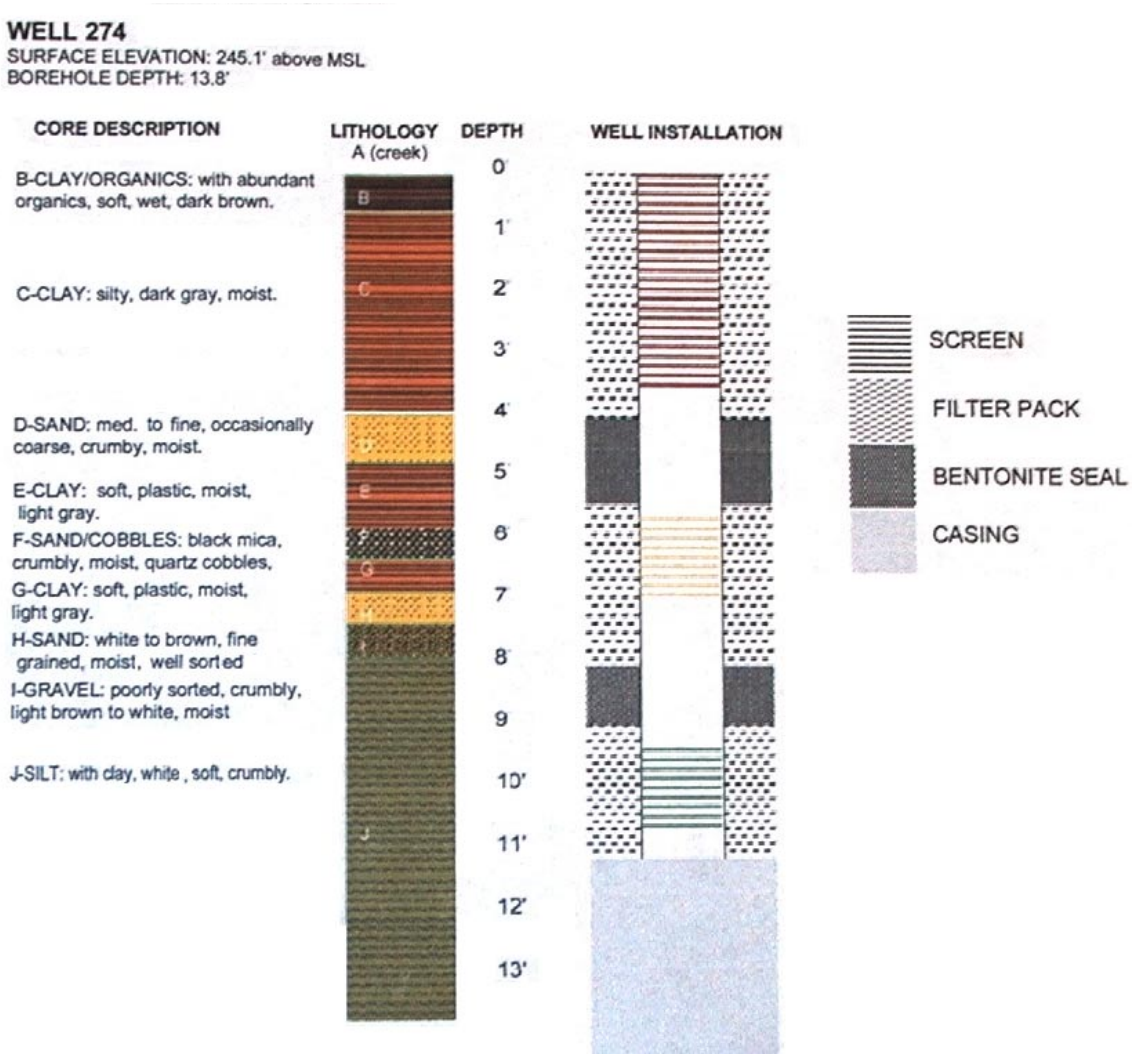

Figure 14. Lithologic description of a Well 274 from the Four Mile Creek field site. The well was primarily screened in the sandy (conductive) horizons. Bentonite was used to separate screened intervals, which were surrounded by conductive filter pack.

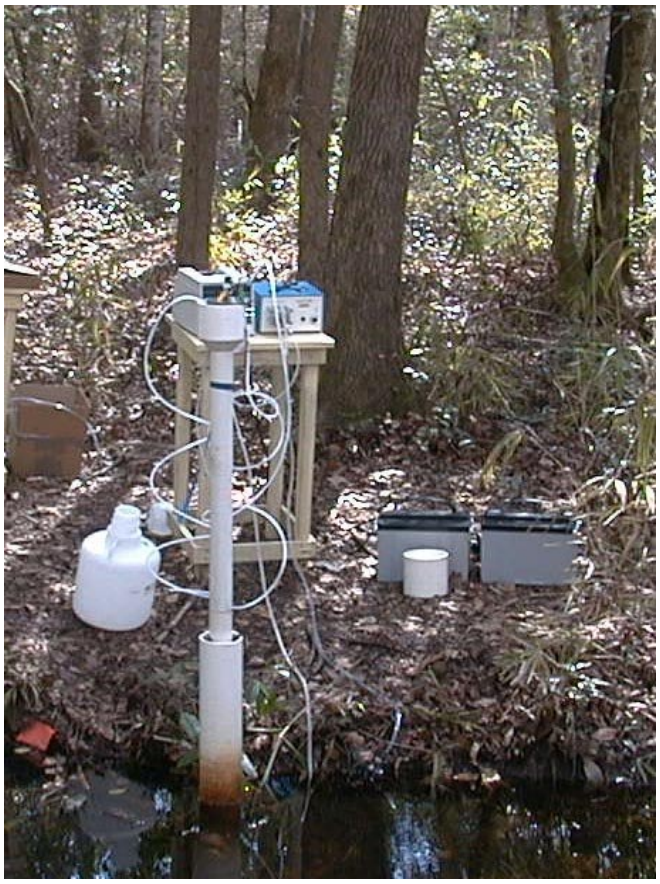

Figure 15. Photograph of Well 274 during an injection. Tracer was pumped from a carboy into the lowest (green) screened interval. A second pump was attached to the middle (yellow) screened interval, so that the upward movement of tracer could be monitored.

reversed; ~ 20 L was removed from Well 335R and ~ 150 L was removed from Well 274G at the same flow rate as it was injected.

2.7. *DISSOLVED GAS LOSS DUE TO PERISTALTIC PUMP*

Because tracer labeled water was injected and retrieved from the formation using a peristaltic pump, water had to pass through the peristaltic pump tubing twice before sample collection. Concerns were raised that the constant flexing of tubing promoted degassing of dissolved gases as water passed through the pump tubing. This problem was examined by performing an experiment where tracer solution was sampled, pumped into a carboy with a peristaltic pump and then pumped out and sampled again. In all cases, tritium concentration was identical to the original solution, but dissolved Kr and SF_6 concentrations decreased ~ 30 % (APPENDIX D). This loss of dissolved gas may have occurred because the contraction of silicone tubing promoted the diffusion and exsolution of dissolved gas through the tubing (silicone tubing is known to be soluble to gases). This problem was circumvented by defining the initial concentration (C_o) of tracer solution as the concentration measured after it was cycled through the pump twice rather than the concentration of tracer in the carboy before injection.

CHAPTER 3
COLUMN EXPERIMENTS

Three sets of column experiments (M, SI, and Large Pulse series) were performed to examine and quantify gas-liquid partitioning of dissolved Kr and SF_6 (Figs. 16-28; APPENDIX F). All three sets of experiments were conducted in the manner described in Chapter Two of this thesis. The ratio of gas-filled void space (θ_g) to water-filled void space (θ_{aq}) varied within each set of experiments and the volume of tracer injected (M < SI < Large Pulse) varied between each set of experiments. A value for (θ_g/θ_{aq}) was recorded before and after each experiment. The volume of tracer solution used was expressed in terms of pore volumes, where one pore volume is defined as the internal volume of the column multiplied by the porosity (Fetter 1993). As described in the Chapter Two, porosity was determined gravimetrically based on the saturated and dry weight of each column. In all experiments, ^{3}H-enriched water was used as the ultimate conservative tracer to which dissolved gas tracer behaviors were compared. Tritium transport occurred by "piston flow", where the concentration of tracer in the effluent followed a step function from background to a concentration (C) equal to that of the pure tracer solution (C_o), i.e. $C/C_o = 1$. Likewise, with the passage of tracer through the system, the concentration (C) of tracer, returned to background level as a single step ($C/C_o = 0$). The tritiated water data were used to calibrate a numerical model (described later in this section) so that nonconservative behavior of dissolved gases could be quantified.

3.1. *RESULTS OF SMALL PULSE (M-SERIES) EXPERIMENTS*

The first set of experiments (M columns) were conducted with ~ 1 pore volume pulses of tritiated water containing dissolved Kr and/or SF_6 in fully saturated columns (M-1, M-2, M-3, and M-6) or columns with different volumes of unsaturated pore space (M-5 and M-7). These experiments were conducted to evaluate the effect of water saturation on the transport of dissolved gases through a simple isotropic medium.

Compared to tritiated water, the dissolved gas tracers did not behave conservatively in experiments M-1 and M-2 (Figs. 16 and 17). In column experiment M-1, ^3H, Kr and SF_6 initially co-eluted at one pore volume. Tritium and Kr reached $C/C_o \approx 1.0$, while SF_6 only reached a maximum of ~ 0.6. Tritium returned to background concentration after ~ 2.3 pore volumes, Kr after ~ 3 pore volumes, and SF_6 after > 5 pore volumes. In column experiment M-2, Kr and SF_6 co-eluted slightly after ^3H eluted at one pore volume. Kr and SF_6 both reached a maximum relative concentration of $C/C_o \approx 0.7$ and SF_6 reached this concentration slightly before Kr. Tailing was greater for Kr than SF_6. These results are dissimilar to later column experiments.

In column experiment M-3 (Fig. 18), the dissolved Kr breakthrough curve was nearly identical to the curve for tritiated water. In the same manner as tritium, dissolved Kr reached a relative concentration of $C/C_o \approx 1$ and did not exhibit any tailing. SF_6 was not used in this experiment. In column experiment M-6 (Fig. 19), dissolved Kr and SF_6 reached a maximum relative concentration of $C/C_o \approx 0.9$ and returned $C/C_o \approx 0$ after ~2.3 pore volumes. SF_6 co-eluted and declined in a manner similar to ^3H, but the elution of Kr occurred ~ 0.1 pore volumes later than ^3H and SF_6.

In experiments M-5 and M-7 (Figs. 20 and 21), the dissolved gases behaved drastically different because of unsaturated pore space that was created in the column. In experiment M-5 (Fig. 20), all three tracers appeared in effluent simultaneously at ~ 1 pore volume. However, unlike tritiated water, the dissolved gas tracers did not exhibit “piston flow” type transport characteristics. Dissolved Kr concentration reached a maximum of

$C/C_o \approx 0.5$ only after two to three pore volumes of tracer solution passed through the column, after which C/C_o slowly decreased to near $C/C_o \approx 0$ after ~ 5.5 pore volumes. Dissolved SF_6 concentration rose only slightly above background after ~ 1 pore volume and slowly increased for the duration of the experiment to a maximum value ≈ 0.1.

In column experiment M-7 (Fig. 21), only dissolved Kr and tritiated water were used as tracers. Krypton eluted slightly after ^3H (~ 0.1 pore volumes) and almost immediately reached a maximum relative concentration of $C/C_o \approx 0.6$ (excluding a single measurement ≈ 1.0). The relative concentration of ^3H dropped almost instantaneously at ~ 2 pore volumes, while Kr tailed before returning to background after ~ 3.5 pore volumes.

3.2. *RESULTS OF MEDIUM PULSE (SI-SERIES) EXPERIMENTS*

To further investigate the transport behavior of dissolved Kr and SF_6, a second series of laboratory columns (SI columns) was conducted where a larger pulse of dissolved Kr and/or SF_6 (~5-7.5 pore volumes) was injected into a column containing a known volume of unsaturated pore space. In these experiments (SI-3, SI-4, and SI-5), ^3H was not mixed into the dissolved gas tracer solution. Instead, one pore volume of tritiated water was injected at the conclusion of an experiment; the purpose of injecting the pulse of tritiated water after the dissolved gases was to confirm "piston flow" transport of water through the column. In all three cases the transport of tritiated water was as a non-dispersed plug.

For experiment SI-3 (Fig. 22), water was drained from a fully saturated column to create gas-filled pore space and an initial θ_g/θ_{aq} value of 0.018 (0.041 at the conclusion of the experiment). Five pore volumes of tracer were injected at a constant flow rate of 4 mL/min. The breakthrough curve for dissolved SF_6 (Kr not used) displayed an asymmetric shape. At one pore volume, C/C_o immediately climbed to ~ 0.4; it continued to slowly increase thereafter, reaching a maximum value of ~ 0.8 at ~six pore volumes.

SMALL PULSE SIZE TRACER TESTS

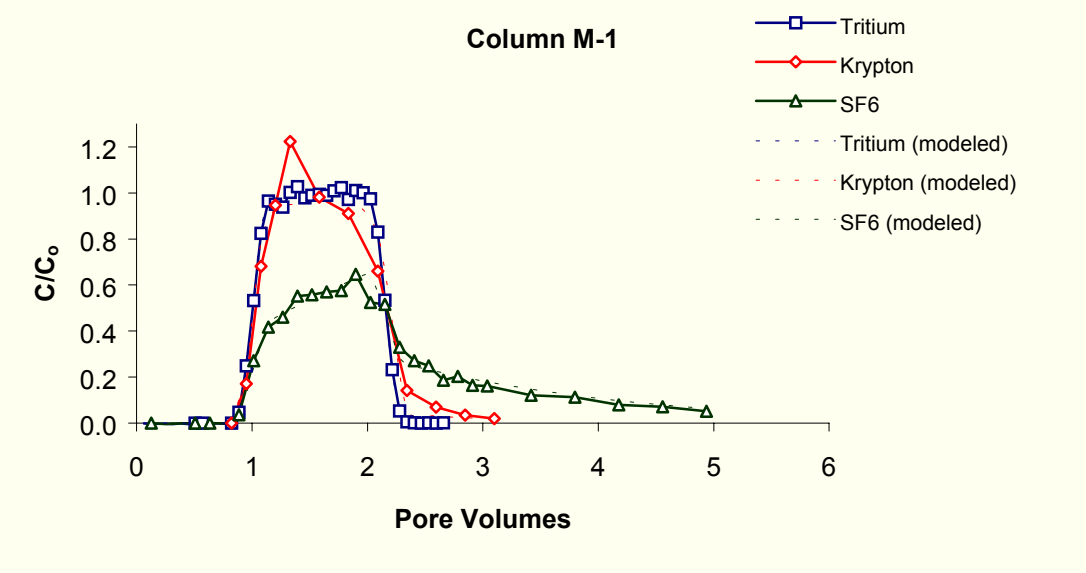

Pre-exp θ_g/θ_{aq} not measured
Post-exp θ_g/θ_{aq} not measured

Physical Parameters of the Column

Q (mL/min)[a]	v_{aq} (cm/sec)[b]	P[c]	δ (cm)[d]	L (cm)[e]	ϕ[f]
4	0.034	334.67	0.090	*30*	*0.39*

Estimated Tracer Parameters

Tracer	R[g]	ω[h]	α (sec^{-1})[i]	θ_g (cm^3/cm^3)[j]	θ_{aq} (cm^3/cm^3)[k]	θ_g/θ_{aq}[l]
^3H_2O	*1.00*	-	-	-	-	-
Kr	1.06	0.08	1.51E-03	0.0016	0.39	0.0040
SF_6	2.07	0.92	9.72E-04	0.0028	0.39	0.0071
			average	0.0022	0.39	0.0056

Figure 16. Experiment where ~ one pore volume of tracer was injected into the column at a pore water velocity of 0.034 cm/sec. The parameters are: (a) flow rate, (b) average linear velocity, (c) Peclet number, (d) dispersivity, (e) column length, (f) porosity, (g) retardation factor, (h) fitting parameter, (i) mass transfer coefficient, (j) volumetric gas content, (k) volumetric water content, and (l) volumetric gas-volumetric water ratio. Parameters (c), (d), (f) (g), (h), and (i) were obtained from modeling and are explained in the discussion section of this thesis. $CV_{tritium} \approx 6.6$ %, $CV_{Kr} \approx 13.9$ %, and $CV_{SF6} \approx 7.3$ %.

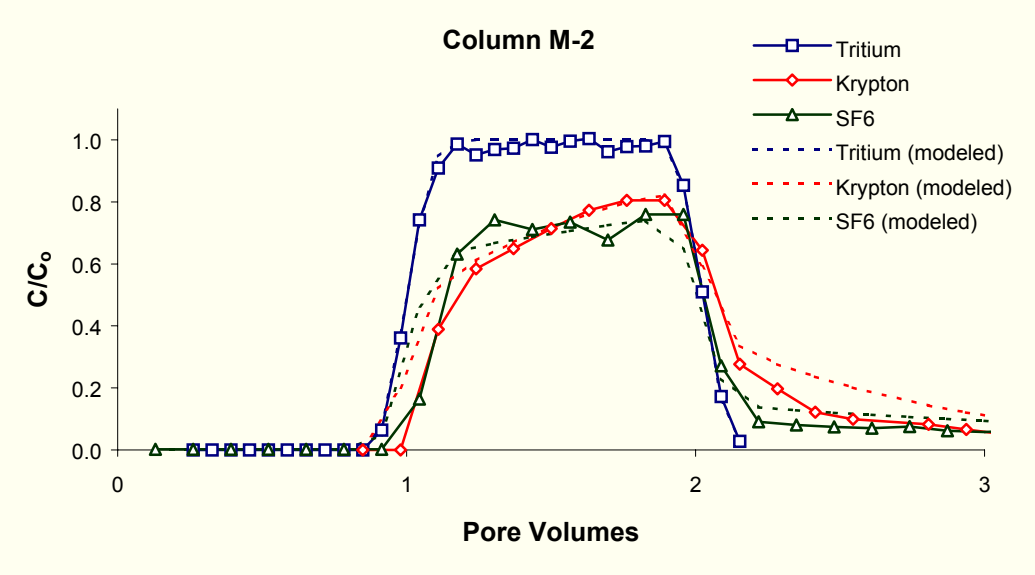

Pre-exp θ_g/θ_{aq} not measured

Post-exp θ_g/θ_{aq} not measured

Physical Parameters of the Column

Q (mL/min)	v_{aq} (cm/sec)	P	δ (cm)[a]	L (cm)	ϕ
2	0.019	477.98	0.063	*30*	*0.40*

Estimated Tracer Parameters

Tracer	R	ω	α (sec^{-1})[b]	θ_g (cm^3/cm^3)[c]	θ_{aq} (cm^3/cm^3)	θ_g/θ_{aq}
^3H_2O	*1.00*	-	-	-	-	-
Kr	1.40	0.73	1.14E-03	0.0104	0.39	0.0267
SF_6	1.78	0.49	3.94E-04	0.0021	0.40	0.0052
			average	0.0062	0.39	0.0159

Figure 17. Experiment where ~ one pore volume of tracer was injected into the column at a pore water velocity of 0.019 cm/sec . For explanation of parameters, see Fig. 16. $CV_{tritium} \approx 2.9$ %, $CV_{Kr} \approx 5.5$ %, and $CV_{SF6} \approx 6.2$ %.

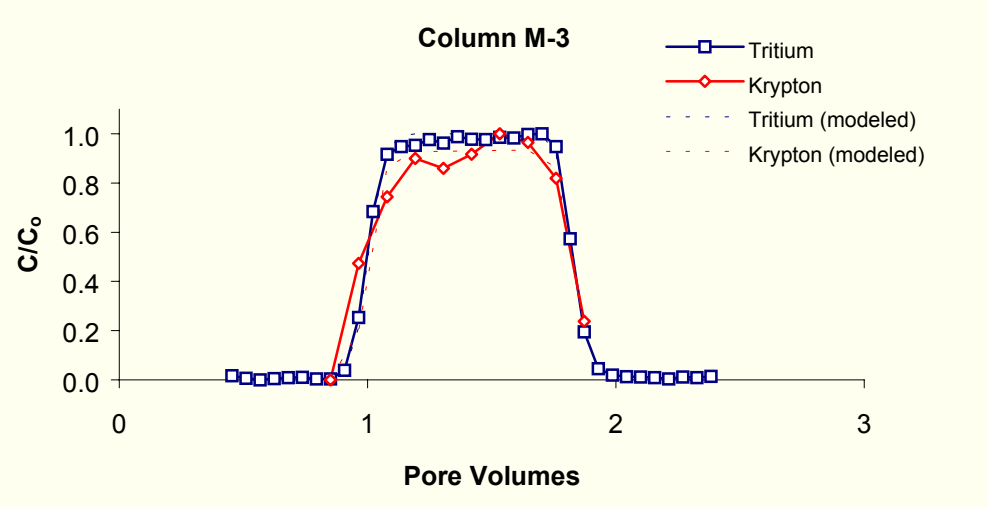

Pre-exp θ_g/θ_{aq}	not measured
Post-exp θ_g/θ_{aq}	not measured

Physical Parameters of the Column

Q (mL/min)	v_{aq} (cm/sec)	P	δ (cm)[a]	L (cm)	ϕ
2	0.017	757.41	0.040	*30*	*0.39*

Estimated Tracer Parameters

Tracer	R	ω	α (sec^{-1})[b]	θ_g (cm^3/cm^3)[c]	θ_{aq} (cm^3/cm^3)	θ_g/θ_{aq}
^3H_2O	*1.00*	-	-	-	-	-
Kr	1.40	0.08	1.15E-04	0.0101	0.38	0.0267
			average	0.0101	0.38	0.0267

Figure 18. Experiment where ~ one pore volume of tracer was injected into the column at a pore water velocity of 0.017 cm/sec. For explanation of parameters, see Fig. 16. $CV_{tritium} \approx 9.9$ % and $CV_{Kr} \approx 6.4$ %.

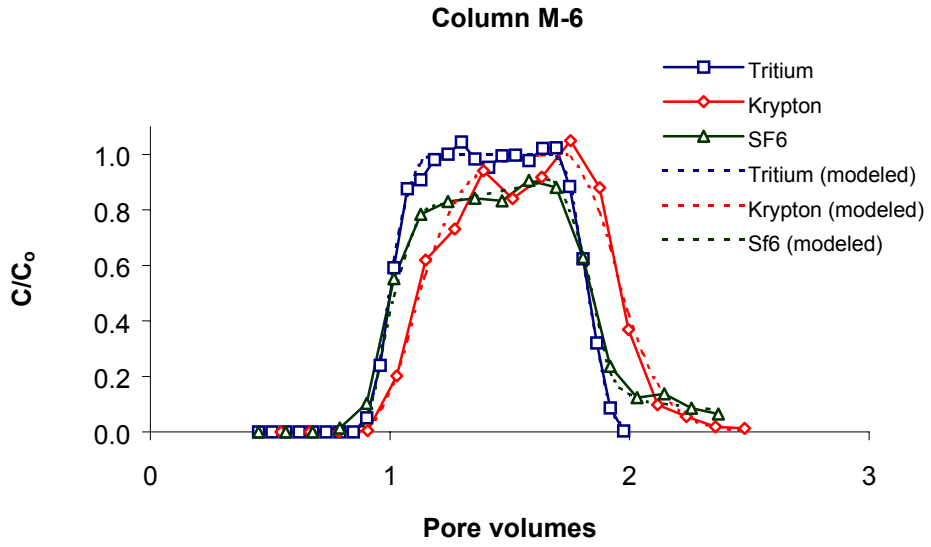

Pre-exp θ_g/θ_{aq} not measured
Post-exp θ_g/θ_{aq} not measured

Physical Parameters of the Column

Q (mL/min)	v_{aq} (cm/sec)	P	δ (cm)[a]	L (cm)	ϕ
4	0.035	475.57	0.063	*30*	*0.38*

Estimated Tracer Parameters

Tracer	R	ω	α (sec^{-1})[b]	θ_g (cm^3/cm^3)[c]	θ_{aq} (cm^3/cm^3)	θ_g/θ_{aq}
^3H_2O	*1.00*	-	-	-	-	-
Kr	1.14	2.95	2.46E-02	0.0035	0.38	0.0093
SF_6	1.19	0.26	1.59E-03	0.0005	0.38	0.0013
			average	0.0020	0.38	0.0053

Figure 19. Experiment where ~ one pore volume of tracer was injected into the column at pore water velocity of 0.035 cm/sec. For explanation of parameters, see Fig. 16. $CV_{tritium} \approx 14.6$ %, $CV_{Kr} \approx 9.2$ %, and $CV_{SF6} \approx 7.1$ %.

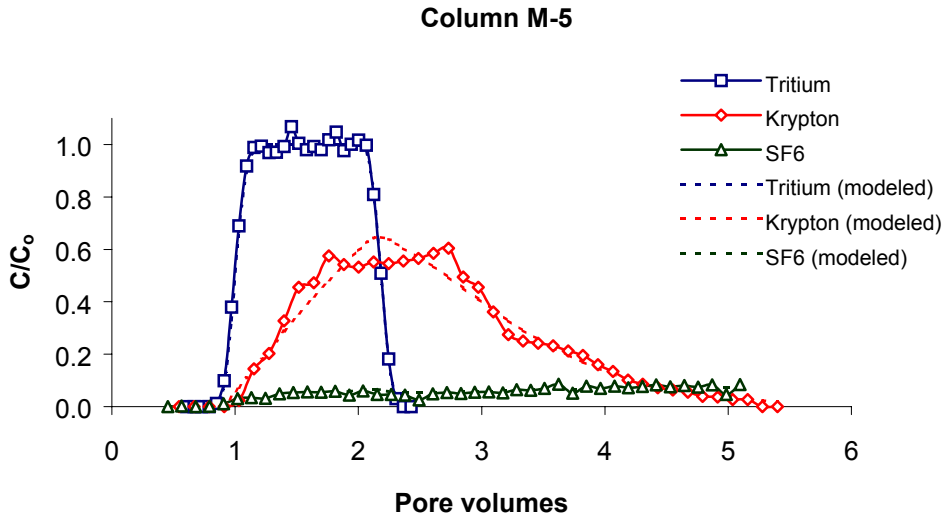

Pre-exp θ_g/θ_{aq} 0.054

Post-exp θ_g/θ_{aq} not measured

Physical Parameters of the Column

Q (mL/min)	v_{aq} (cm/sec)	P	δ (cm)[a]	L (cm)	ϕ
4	0.038	418.43	0.072	*30*	*0.37*

Estimated Tracer Parameters

Tracer	R	ω	α (sec^{-1})[b]	θ_g (cm^3/cm^3)[c]	θ_{aq} (cm^3/cm^3)	θ_g/θ_{aq}
^3H_2O	*1.00*	-	-	-	-	-
Kr	1.97	2.74	3.57E-03	0.0225	0.35	0.0647
SF_6	10.75	3.82	4.95E-04	0.0226	0.35	0.0650
			average	0.0225	0.35	0.0648

Figure 20. Experiment where ~ one pore volume of tracer was injected into the column at pore water velocity of 0.038 cm/sec. For explanation of parameters, see Fig. 16. $CV_{tritium} \approx 2.8$ %, $CV_{Kr} \approx 3.2$ %, and $CV_{SF6} \approx 5.2$ %.

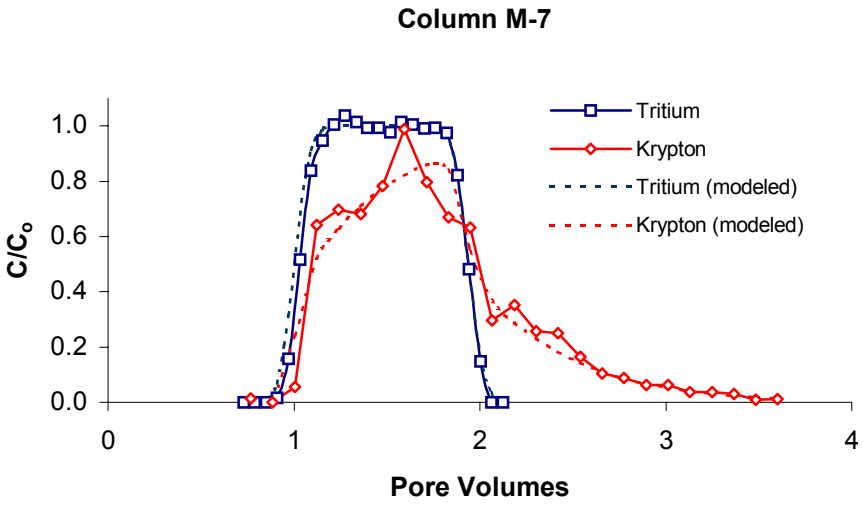

Pre-exp θ_g/θ_{aq} 0.011

Post-exp θ_g/θ_{aq} not measured

Physical Parameters of the Column

Q (mL/min)	v_{aq} (cm/sec)	P	δ (cm)[a]	L (cm)	ϕ
4	0.035	496.15	0.060	*30*	*0.38*

Estimated Tracer Parameters

Tracer	R	ω	α (sec^{-1})[b]	θ_g (cm^3/cm^3)[c]	θ_{aq} (cm^3/cm^3)	θ_g/θ_{aq}
^3H_2O	*1.00*	-	-	-	-	-
Kr	1.28	0.88	3.70E-03	0.0070	0.37	0.0187
			average	0.0070	0.37	0.0187

Figure 21. Experiment where ~ one pore volume of tracer was injected into the column at a pore water velocity of 0.035 cm/sec. For explanation of parameters, see Fig. 16. $CV_{tritium} \approx 2.3$ %, $CV_{Kr} \approx 13.5$ %, and $CV_{SF6} \approx 5.2$ %.

After this point, C/C_o dropped sharply because the ~ 5 pore volumes of tracer solution eluted from the column. Nevertheless, SF_6-enriched water continued to elute for the remainder of the experiment.

In experiments SI-4 and SI-5 (Figs. 23 and 24), dissolved Kr and SF_6 were used as tracers for column experiments having an initial θ_g/θ_{aq} ratio of 0.039 and 0.081, respectively (final ratios were 0.063 and 0.088). Flow rate was held constant at 4 mL/min for both experiments. In experiment SI-4, where ~ six pore volumes of tracer solution was injected, both dissolved gas tracers first appeared at one pore volume. The relative concentration of Kr (C/C_o) increased for ~ four pore volumes reaching a maximum C/C_o ≈ 0.9 at six pore volumes followed by a steep decline until approximately eight pore volumes and a slower decrease thereafter. The relative concentration of SF_6 (C/C_o) increased at a fairly steady rate for the duration of the experiment reaching a maximum value of ≈ 0.3. Because only a small fraction of the injected mass of SF_6 was recovered even after 10 pore volumes, presumably SF_6 would have continued to elute for some time had the duration of the experiment been extended.

Experiment SI-5 yielded similar results, but in this case ~ 7.5 pore volumes of tracer were injected into the column. As in experiment SI-4, the dissolved gas tracers appeared at ~ one pore volume. The relative concentration of Kr (C/C_o) increased at a steady rate until ~ 4.5 pore volumes (C/C_o ≈ 0.8), and then more slowly thereafter to a C/C_o of ~ 0.98. At ~ eight pore volumes, C/C_o began to decrease at a steady rate until ~ 10 pore volumes, at which time the rate of decrease began to slow. Krypton elution was complete at ~12 pore volumes. The relative concentration of SF_6 increased above a background value at 1 pore volume and increased at a steady rate for the duration of the experiment to a maximum value of ≈ 0.4.

INTERMEDIATE PULSE SIZE TRACER EXPERIMENTS

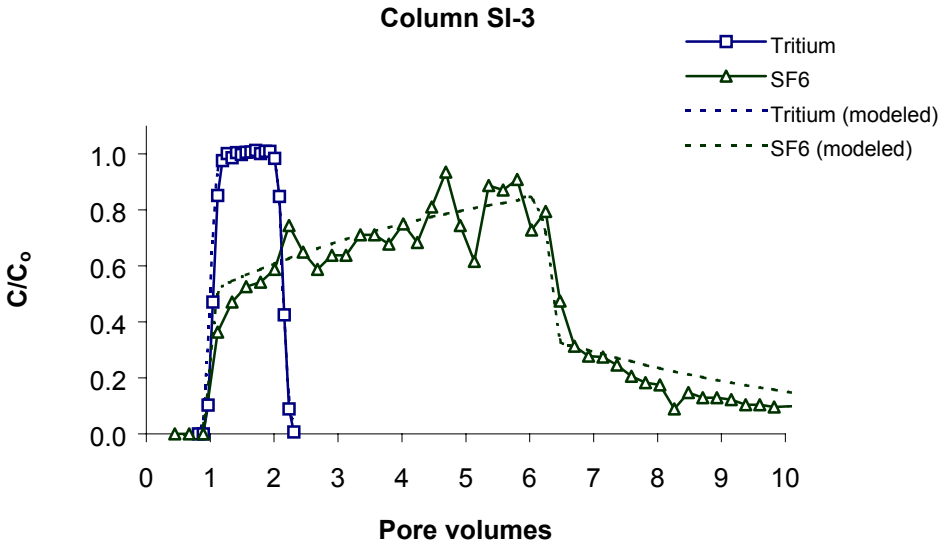

Pre-exp θ_g/θ_{aq} 0.018
Post-exp θ_g/θ_{aq} 0.041

Physical Parameters of the Column

Q (mL/min)	v_{aq} (cm/sec)	P	δ (cm)[a]	L (cm)	ϕ
4	0.037	385.22	0.078	*30*	*0.36*

Estimated Tracer Parameters

Tracer	R	ω	α (sec^{-1})[b]	θ_g (cm^3/cm^3)[c]	θ_{aq} (cm^3/cm^3)	θ_g/θ_{aq}
^3H_2O	*1.00*	-	-	-	-	-
Kr	1.75	0.51	8.29E-04	0.0171	0.34	0.0500
SF_6	3.14	0.67	3.81E-04	0.0051	0.35	0.0143
			average	0.0111	0.35	0.0321

Figure 22. Experiment where ~ six pore volumes of tracer were injected into the column at a pore water velocity of 0.037 cm/sec. For explanation of parameters, see Fig. 16. $CV_{tritium} \approx 7.4$ %, $CV_{Kr} \approx 2.5$ %, and $CV_{SF6} \approx 11.3$ %.

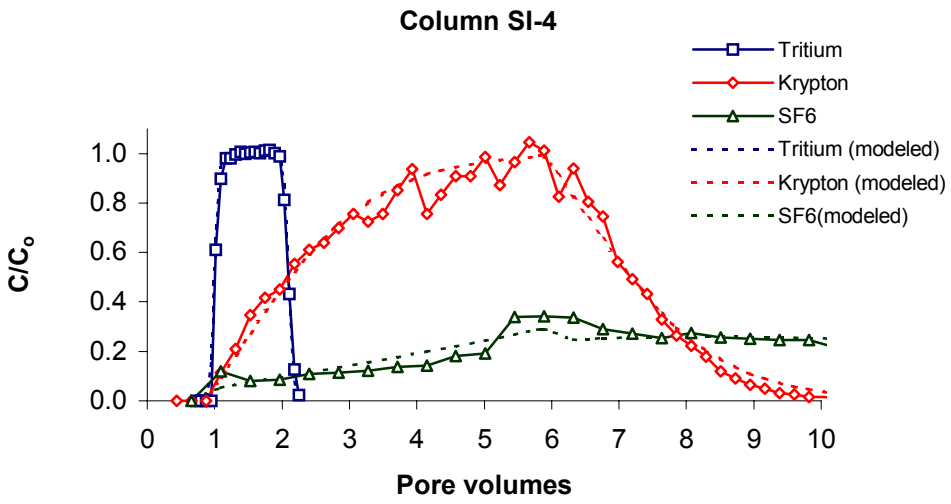

Pre-exp θ_g/θ_{aq}	0.039
Post-exp θ_g/θ_{aq}	0.063

Physical Parameters of the Column

Q (mL/min)	v_{aq} (cm/sec)	P	δ (cm)[a]	L (cm)	ϕ
4	0.037	692.87	0.043	*30*	*0.36*

Estimated Tracer Parameters

Tracer	R	ω	α (sec^{-1})[b]	θ_g (cm^3/cm^3)[c]	θ_{aq} (cm^3/cm^3)	θ_g/θ_{aq}
^3H_2O	*1.00*	-	-	-	-	-
Kr	2.40	2.73	2.38E-03	0.0307	0.33	0.0933
SF_6	12.06	2.98	3.28E-04	0.0247	0.34	0.0737
			average	0.0277	0.33	0.0835

Figure 23. Experiment where ~ six pore volumes of tracer were injected into the column at a pore water velocity of 0.037 cm/sec. For explanation of parameters, see Fig. 16. $CV_{tritium} \approx 9.1$ %, $CV_{Kr} \approx 7.8$ %, and $CV_{SF6} \approx 6.8$ %.

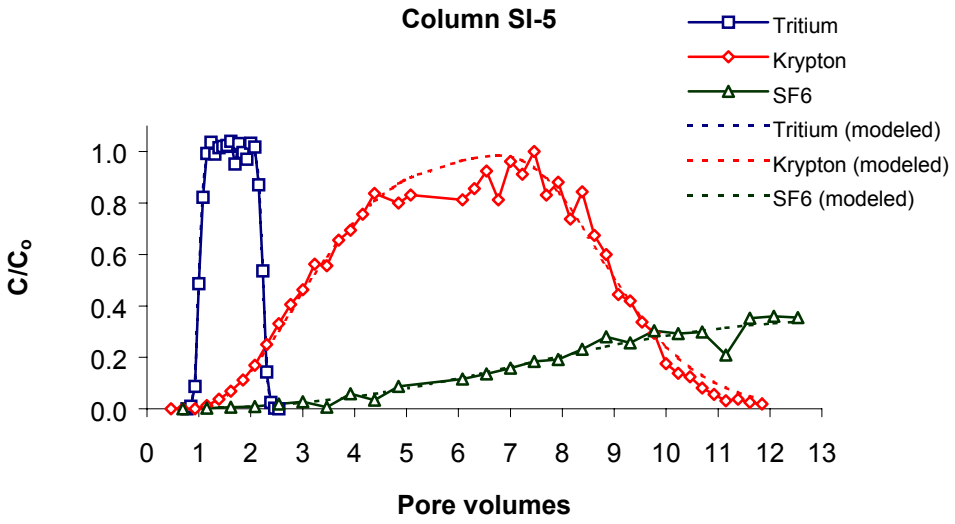

Pre-exp θ_g/θ_{aq}	0.081
Post-exp θ_g/θ_{aq}	0.088

Physical Parameters of the Column

Q (mL/min)	v_{aq} (cm/sec)	P	δ (cm)[a]	L (cm)	ϕ
4	0.036	396.62	0.076	*30*	*0.37*

Estimated Tracer Parameters

Tracer	R	ω	α (sec^{-1})[b]	θ_g (cm^3/cm^3)[c]	θ_{aq} (cm^3/cm^3)	θ_g/θ_{aq}
^3H_2O	*1.00*	-	-	-	-	-
Kr	3.32	6.61	3.38E-03	0.0496	0.32	0.1547
SF_6	13.71	6.74	6.29E-04	0.0289	0.34	0.0847
			average	0.0392	0.33	0.1197

Figure 24. Experiment where ~ six pore volumes of tracer were injected into the column at a pore water velocity of 0.36 cm/sec. For explanation of parameters, see Fig. 16. $CV_{tritium} \approx 2.8$ %, $CV_{Kr} \approx 4.6$ %, and $CV_{SF6} \approx 6.0$ %.

3.3. *RESULTS OF LARGE PULSE EXPERIMENTS*

Trends in the shapes of the tracer breakthrough curves became more distinct when the length of the tracer pulse was increased (M-series vs. SI-series). However, in the SI series of column experiments, it was observed that the relative concentration of SF_6 was still not sufficient to produce well defined breakthrough curves in the presence of unsaturated pore space. It was thought that longer pulse injections would better define the breakthrough curves for SF_6. Therefore, four additional experiments (Figs. 25-28) were conducted where the size of the pulse was increased to ~ 20 pore volumes and average pore water velocities were varied from ~0.009 to ~0.15 cm/sec. In these experiments, the dissolved gas tracer solution included Kr, SF_6, and tritiated water. As in the previous experiments, the transport of tritiated water followed "piston flow" conditions and the appearance of gas tracers in effluent occurred simultaneously with tritiated water.

The 20 PV Column (Fig. 25) and High V_x Column (Fig. 26) experiments yielded similar results despite differences in average linear velocities (v_x) of 0.073 and 0.152 cm/sec and initial θ_g/θ_{aq} ratios of ~ 0.026 and 0.022, respectively. The High V_x Column experiment was conducted using a smaller diameter column (1 cm ID) than all other experiments (2.5 cm ID). This small diameter column was chosen so that the effect of a significantly higher average linear velocity could be examined. In both experiments, the SF_6 breakthrough curves were more asymmetric than the Kr breakthrough curves. In the 20 PV Column experiment, Kr reached a relative concentration (C/C_o) ≈ 1 within ~ four pore volumes. Krypton remained at this concentration until ~ twenty pore volumes passed through the column. The relative concentration of Kr decreased at a linear rate thereafter and tailed for several pore volumes until it fell below the detection limit at ~ twenty-five pore volumes. The relative concentration of SF_6 (C/C_o) increased at a rate nearly identical to Kr and tritiated water for the first pore volume to ($C/C_o \approx 0.4$), after which it slowed drastically but continued to increase to 0.9 by the time ~ twenty pore volumes eluted. The relative concentration of SF_6 fell quickly after this point to $C/C_o \approx$

0.6 over < 1 pore volume and then continued to decrease at a slower rate for the remainder of the experiment. SF_6 concentration reached a C/C_o of ≈ 0.15 after ~30 pore volumes.

In the High V_x Column experiment, Kr again reached a relative concentration of C/C_o ≈ 1 within ~ four pore volumes and remained at this concentration for an additional 18 pore volumes. Kr concentration decreased at a linear rate for ~ 3 pore volumes thereafter and tailed for ~five additional pore volumes until a C/C_o of ≈ 0 was reached. The relative concentration of SF_6 increased at a linear rate to a C/C_o ≈ 0.5 within ~ one pore volume. After this C/C_o increased to a value of ≈ 0.9 at a much slower rate until ~ 18 pore volumes, at which time C/C_o dropped to ≈ 0.4 within ~ two pore volumes; the relative concentration of SF_6 decreased more slowly thereafter at a linear rate until C/C_o ≈ 0.2 when the experiment was terminated (at ~ 28 pore volumes).

The final two experiments, LT1 (Fig. 27) and LT2 (Fig. 28), where ≈ 25 pore volumes of tracer solution was injected, yielded similar results yet were conducted with different average linear velocities (v_x) of 0.009 and 0.020 cm/sec and initial unsaturated volumes of θ_g/θ_{aq} of ~ 0.010 and 0.022, respectively. These results were also similar to the 20 PV Column and High V_x Column experiments, however there were also some significant differences. As in the 20 PV Column and High V_x Column experiments, SF_6 breakthrough curves were more asymmetric than Kr breakthrough curves. In the LT1 experiment, Kr reached a relative concentration of C/C_o ≈ 1 within ~ two pore volumes. Krypton remained at or near this concentration until ~ 25 pore volumes passed through the column. The relative concentration of Kr decreased linearly for ~ 2 pore volumes thereafter and tailed for an additional ~1.5 pore volumes until it fell below the detection limit at ~ 27 pore volumes. The relative concentration of SF_6 increased at rate nearly identical to Kr and tritiated water for the first ~ 1.5 pore volumes (C/C_o ≈ 0.3), after which it slowed but continued to rise until ~ 25 pore volumes eluted. The relative concentration fell after this point from ≈ 0.8 to ≈ 0.5 for the remainder of the experiment

(terminated at ~ 33 pore volumes). In experiment LT2, Kr again reached a relative concentration of ≈ 1 within ~ two pore volumes and remained at this concentration for ~ 22 pore volumes. Krypton concentration decreased quickly thereafter for ~ 2 pore volumes and tailed for an additional ~ 3 pore volumes until C/C_o reached baseline. The relative concentration of SF_6 increased at a linear rate to a C/C_o of ≈ 0.7 within ~ three pore volumes, and reached a C/C_o of ≈ 1.0 by five pore volumes after which it decreased slowly to 20 pore volumes before reaching a value of 1.0 near 25 pore volumes. After this point, the relative concentration dropped quickly to a $C/C_o \approx 0.5$ within ~ 2 pore volumes, and more slowly thereafter to a $C/C_o \approx 0.2$ when the experiment was terminated at ~ 28 pore volumes.

3.4. DISCUSSION OF COLUMN EXPERIMENTS

It is known that dissolved gas tracers behave conservatively in fully saturated media (Wilson and MacKay 1993; Fry et al. 1995; Sanford et al. 1996). In the M-series experiments, an attempt was made to replicate this conservative behavior. In experiments M-3 (Fig. 18) and less so in M-6 (Fig. 20) the dissolved gases essentially behaved conservatively. In experiment M-6 the gas tracers essentially eluted as plugs, however there is a slight unexplained phase shift for Kr. In other experiments, such as M-1 (Fig. 16) and M-2 (Fig. 17), the dissolved gases did not behave conservatively even though the columns were thought to be fully saturated. It was realized from these early experiments that maintaining full saturation of a column was a critical element to achieve conservative behavior for dissolved Kr and SF_6. In experiment M-5 (Fig. 19), a predetermined volume of unsaturated pore space was created to demonstrate the transport of dissolved gases in a two phase (gas-liquid) system. These results were similar to those of Fry et al. (1995), who showed that retardation could be described by eq. 7 (see pg. 12). The SI-series

LARGE PULSE SIZE EXPERIMENTS

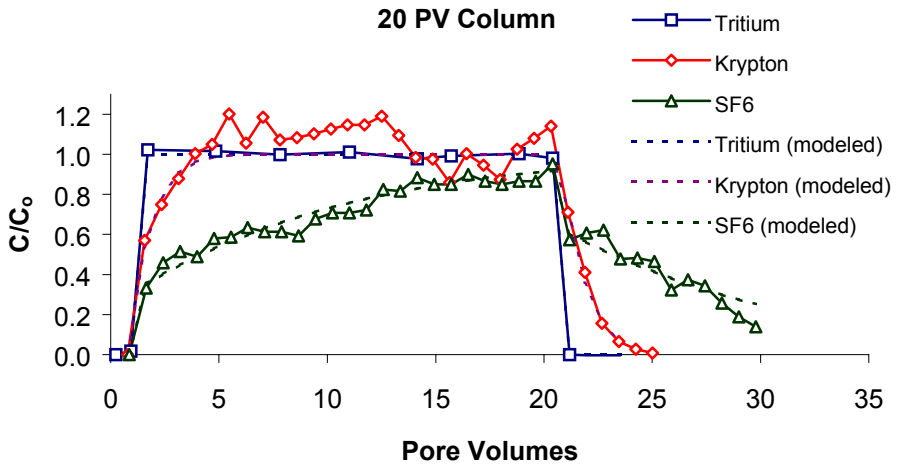

Pre-exp θ_g/θ_{aq}	0.026
Post-exp θ_g/θ_{aq}	0.049

Physical Parameters of the Column

Q (mL/min)	v_{aq} (cm/sec)	P	δ (cm)[a]	L (cm)	ϕ
8	0.073	2201.65	0.014	*30*	*0.36*

Estimated Tracer Parameters

Tracer	R	ω	α (sec^{-1})[b]	θ_g (cm^3/cm^3)[c]	θ_{aq} (cm^3/cm^3)	θ_g/θ_{aq}
^3H_2O	*1.00*	-	-	-	-	-
Kr	1.79	1.39	4.29E-03	0.0180	0.34	0.0527
SF_6	7.40	1.16	4.42E-04	0.0147	0.35	0.0427
			average	0.0164	0.34	0.0477

Figure 25. Experiment where ~ twenty pore volumes of tracer were injected into the column at a pore water velocity of 0.073 cm/sec. For explanation of parameters, see Fig. 17. $CV_{tritium}$ = 1.5 %, CV_{Kr} = 9.7 %, and CV_{SF6} = 2.0 %.

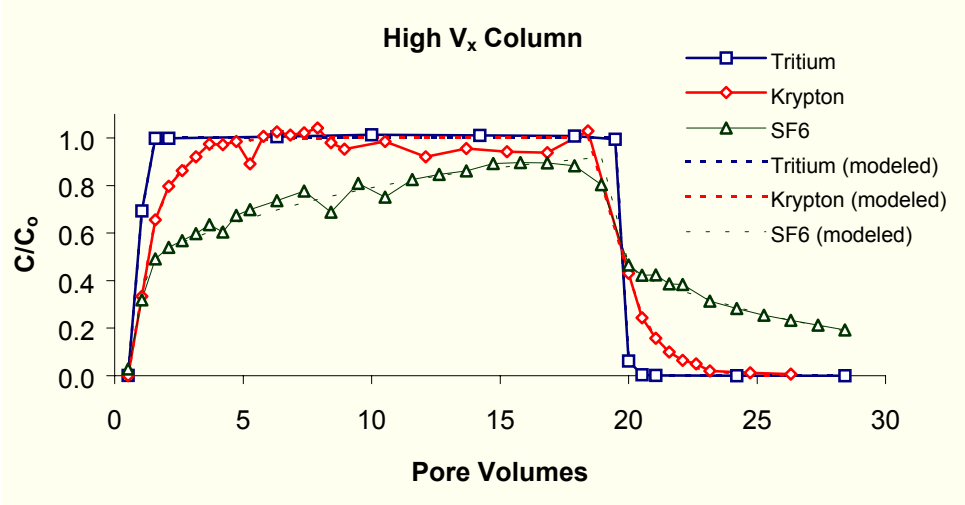

Pre-exp θ_g/θ_{aq}	0.022
Post-exp θ_g/θ_{aq}	not measured

Physical Parameters of the Column

Q (mL/min)	v_{aq} (cm/sec)	P	δ (cm)[a]	L (cm)	ϕ
2.5	0.152	205.73	0.146	*30*	*0.35*

Estimated Tracer Parameters

Tracer	R	ω	α (sec^{-1})[b]	θ_g (cm^3/cm^3)[c]	θ_{aq} (cm^3/cm^3)	θ_g/θ_{aq}
^3H_2O	*1.00*	-	-	-	-	-
Kr	1.61	0.84	6.96E-03	0.0137	0.34	0.0407
SF_6	5.98	0.72	7.31E-04	0.0112	0.34	0.0332
			average	0.0125	0.34	0.0369

Figure 26. Experiment where a small diameter column (1 cm ID) was used so that a relatively high pore water velocity of 0.152 cm/sec was obtained. Due to experimental difficulties, post experiment θ_g/θ_{aq} was not measured. For explanation of parameters, see Fig. 16. $CV_{tritium} \approx 0.3$ %, $CV_{Kr} \approx 4.2$ %, and $CV_{SF6} \approx 9.8$ %.

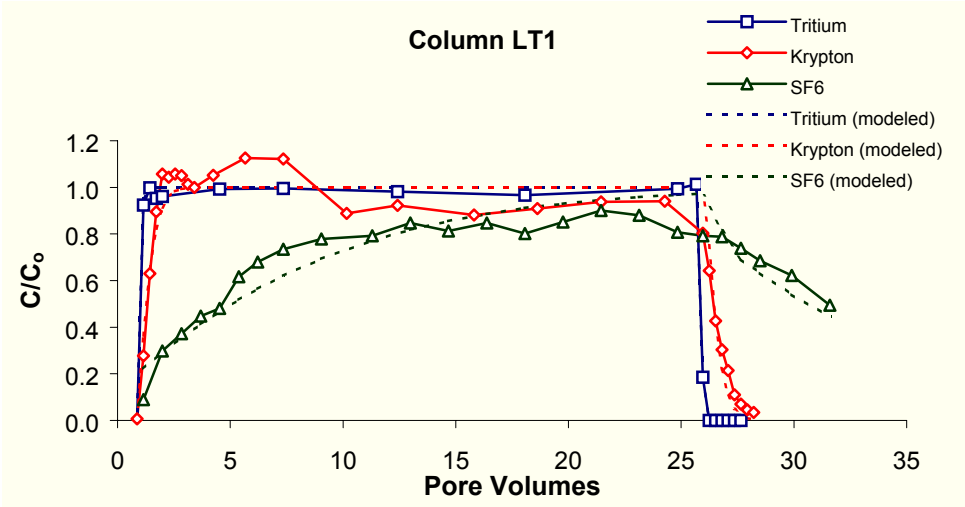

Pre-exp θ_g/θ_{aq}	0.010
Post-exp θ_g/θ_{aq}	0.031

Physical Parameters of the Column

Q (mL/min)	v_{aq} (cm/sec)	P	δ (cm)[a]	L (cm)	ϕ
1	0.009	285.1	0.105	*30*	*0.36*

Estimated Tracer Parameters

Tracer	R	ω	α (sec^{-1})[b]	θ_g (cm^3/cm^3)[c]	θ_{aq} (cm^3/cm^3)	θ_g/θ_{aq}
^3H_2O	*1.00*	-	-	-	-	-
Kr	1.37	1.77	1.46E-03	0.0087	0.35	0.0247
SF_6	7.32	1.53	7.37E-05	0.0146	0.35	0.0421
			average	0.0116	0.35	0.0334

Figure 27. Experiment where ~ twenty pore volumes of tracer were injected into the column at a relatively low pore water velocity of 0.009 cm/sec. For explanation of parameters, see Fig. 16. $CV_{tritium} \approx 1.5$ %, $CV_{Kr} \approx 3.2$ %, and $CV_{SF6} \approx 4.2$ %.

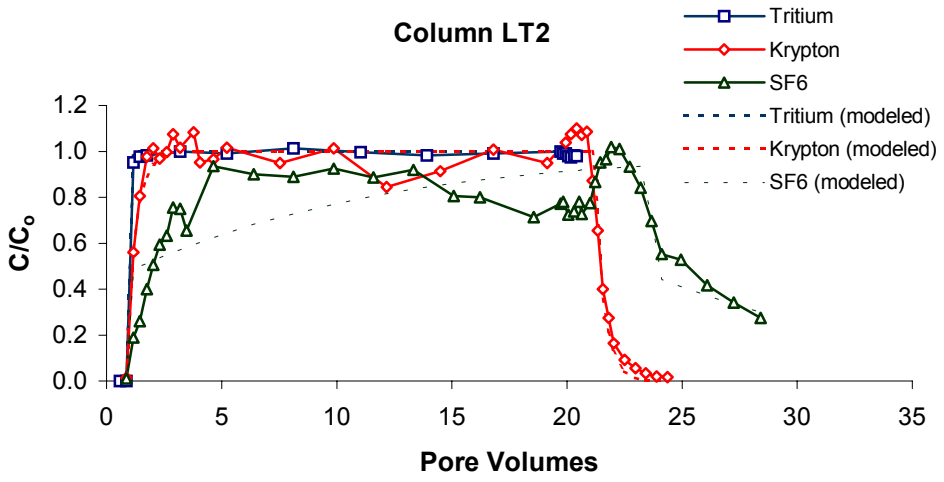

Pre-exp θ_g/θ_{aq} 0.022

Post-exp θ_g/θ_{aq} 0.035

Physical Parameters of the Column

Q (mL/min)	v_{aq} (cm/sec)	P	δ (cm)[a]	L (cm)	ϕ
2	0.020	389.88	0.077	*30*	*0.36*

Estimated Tracer Parameters

Tracer	R	ω	α (sec^{-1})[b]	θ_g (cm^3/cm^3)[c]	θ_{aq} (cm^3/cm^3)	θ_g/θ_{aq}
^3H_2O	*1.00*	-	-	-	-	-
Kr	1.25	0.85	2.22E-03	0.0059	0.35	0.0167
SF_6	6.50	0.74	8.77E-05	0.0127	0.35	0.0367
	.		average	0.0093	0.35	0.0267

Figure 28. Experiment where ~ twenty pore volumes of tracer were injected into the column at relatively low pore water velocity of 0.020 cm/sec. For explanation of parameters, see Fig. 16. $CV_{tritium}$ = 1.0 %, CV_{Kr} = 5.3 %, and CV_{SF6} = 15.7 %.

experiments were conducted to explore transport behavior using a larger pulse of tracer (~ five to six pore volumes instead of ~ one pore volume). This volume of tracer facilitated the modeling of transport behavior because the effects of partitioning could be observed over longer time intervals. It was noted in experiments SI-4 and SI-5 that dissolved SF_6 partitioned to gas-filled void space so strongly that only a small proportion of SF_6 was recovered in the effluent over the duration of an experiment. To improve the mass recovery of SF_6, the volume of tracer solution injected was increased to ~ twenty to twenty – five pore volumes (large pulse experiments). Increasing the mass of injected tracer improved the mass recovery of SF_6 to the extent that resolvable transport phenomena could be modeled.

CHAPTER 4
MODELING OF COLUMN EXPERIMENTS

4.1. DESCRIPTION

To better understand and quantify the transport behavior of dissolved Kr and SF_6 in the column experiments, the computer model CFITIM was used (van Genuchten 1981). Donaldson et al. (1996) used this model successfully on similar dissolved gas data. CFITIM is FORTRAN code that can be used to determine transport parameters for nonequilibrium column experiments. Specifically, a version of the convection-dispersion equation (CDE) which accounts for one-site, kinetic-nonequilibrium adsorption is solved:

$$R\frac{\partial C_l}{\partial t}+\frac{\rho}{\theta}\frac{\partial S}{\partial t}=D\frac{\partial^2 C_l}{\partial z^2}-V\frac{\partial C_l}{\partial z} \qquad [12]$$

where t = time, ρ = soil bulk density (length^3/mass), θ = porosity, R = retardation factor, S = adsorbed concentration (mass/volume), D = dispersion coefficient (length), C_l = longitudinal tracer concentration, V = the average linear flow velocity (length/time), and z = the length of transport. Based on the asymmetric nature of the breakthrough curves, a nonequilibrium model was needed to explain dissolved gas transport. Because it was assumed that dissolved gases were not interacting with the porous media, only one type of site (gas-filled void space) was responsible for the nonequilibrium behavior. This solution simplified to eq. 2 for a symmetrical breakthrough curve because the sorption term becomes insignificant as equilibrium behavior is approached. The only difference in the application of eq. 12 in this study versus the way it has classically been applied is that gas-liquid interactions are the root cause for partitioning rather than solid-liquid interactions. The input data for the model consists of some dimensionless parameters: P (Peclet number), T (dimensionless time or pore volumes), and ω (a fitting parameter),

. where $P = \frac{vL}{D}$, $T = \frac{vt}{L}$, and $R = 1 + \frac{\rho k}{\theta}$ for v = pore water velocity (length/time), D = dispersion coefficient (length), L=column length, ρ=soil bulk density (mass/volume), t = time, k = the distribution coefficient (volume/mass), and θ = porosity. However, retardation was redefined in this study as $R = 1 + K_H^{'} \frac{\theta_g}{\theta_{aq}}$ (Fry et al 1995). Because the Peclet number is strictly a physical parameter (where v and L are specified at the outset of an experiment), this variable can be accurately determined using the tritium breakthrough curve to solve for D in eq. 2 when R = 1. The Peclet number can then be utilized to model the dissolved gas behavior where R is unknown. The dimensionless fitting parameter (ω) is defined as $\omega = \frac{\alpha(R-1)L}{v}$, where α = mass transfer coefficient (time^{-1}). An initial estimate for the parameter (ω) is made and the value is recalculated by the model until the solution mimics the shape of the observed breakthrough curve. The value of α can be calculated for any experiment using the values derived as specified above; α is the inverse of the time needed for interphase partitioning to take place. The model also requires that either a constant concentration, [$c(0,t) = C_o$], or a constant flux $\left[\left(-D\frac{\partial c}{\partial x} + vc\right)_{x=0} = vC_o\right]$ boundary condition be used for the column inlet. The constant flux boundary condition was chosen for this study because the constant concentration boundary condition led to mass conservation errors at large values of (D/v). Further, the constant flux boundary condition is typically applied to laboratory column experiments (van Genuchten 1981). However, dispersion was very small relative to velocity in the column experiments and changing the boundary condition resulted in negligible differences for the modeled results. For the column outlet, a boundary condition of $\frac{\partial c}{\partial x}(\infty, t) = 0$ was applied. Strictly speaking, a packed soil column is not an infinite domain, but van Genuchten, (1981) found that this boundary condition provided model solutions that did not vary significantly over a range of column diameters or lengths.

4.2. SUMMARY

In summary, the CFITIM model was used to quantify experimental results by fitting a mathematically derived curve to the data. The model was used first to obtain a value for *D*. This was accomplished by modeling tritium data where it was assumed that $R = 1$, for any given value of *T* (pore volumes injected). The Peclet number (*P*) was estimated and refined by iterative solution. Values for *P* and *D* were used for all subsequent tracer experiments using a particular column setup because they are based entirely on the physical attributes of the packed medium. The data for dissolved gases can then be modeled for unknown values of *R*. With *R* determined, θ_g/θ_{aq} can be solved for theoretically from eq. 7. The mass transfer coefficient (α) for a particular non-conservative tracer was determined from the appropriate value for the fitting parameter (ω) which was taken from the model solution, where $\alpha = (\omega)(v)/(R\text{-}1)(L)$.

In all cases the modeled curves provided close matches to the empirical data (Figs. 16 – 28). For the dissolved gas tracer experiments conducted at near complete saturation and for all tritium curves, the modeled curves exhibited the same symmetric shape as the empirical curves. In the intermediate and large pulse size experiments, the dissolved gas tracer modeled curves exhibited the same asymmetric shapes. Unlike the empirical curves, the modeled curves do not show the noise caused by variation due to measurement techniques.

4.3. DETERMINATION OF (θ_g/θ_{aq})

A complication in modeling efforts was acknowledged when it was noted from empirical measurements that (θ_g/θ_{aq}) increased during experiments where unsaturated pore space was created, i.e. most columns contained slightly less water at the end of an experiment than at the beginning. This observation was also noted by Donaldson et al. (1996). Beginning with the SI-series experiments, pre-experiment and post-experiment measurements of *(θ_g/θ_{aq})* were made to better understand this process.

Pre-experiment and post-experiment empirical values for θ_g/θ_{aq} are plotted against the CFITIM derived value of R in Fig. 29 (experiments SI-3, SI-4, SI-5, LT1, LT2, and 20 PV). Values for R are overestimated using the pre-experiment empirical values for θ_g/θ_{aq} compared with modeled R values for both SF_6 and Kr, and deviations are greatest for SF_6, especially at low values of θ_g/θ_{aq}. Using the post-experiment values for θ_g/θ_{aq} provided a much closer fit between empirically derived values of R and those predicted using the CFITIM model.

Post-experiment retardation factors (R) calculated from values of θ_g/θ_{aq} are still not an exact match to modeled R values but they are much closer than pre-experiment values. Differences in the relationship between R and θ_g/θ_{aq} for SF_6 and Kr were strongly dependent on $K_H^{'}$ for these two gases. Fry et al. (1995) also underestimated R using pre-experiment values for θ_g/θ_{aq} to predict the retardation of dissolved oxygen. It is hypothesized that a post-experiment estimate would have provided a closer estimate in their case as well. It is also possible that the initial value for θ_g/θ_{aq} increases when tracer enriched water first comes in contact with trapped gas pockets, but it soon stabilizes.

Donaldson et al. (1996) hypothesized that dissolved gases partitioned into trapped gas pockets and expanded the volume of unsaturated pore space in a column during an experiment. They assumed that the partitioning of tracer gas to air-filled void space (based on dissolved gas concentration and $K_H^{'}$) required the volume of gas-filled voids to increase as equilibrium was approached if the gas pressure of the bubbles remained constant. However, when a column is purged with tracer free solution, tracer gases should partition back into solution and the volume of unsaturated pore space should return to its original value. Donaldson et al. (1996) recovered the entire mass of tracer by the end of an experiment and this is inconsistent with their model. In the 20 PV Column experiment of this study, almost all of the Kr and SF_6 were recovered in the effluent, however, θ_g/θ_{aq} still increased significantly over the course of the experiment (0.026 to 0.049). These

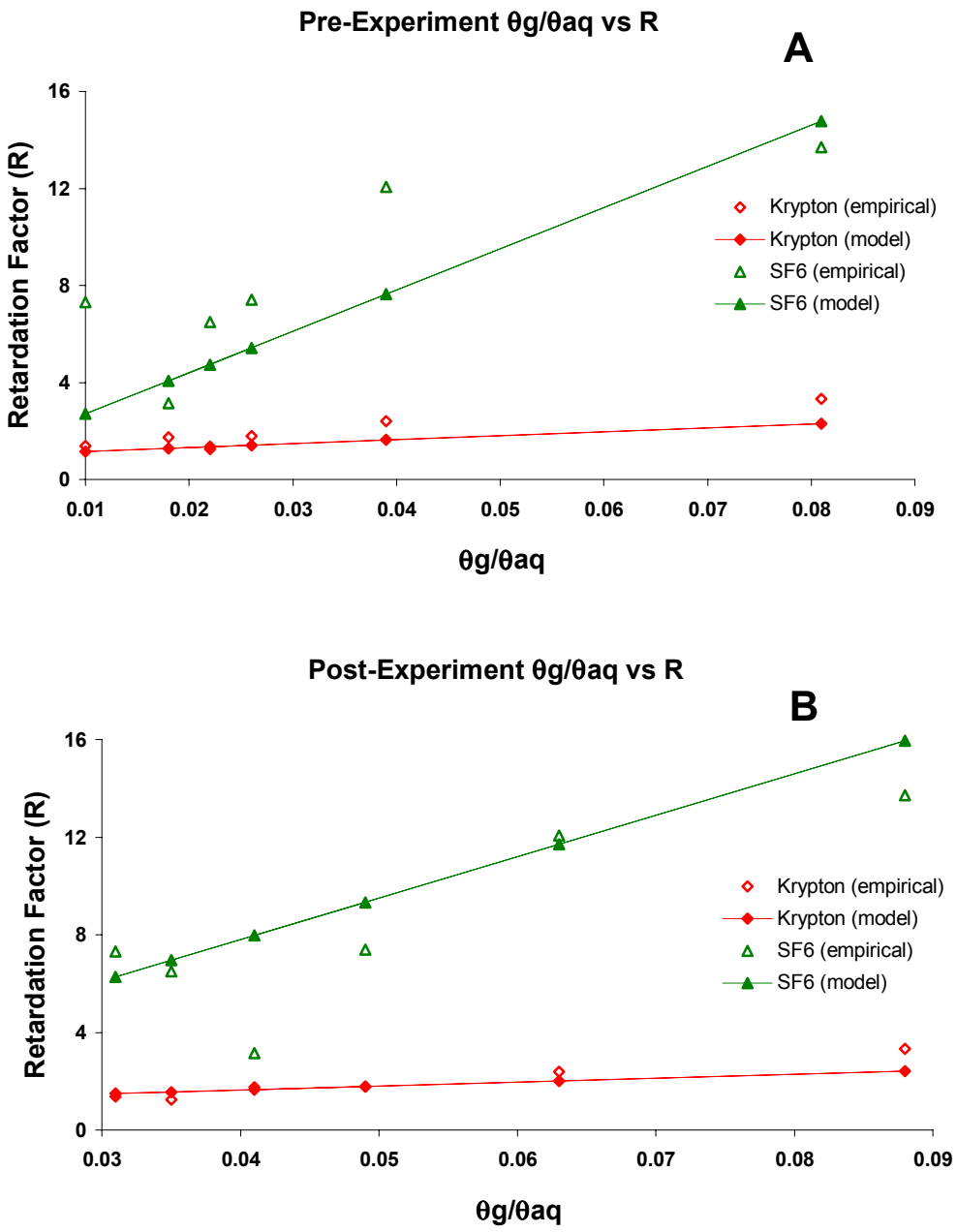

Figure 29. a) Values for R and θ_g/θ_{aq} calculated using pre-experiment data compared to CFITIM model results. b) Values for R and θ_g/θ_{aq} calculated using post-experiment data.

observations suggest another process was responsible for the growth of gas-filled void space over time.

A possible explanation is that as the tracer gas dissolved back into solution, it was replaced by dissolved air present in the tracer free water. In the process of creating a tracer solution, it is probable that much of the dissolved air is stripped from solution as the tracer is bubbled through the solution. This would result in partitioning effects that do not include the two most common dissolved gases in water, nitrogen and oxygen. When tracer was circulated through the column, N_2 and O_2 would preferentially partition into solution while Kr and SF_6 would move into the air-filled void space. When tracer free water in equilibrium with air, was circulated through the column after the tracer it became a source of N_2 and O_2 for the gas-filled void space while Kr and SF_6 moved into solution. Dissolution and exsolution rates probably differed for tracer and air resulting in the net growth of gas-filled void space during an experiment.

4.4. MASS TRANSFER COEFFICIENT (α)

A relationship between mass transfer coefficient (α), a first order rate coefficient, and pore water velocity was observed in column experiments where tracer solution was continuously injected for multiple pore volumes (Fig. 30; SI-series and large pulse size columns). The slope of the relationship between pore water velocity (v_x) and α was one order of magnitude greater for Kr (0.04) than SF_6 (0.004). The Pearson correlation coefficient (R^2) was significant for Kr (~0.96) but not for SF_6 (~0.61) at $\alpha = 0.05$ for n= 6. Barry and Li (1994) presented a simple model to conceptualize mass transfer in a two-phase system (Fig. 31). In this model, the time needed for transport by simple advection (t_a) was compared to the time required for reactive transport (t_r). Under equilibrium conditions where there is no reaction with the media, t_a and t_r will be the same. If the advective time scale is less than t_r (which is true in the data presented here), then the likelihood that the system will attain equilibrium decreases accordingly. In Table 5, data

are presented that demonstrate that for Kr $t_r < t_a$ so the gaseous and fluid phases were capable of attaining equilibrium, while for SF_6 $t_r > t_a$ and the phases could not reach equilibrium.

One important influence that was neglected is the shape, size, and distribution of the unsaturated pore space. The experimental design used in these experiments did not allow for control of the shape or size of the unsaturated pore space. Presumably, unsaturated pore space with a high surface area to volume ratio would facilitate mass transfer compared to pore space with low surface area to volume ratio. Further, the distribution of pore space in the columns was not controlled with the experimental design used. If flow paths do not intersect unsaturated pore space, partitioning cannot occur. According to a model presented by Schwartzenbach et al. (1993), the aqueous diffusion coefficient of a gas plays an important role in mass transfer. A gas of relatively greater mass such as SF_6 needs more time to diffuse across the air-water interface than Kr. The results of this research support the hypothesis that the kinetics of mass transport of in a two-phase system (liquid and gas) limits the utility of SF_6 as an effective groundwater tracer.

Table 5. Data showing that dissolved Kr equilibrated with trapped gas pockets while SF_6 did not over the range of pore water residence times observed.

			Krypton		SF_6	
Column	Pore Volume (mL)	t_a (min)	t_r (min)	Krypton t_r/t_a*	t_r (min)	SF_6 t_r/t_a*
20PV	49.98	6.25	3.89	0.62	37.73	6.04
High V_x	8.24	3.30	2.40	0.73	22.81	6.92
LT1	51.54	51.54	11.44	0.22	226.01	4.39
LT2	51.07	25.54	7.52	0.29	189.96	7.44
SI4	49.76	12.44	7.01	0.56	50.77	4.08
SI5	50.08	12.52	4.93	0.39	26.51	2.12

* -If <1 equilibrium conditions are possible

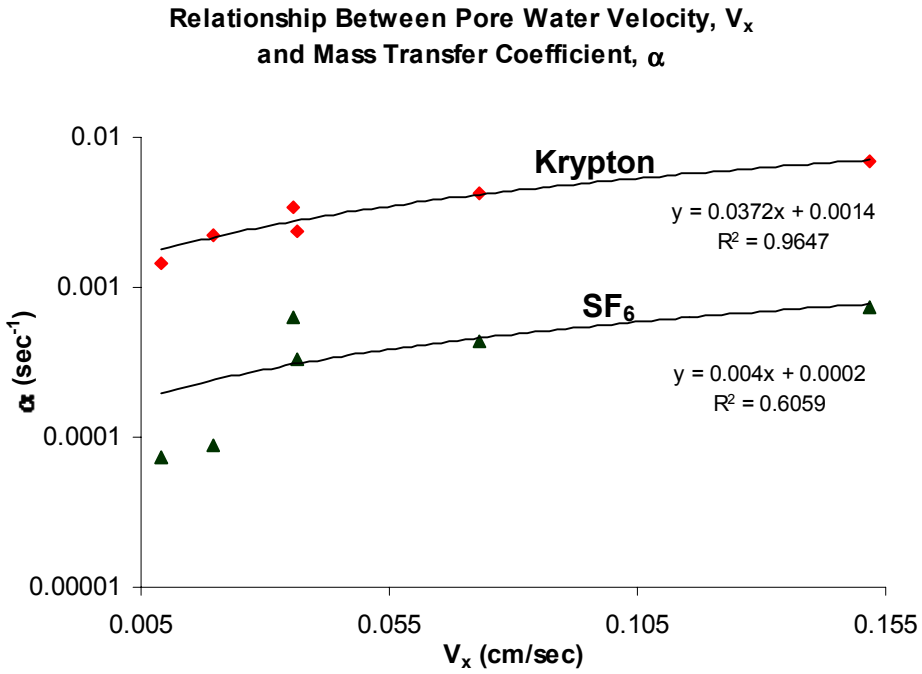

Figure 30. Plot showing the positive correlation between pore water velocity and mass transfer coefficient. The slope for krypton is almost one order of magnitude greater than for SF_6.

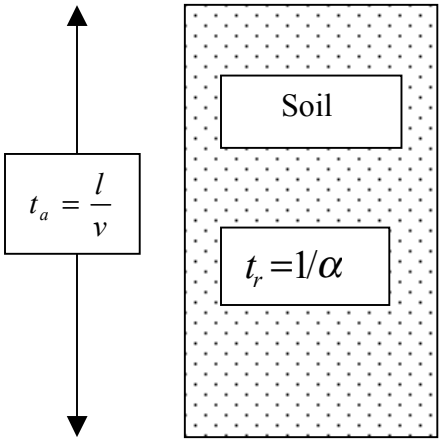

Figure 31. Model presented by Barry and Li (1994) to show the relationship between pore volume residence time and a first order mass transfer coefficient, α. Where t_a = advection time scale (sec), l = column length (cm), v = pore water velocity (cm/sec), t_r = reaction time (sec) scale, and α = mass transfer coefficient (sec).

CHAPTER 5
FIELD EXPERIMENTS

5.1. *SMALL VOLUME PUSH-PULL EXPERIMENTS*

Results

Six small-scale push-pull tracer tests were conducted in three different wells at the Four Mile Creek well site (Figs. 32-37; Tables G1-G6 in APPENDIX G). In each experiment, ~5 L of tracer was injected and except for the 01/06/00 experiment, all flow rates were ~ 0.9 L/minute. The distance the tracers traveled in the aquifer (~ 4.0 to 7.3 cm assuming radial flow and homogeneous media) and the calculated average pore water velocities varied (~ 3 x 10^{-2} to ~ 8 x 10^{-2} cm/sec) because the screened intervals were not all the same lengths for each experiment (30 cm for Well 274 and 90 cm for Wells 335 and 356). The pump was reversed after injection and water was withdrawn at the same flow rate. Most of the mass of injected tracer was recovered in the first 10 minutes of an experiment and in all cases, the tracer concentration returned to nearly background in a relatively short length of time (< ~ 30 min.). However, with the exception of the 04/03/00 experiment, dissolved gas tracer concentrations remained slightly above background with continued pumping for up to 2 hrs. The data are plotted as measured values starting at the point in time when the pump was reversed and water was withdrawn from the well (t = 0). Data were also plotted as log transformed values to accentuate the differences in effluent tracer recovery.

In the first two experiments (01/06/00 and 02/16/00; Figs. 32 and 33), the tracers included ^{3}H, ± Kr, SF_6, and Br^- (10,000 ppm). In these experiments, the tracer solution was injected into the lowest (green) screened interval of Well 274, at ~0.57 L/min and 0.92 L/min respectively, and then immediately withdrawn at the same rate. The middle

(yellow) screened interval was sampled intermittently or continuously to detect for the presence of tracer in the overlying water table. In the 01/06/00 experiment, the middle (yellow) screened interval was pumped long enough only to collect a 40 mL water sample while in the 02/16/00 experiment, the middle (yellow) interval was pumped continuously at a low flow rate of ~0.09 L/min. In both cases, the gas tracers were detected in the middle (yellow) screened interval while Br^- and tritium were not. In both experiments, the tailing of the gas tracers was less severe than tritium and bromide. This more rapid decline is clearer when the log-transformed data are plotted. In the 01/06/00 experiment (Fig. 32), SF_6 concentrations drop at a faster rate than tritium and bromide; Kr repeats this behavior in the 02/16/00 experiment (Fig. 33).

To determine the cause of the upward movement of the gas tracers, a third experiment was conducted on 02/26/00 (Fig. 34). In this experiment, Br^- was not included as a component of the tracer, only Kr and SF_6 were mixed with tritiated water. All other experimental parameters were identical to the 2/16/00 experiment. In this case, no upward movement of dissolved gas tracer was observed. However, while the behavior of Kr and tritium were similar, SF_6 was still detected after Kr and tritium returned to baseline levels. This behavior was duplicated in an experiment conducted on 04/03/00 (see Fig. 35), where only the lowest (green) screened interval of Well 274 was sampled.

Two additional ~5 L push-pull experiments were conducted on 03/20/00 and 03/23/00 (Figs. 35 and 36). The purpose of these two experiments was to determine if significant partitioning could be observed in a region of the water table aquifer that historically fluctuated between saturated and partially saturated conditions (or was thought to extend into the capillary fringe). The upper (red) screened intervals of Wells 335 and 356 were chosen for these experiments because portions of these intervals were observed above the water table in the past ~1.5 years (Dunn et al. 1998). It was thought that these intervals may contain trapped gas pockets and would be good locations to observe gas-liquid partitioning behavior. Both experiments were conducted with 5 L (no

Br^-) of tracer in a manner identical to that described for the previous experiments, except that injection and recovery were performed only through the upper (red) screened horizon. In both experiments, some chromatographic separation of gases occurred compared with the tritium spike where the gas concentrations approached baseline at a slower rate than tritium; this effect was observed for both Kr and SF_6 in well 335 (Fig. 36) and for SF_6 in well 356 (Fig. 37).

Discussion

In the field experiments conducted on 01/06/00 and 02/16/00 (Figs. 32 and 33), the concentration of dissolved gas tracers appeared to decrease at a faster rate than the conservative tracers in effluent collected from the lower (green) screened interval. Upon first analysis this is counterintuitive because if partitioning of dissolved gas tracers was taking place, then the decrease in concentration for the nonconservative tracers should be slower than the conservative tracers. However, the more rapid decrease in dissolved gas concentration than tritium and bromide can be attributed to a sink. Dissolved gas tracers appeared in the middle (yellow) screened interval, while the conservative tracers did not. This result led to the conclusion that the transport of dissolved gas tracer was complicated by ionic strength gradients created by dissolved KBr. This effect was further examined in laboratory column experiments (Chapter 6) and dissolved salts were not used in subsequent field experiments.

In the field tests conducted on 02/26/00, 03/20/00, and 03/23/00 (Figs. 34, 35 and 36), the dissolved gas tracers approached background concentration at a faster rate than tritium between 0- ~ 10 min and then more slowly (after ~ 10 min). In all three experiments, the degree of tailing was greater (≥ 10 min interval) for SF_6 than Kr. The areas under the tails were a small percentage of the total peak area, but this effect is indicative of partitioning to another phase. The rapid early decline in dissolved gas tracer concentration (0 – 10 min) is interpreted to be partitioning to another phase and the later

slower rate of decline is interpreted to be gas partitioning back into solution. If gas-liquid partitioning were the sole factor controlling the shape of these curves, then the effect should be enhanced for SF_6 compared to Kr because of the higher K'_H for this gas. However, SF_6 also has a higher octanol-water partition coefficient *(K_{ow})* than Kr (47.9 and 7.8). Previously, it has been shown that K_{ow} crudely correlates with organic matter partitioning (Schwartzenbach et al. 1993). Hence, the greater tailing of SF_6 may also be caused by partitioning onto organic matter (Schwartzenbach et al. 1993). Tailing was most pronounced in the 03/20/00 and 03/23/00 experiments (Figs. 36, 37) where tracer was injected in the upper (red) screened intervals of the wells. These intervals may contain media that are highly reactive (trapped air or organic matter) compared with aquifer materials lower in the section. Based on the laboratory column experiments, if the phase that caused the partitioning of the dissolved gases was air, then the percentage of gas-filled void space was small (< 1%). The dissolved gases (particularly SF_6) would have largely been lost if even a few percent of the pore space was trapped gas. The fact that the capillary fringe of the water table may extend at least several feet above the measured water level may prevent the aquifer sediments from becoming completely unsaturated even when the water level is below the screen.

The slight tailing of SF_6 relative to tritium in the 2/26/00 experiment (Fig. 34) was an unexpected result because the interval in which the tracer was injected [lowest (green) screened interval] was located at a depth (~ 7.5'-8.5' below surface) below any historical seasonal groundwater fluctuations; further, organic rich layers were not observed in lithologic logs. In the 04/03/00 experiment conducted on the same screened interval (Fig. 35), SF_6 behaved virtually the same of tritium. One possible explanation for this is that the 2/26/00 experiment took place only ten days after a tracer experiment that used Br^-. It is possible that residual Br^- complicated the interpretations of the 2/26/00 experiment.

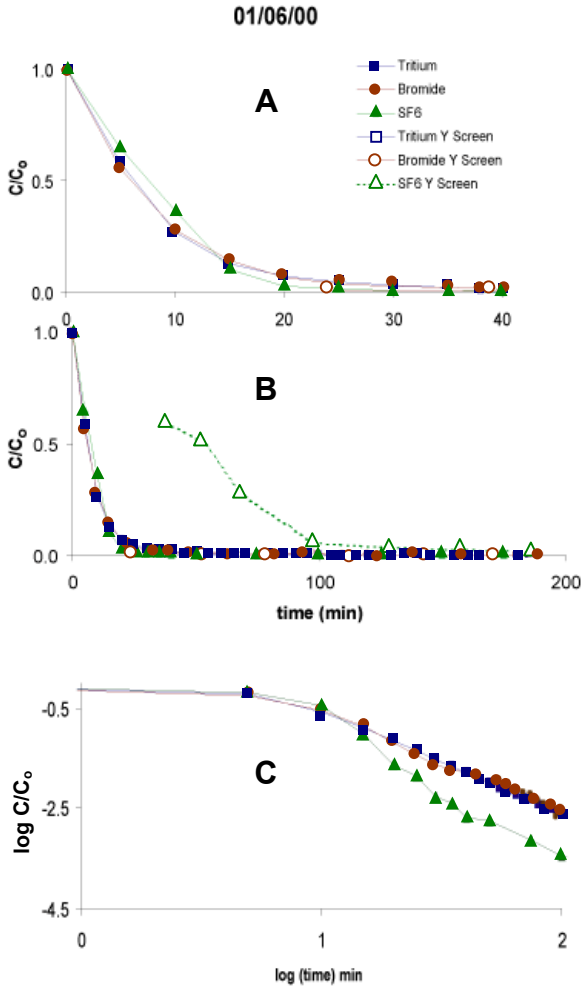

01/06/00 "Push-Pull" Experiment

Well:	274 G
Vol. Injected:	5L
Q:	9.50cm^3/sec
n:	*0.40*
b:	30cm
r:	2.54cm
v*:	4.96E-02cm/sec
L:	7.28cm

where: Q = pump rate, n = porosity (arbitrary value),
b = screen thickness, r = well radius,
v = pore water velocity*, and L = max tracer distance

*-calculated from the equation: $v = \frac{Q}{2\pi b\theta r}$
(Haggerty et al. 1998)
Assuming radial flow (all exps.)

Figure 32. a) Push-pull experiment where tracer solution (containing ^3H, SF_6, and Br^-) was injected into the lower (green) interval and immediately withdrawn. b) The overlying screened interval (yellow) was intermittently sampled for tracer (lower interval data are plotted for comparison). c) log transformed data for lower (green) interval. No data available to compute CVs.

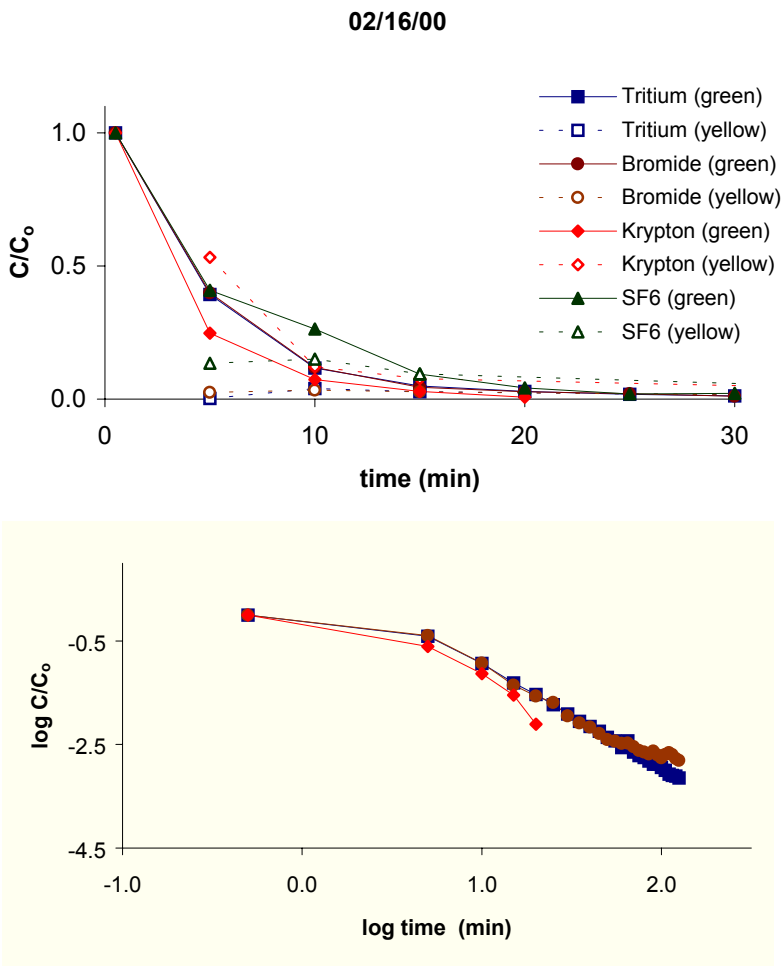

02/16/00 "Push-Pull" Experiment

Well:	274 G
Vol. Injected:	5L
Q:	15.33cm^3/sec
n:	*0.40*
b:	30cm
r:	2.54cm
v*:	8.01E-02cm/sec
L:	7.28cm

where: Q = pump rate, n = porosity (arbitrary value),
b = screen thickness, r = well radius,
v = pore water velocity*, and L = max tracer distance

*-calculated from the equation: $v = \frac{Q}{2\pi b\theta r}$
(Haggerty et al. 1998)

Figure 33. Push-pull experiment where tracer solution (containing ^{3}H, Kr, SF_6, and Br^-) was injected into the lower (green) interval and immediately withdrawn. The overlying screened interval (yellow) was continuously sampled for tracer concentrations, but at ~ 10% the flow rate of the lower (green) level so that only minimal upward flow was induced. $CV_{tritium} \approx 16.2$ %, $CV_{bromide} \approx 1.7$ %, $CV_{Kr} \approx 7.0$ %, and $CV_{SF6} \approx 8.2$ %.

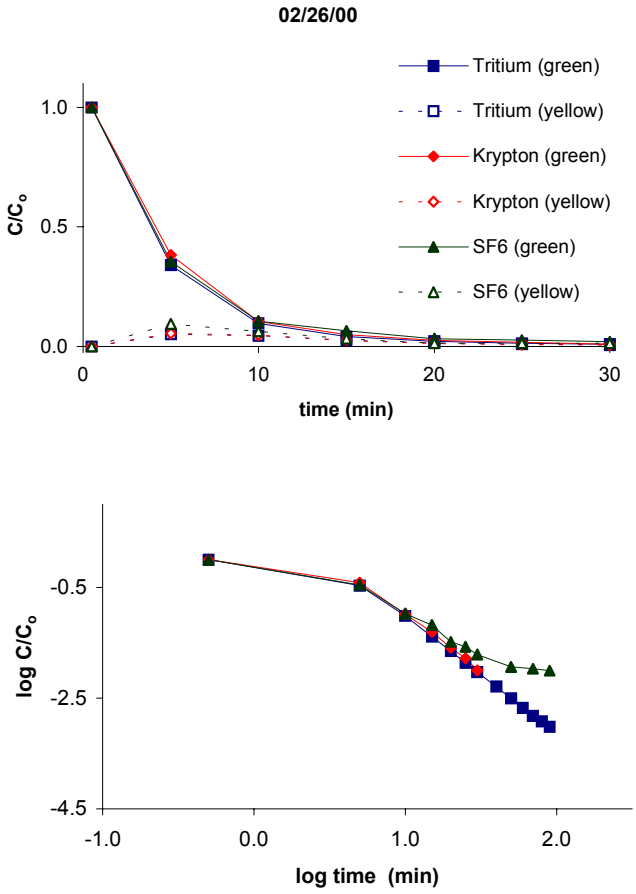

02/26/00 "Push-Pull" Experiment

Well:	274 G
Vol. Injected:	5L
Q:	15.17cm^3/sec
n:	*0.40*
b:	30cm
r:	2.54cm
v*:	7.92E-02cm/sec
L:	7.28cm

where: Q = pump rate, n = porosity (arbitrary value),
b = screen thickness, r = well radius,
v = pore water velocity*, and L = max tracer distance

*-calculated from the equation: $v = \frac{Q}{2\pi b \theta r}$
(Haggerty et al. 1998)

Figure 34. Push-pull experiment where tracer solution (containing ^{3}H, Kr, and SF_6) was injected into the lowest (green) interval and immediately withdrawn. The overlying middle (yellow) screened interval was continuously sampled for tracer concentrations, but at ~ 10% the flow rate of the lower (green) level so that minimal upward flow was induced. Bromide was excluded so that the behavior of the gas tracers could be examined in the absence of a dissolved salt. $CV_{tritium} \approx 0.5$ %, $CV_{Kr} \approx 2.2$ %, and $CV_{SF6} \approx 6.8$ %.

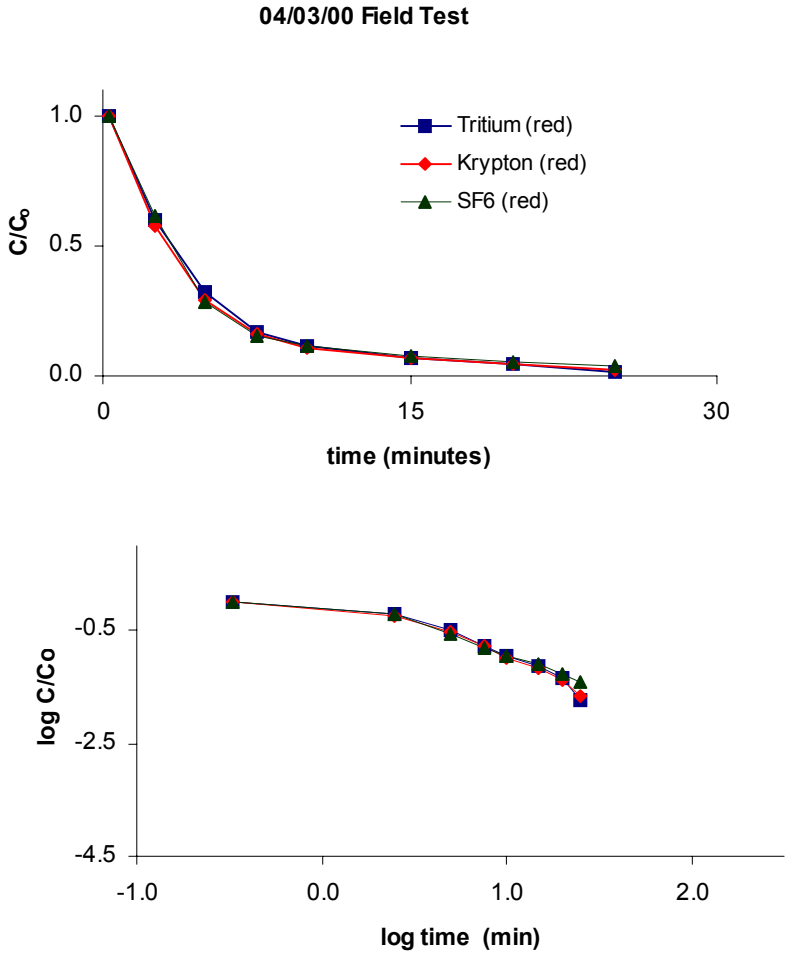

04/03/00 "Push-Pull" Experiment

Well:	274 G
Vol. Injected:	4.95L
Q:	14.17cm^3/sec
n:	*0.40*
b:	30cm
r:	2.54cm
v*:	7.40E-02cm/sec
L:	7.25cm

where: Q = pump rate, n = porosity (arbitrary value),
b = screen thickness, r = well radius,
v = pore water velocity*, and L = max tracer distance

*-calculated from the equation: $v = \frac{Q}{2\pi b \theta r}$
(Haggerty et al. 1998)

Figure 35. Push-pull experiment where tracer solution (containing ^{3}H, Kr, and SF_6) was injected into the lower (green) interval of Well 274 and immediately withdrawn. $CV_{tritium} \approx 1.0$ %, $CV_{Kr} \approx 9.2$ %, and $CV_{SF6} \approx 13.9$ %.

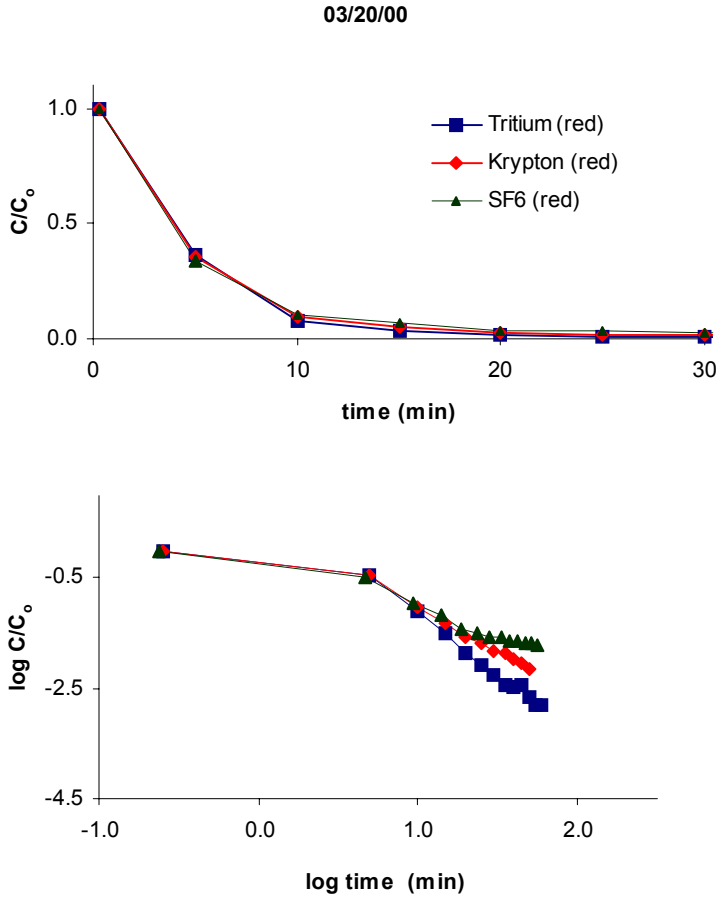

03/20/00 "Push-Pull" Experiment

Well:	335 R
Vol. Injected:	4.55L
Q:	15.67cm^3/sec
n:	*0.40*
b:	90cm
r:	2.54cm
v*:	2.73E-02cm/sec
L:	4.01cm

where: Q = pump rate, n = porosity (arbitrary value),
b = screen thickness, r = well radius,
v = pore water velocity*, and L = max tracer distance

*-calculated from the equation: $v = \frac{Q}{2\pi b \theta r}$
(Haggerty et al. 1998)

Figure 36. Push-pull experiment where tracer solution (containing ^{3}H, Kr, and SF_6) was injected into the upper (red) interval of Well 335 and immediately withdrawn. Part of this screen was above the water table in the past ~1.5 years (Dunn et al. 1998) so it was thought this interval may contain trapped gas pockets that would cause the gas tracers to behave differently than tritium. $CV_{tritium} \approx 5.3$ % and $CV_{Kr} \approx 11.2$ %.

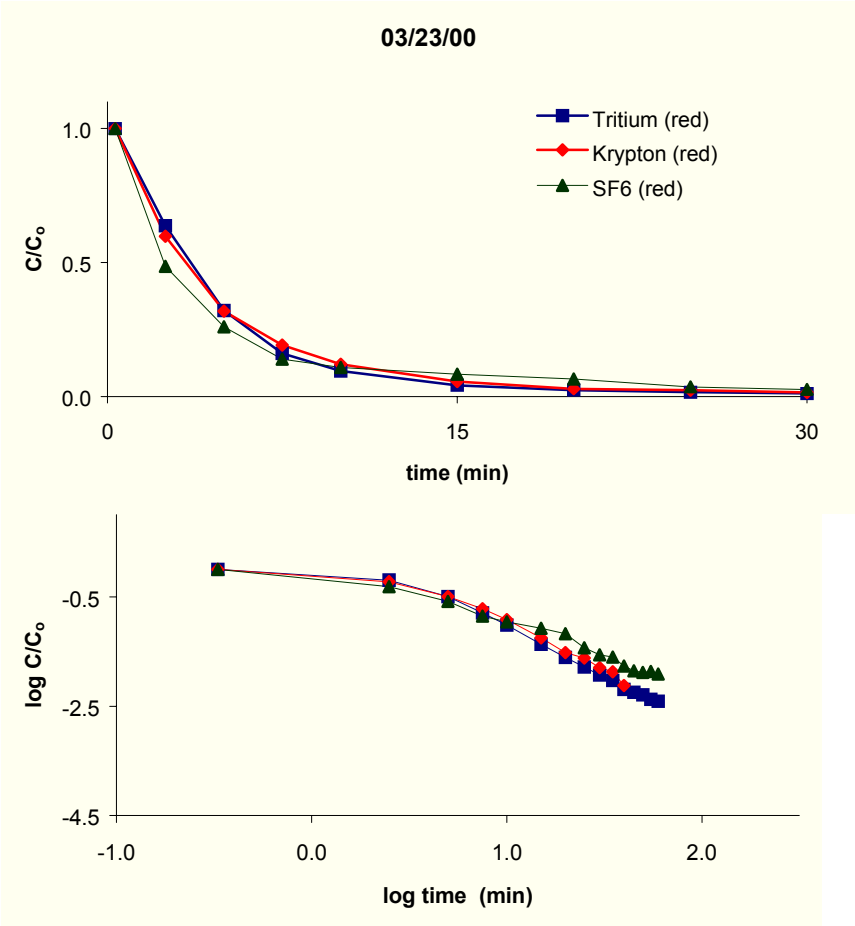

03/23/00 "Push-Pull" Experiment

Well:	356 R
Vol. Injected:	4.99L
Q:	15.33cm^3/sec
n:	*0.40*
b:	90cm
r:	2.54cm
v*:	2.67E-02cm/sec
L:	4.20cm

where: Q = pump rate, n = porosity (arbitrary value), b = screen thickness, r = well radius, v = pore water velocity*, and L = max tracer distance

*-calculated from the equation: $v = \frac{Q}{2\pi b \theta r}$ (Haggerty et al. 1998)

Figure 37. Push-pull experiment where tracer solution (^{3}H, Kr, and SF_6) was injected into the upper (red) interval of Well 356 and immediately withdrawn. Part of this screen was above the water table in the past ~1.5 years (Dunn et al. 1998), so it was thought that this interval may contain trapped gas pockets that would cause the gas tracers to behave differently than tritium. $CV_{tritium} \approx 1.6$ % and $CV_{Kr} \approx 1.9$ %.

5.2. *LARGE VOLUME PUSH-PULL EXPERIMENTS*

Results

Two larger scale push-pull tracer experiments were conducted on 5/5/00 (Fig. 38; Table G7) and 5/11/00 (Fig. 39; Table G8), the former in the upper (red) screened interval of Well 335 thought to contain some unsaturated pore space and the latter in the lower (green) screened interval of Well 274 that was thought to be completely saturated. The tests were conducted by adding a relatively large slug of tracer-charged water (~20L), followed by tracer-free creek water (~30L). The larger mass of tracer was used to push solution further into the aquifer than the ~5 L injections. In these two experiments, the estimated travel distances for the tracer solution were ~13.3 cm and ~21.3 cm (assuming radial flow and homogeneous media), respectively. In the 05/05/00 experiment (Fig. 38), the recovery of tritium was low (~ 2 L out of 20 L injected, based on mass balance considerations) and the recovery of the gas tracers was negligible. During pumping, the flow dropped from ~ 0.87 L/min to ~ 0.16 L/min within a few minutes. This occurred because water was pumped from the well at a rate that could not be sustained by the aquifer. The tracers were detected immediately after the pump was reversed, which indicated they did not move uniformly into the formation by piston flow, but rather mixed to some extent with the formation water. Relative to tritium, dissolved gas tracer recovery was low (maximum tritium $C/C_o \approx 0.12$ while dissolved gas tracers were less than ~ 0.02).

In the 05/11/00 experiment (Fig. 39) conducted at Well 274G, the recovery of the tracers was enhanced. Again, all tracers were detected immediately after the pump was reversed. Initially, the recovery of the dissolved gas tracers was similar to tritium, but after ~ 10 L of effluent was removed, Kr concentration dropped compared to tritium, and after ~ 20 L of removal, SF_6 concentration dropped below tritium. After ~ 30 L of effluent had been removed, Kr concentration exceeded that of SF_6. The tracers continued

to elute in measurable concentrations (^3H > Kr > SF_6) afterward until the experiment was terminated at ~ 110 L.

Discussion

In the 05/05/00 push-pull tracer test (Fig. 38), where ~ 20 L of tracer solution was injected and followed by ~ 30 L of creek water, only a small portion of the original injected mass of tracer was recovered because the well ran dry after only a total of 20 L of effluent was recovered. All tracers were detected immediately after withdrawal began, which indicated mixing was occurring in the immediate vicinity of the screen (tracer did not move out as a piston). Initial ratios of C/C_o were low, indicating only a small amount of tracer solution was not pushed into the formation. The maximum relative concentrations recovered for the dissolved gases occurred after ~ 1 L of effluent was recovered, while the maximum relative concentration of tritium occurred at ~ 6 L.

For the 05/11/00 tracer test (Fig. 39), where ~ 17 L of tracer solution was injected and followed by ~ 26 L of creek water, several interesting observations were made. Based on the breakthrough curves (Fig. 39), there appeared to be some partitioning of the dissolved gases to a second phase. It is possible that the gas partitioned to a trapped gas phase, however, the lower (green) screened interval was thought to be a fully saturated medium based on the results of the 5 L push-pull experiment conducted on 04/03/00 (see Fig. 35). Lithological analyses showed that the sediments of the Fourmile Creek floodplain do contain a significant amount of organic carbon, although concentrations are highest near the surface and decrease quickly with depth. It was curious that the relative concentration of SF_6 was higher than Kr for the first ~ 30 L of recovered effluent. This is the only experiment (field or laboratory) where this result occurred. A possible explanation is that SF_6 partitioned to another phase (a sink) immediately after entering the formation. When the pump was reversed and effluent was collected, this SF_6 partitioned back into solution and the sink became a source. This effect would have also

occurred with Kr, but to a less severe extent due to its subdued partitioning characteristics. After ~ 30 L of effluent was collected, the relative concentration of Kr exceeded that for SF_6. At this point, the source of SF_6 had become depleted. The fact that dissolved gas tracer recoveries were similar to tritium early in the effluent recovery but later diverged indicates the presence of both reactive and non-reactive media in the aquifer. As with the earlier smaller scale experiments, the initial tracer that was recovered only penetrated a short distance into the aquifer, however the effluent collected later was retrieved from further in the aquifer and therefore had the potential to interact to a greater extent with reactive media.

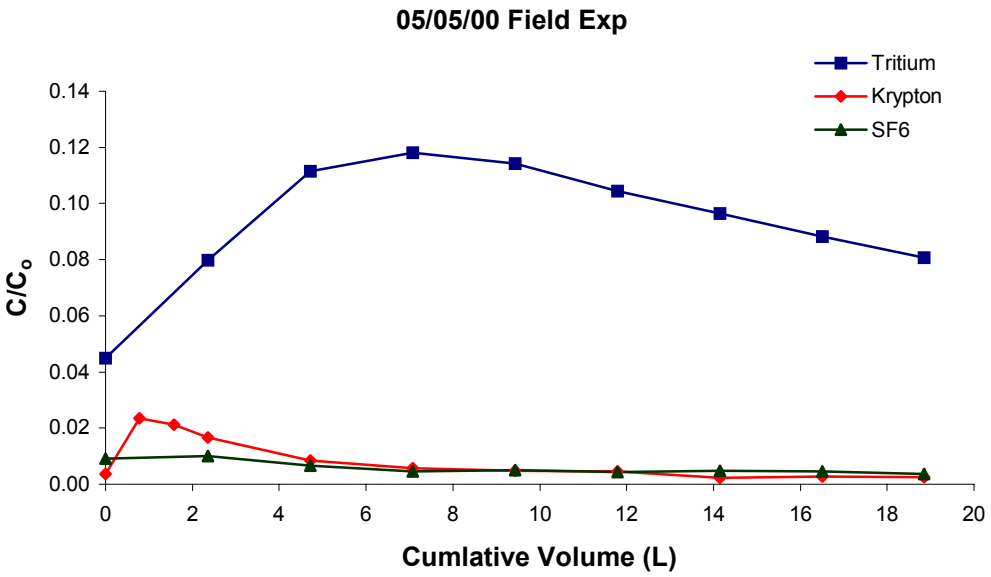

05/05/00 "Push-Pull" Experiment

Well:	335 R
Vol. Injected:	50L
Q:	14.5cm^3/sec
n:	*0.40*
b:	90cm
r:	2.54cm
v*:	2.52E-02cm/sec
L:	13.3cm

where: Q = pump rate, n = porosity (arbitrary value), b = screen thickness, r = well radius, v = pore water velocity*, and L = max tracer distance

*-calculated from the equation: $v = \frac{Q}{2\pi b \theta r}$ (Haggerty et al. 1998)

Figure 38. Push-pull test conducted in the upper (red) screened interval of Well 335. Twenty liters of tracer (containing ^{3}H, Kr, and SF_6) was injected, followed by 30 L of tracer free creek water. After injection, the pump was reversed and effluent was sampled. Cumulative volume is the number of liters withdrawn after injection. After 20 L was removed, the well ran dry and the experiment was terminated. $CV_{tritium} \approx 0.5$ %, $CV_{Kr} \approx 12.0$ %, and $CV_{SF6} \approx 3.9$ %.

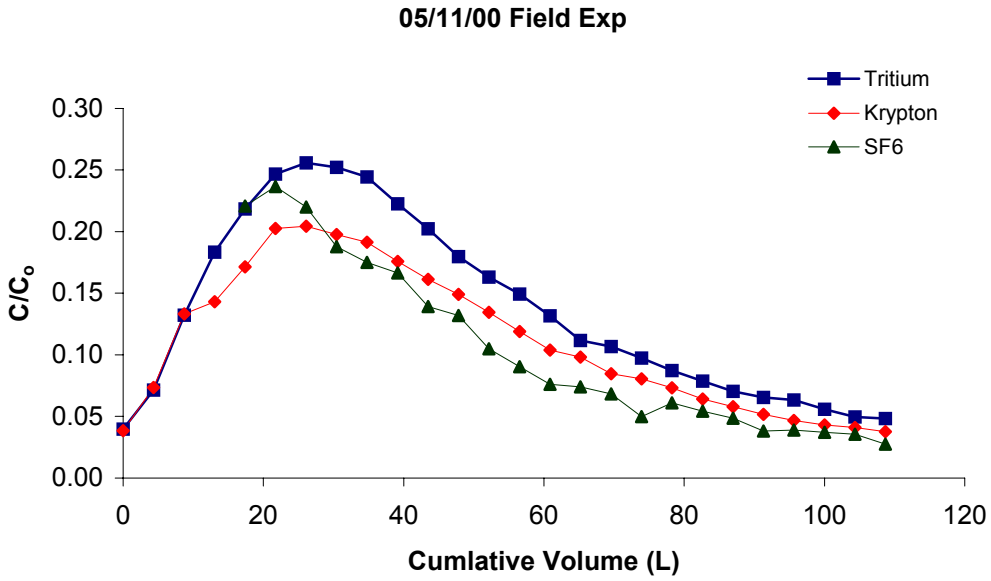

05/11/00 "Push-Pull" Experiment

Well:	274 G
Vol. Injected:	42.7L
Q:	14.83cm^3/sec
n:	*0.40*
b:	30cm
r:	2.54cm
v*:	7.74E-02cm/sec
L:	21.29cm

where: Q = pump rate, n = porosity (arbitrary value), b = screen thickness, r = well radius, v = pore water velocity*, and L = max tracer distance

*-calculated from the equation: $v = \frac{Q}{2\pi b \theta r}$ (Haggerty et al. 1998)

Figure 39. A push-pull test conducted in the lower (green) screened interval of Well 274. Approximately 17 L of tracer (^{3}H, Kr, and SF_6) was injected followed by ~25 L of tracer-free creek water. Cumulative volume is the number of liters withdrawn after injection. $CV_{tritium} \approx 0.9$ %, $CV_{Kr} \approx 13.4$ %, and $CV_{SF6} \approx 11.2$ %.

CHAPTER 6
THE EFFECT OF DISSOLVED SALTS

In the 5 L push-pull experiments conducted on 01/06/00 and 02/16/00 (Figs. 32 and 33), the gas tracers displayed unusual behavior that could not be easily explained. Both Kr and SF_6 were observed in water from the middle (yellow) screened interval almost instantaneously after injection in the lower (green) interval, while tritium and Br^- were not. In the second test conducted on 02/26/00 (Fig. 34) where Br^- was not used, no upward movement of dissolved gas tracers was detected.

From these observations, it was hypothesized dissolved salt was the cause of the rapid upward movement of the dissolved gases. Two column experiments were conducted to further test this hypothesis. The columns were packed in the same manner as in previous experiments and they were saturated with distilled water. Two tracer solutions were mixed one where Kr and SF_6 were dissolved in tritiated water of negligible ionic strength and a second one containing tritiated water plus ~ 10,000 mg/L dissolved NaCl.

One pore volume of high ionic strength tracer solution was introduced to a saturated column. Next, ~ one pore volume of the NaCl free tracer solution was introduced to the column (this step was to provide a benchmark to which the high ionic strength tracer could be compared). Flow rate was held at 4 mL/min for both the high and low salinity tracer injections and samples were collected at regular increments (every ~ 0.1 pore volume) for ~ 1.5 pore volumes (Table H1 in APPENDIX H). The experiment was repeated at a flow rate of 8 mL/min (Table H2 in APPENDIX H). In experiments at both the low and high flow rate, when the dissolved gas tracer was used in conjunction with the dissolved salt, the gas tracer arrived prior to tritium (Fig. 40). When the solution

did not contain a dissolved salt, the dissolved gas tracer arrived slightly after tritiated water. These results suggest the ionic tracer is facilitating the transport of the dissolved gas, probably through an exsolution and redissolution mechanism.

The effect of ionic strength on the solubility of dissolved gases is well known (Colt 1984). Perhaps a solubility gradient promoted the exsolution of dissolved gases when a high ionic strength tracer was injected into a fluid of relatively low ionic strength. If this occurred in the column and field experiments, it would facilitate the accelerated upward movement of Kr and SF_6 in the gaseous state until bubbles redissolved in the overlying low ionic strength waters. This phenomena was observed in the laboratory when high ionic strength, gas charged water was introduced through 1/16" tubing into the bottom of a flask containing distilled water. Bubbles formed at the contact between the dense, high ionic strength fluid and the distilled water. As these bubbles moved upward, they redissolved in the overlying water of low ionic strength. The reason for the exsolution of gas at the interface of high and low ionic strength tracers is not entirely clear but it may be related to diffusional processes at the boundary of these two solutions and/or interfacial surface energies. Such a phenomenon could explain the 01/06/00 and 02/16/00 field experiments where the dissolved gas tracers migrated upward. In subsequent experiments where dissolved ionic tracers were not used this effect was not observed. Based on these results, dissolved salts and dissolved gases should not be used as co-tracers.

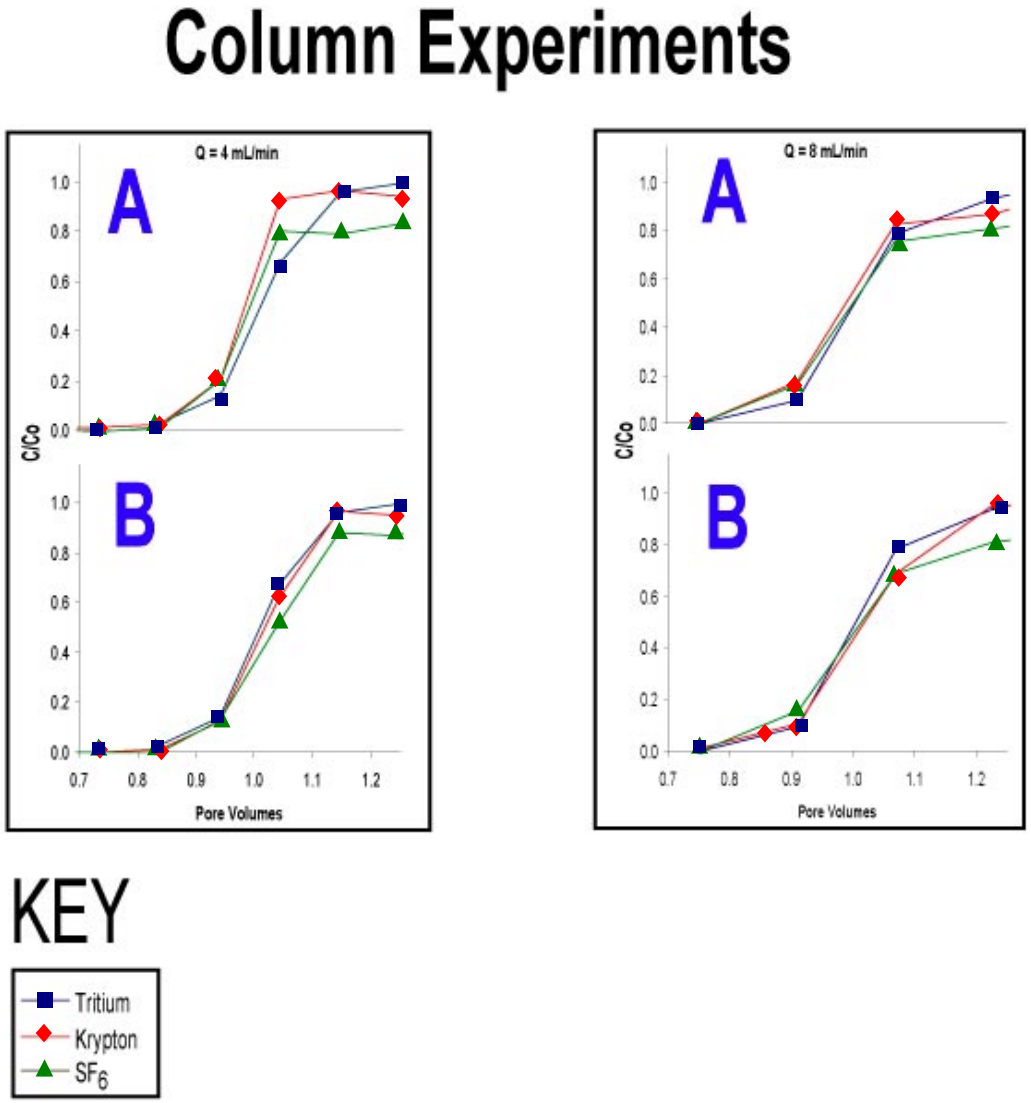

Figure 40. Single pulse column experiments were run at 4 to 8 mL/min using gas tracers with a) 10,000 mg/L dissolved salt or b) no added salt. Injection of dissolved salt tracer solution began at PV = 0.

CHAPTER 7
CONCLUSIONS

Dissolved gas tracers are an attractive alternative to conventional groundwater tracers such as dyes and salts. Limitations associated with conventional tracers such as toxicity, increased solution density, or regulatory concerns are all avoided with inert dissolved gas tracers. Many different inert gases are suitable for use as dissolved gas tracers; an array of different gases with different physical properties can be used to obtain a variety of information. Dissolved gas tracers can be chosen that have different propensities for partitioning into trapped gas filled space or for partitioning onto organic matter. They can also be chosen based on available analytical equipment so the cost of analysis is minimized.

The purpose of this study was to examine the inter-phase partitioning behavior of dissolved gas tracers in laboratory column and field experiments. In the laboratory column experiments, the two phases were gas and liquid and in the field experiments the phases included gas, liquid and/or organic matter. Krypton and SF_6 were the two dissolved gas tracers examined in this study. Under fully saturated conditions, the gases behaved similarly to tritiated water in both laboratory column experiments and field experiments. They displayed different partitioning behavior in media containing trapped gas that could be explained using a numerical model. The presence of even small amounts of trapped gas in media caused the transport of dissolved gas tracers to deviate from conservative behavior. This deviation occurred in a quantifiable manner in laboratory column experiments and yielded information such as the volume of trapped gas phase present in the column, mass transfer coefficients, and retardation factors. In small-scale field tests and laboratory column experiments, it was observed that dissolved

salts at a concentration of ~ 10,000 mg/L interfered with the transport of dissolved gas tracers. Slightly different recoveries of dissolved gas tracers and tritium in field tests indicated that either small amount of trapped gas or organic matter was present in shallow wells.

The potential for future applications of dissolved gas tracers to problems in hydrology is promising. Models developed for the transport of both conservative and reactive tracers are applicable to dissolved gas tracers. However, the issue of partitioning to organic matter or organic contaminants has been dealt with in a very limited manner. Dissolved gas tracers can potentially be used to quantify the area and volume of an organic contaminant in the same manner they were used in this study to quantify the volume of trapped gas phase.

APPENDIX A

HP CHEMSTATION© GC SETTINGS

Table A1. Method used to program HP Chemstation software to run HP5890 GC and HP5970 MSD

TOPLEVEL PARAMETERS

Method information For: C:\HPCHEM\1\METHODS\DEFAULT.M

Method Sections To Run:
( ) Save Copy of Method With Data
( ) Pre-Run Cmd/Macro =
(X) Data Acquisition
(X) Data Analysis
( ) Post-Run Cmd/Macro =

Method Comments:
Method for noble gas analysis.

ACQUISITION PARAMETERS

General Information
Inlet: GC
Tune File: ATUNE.U
Acquisition Mode: Sim

MS Information
Solvent Delay: 0.00 min
EM Absolute: True
Resulting Voltage: 1800.0
[Sim Parameters]
GROUP 1
Group ID: NEON
Dwell Per Ion: 100 msec
Low Resolution: Yes
Start Time: 0.00
Ions In Group: 20.05 21.05 22.05
GROUP 2
Group ID: ARGON
Dwell Per Ion: 50 msec
Low Resolution: No
Start Time: 2.00
Ions In Group: 36.95 37.95 39.95
GROUP 1
Group ID: KRYPTON
Dwell Per Ion: 100 msec

Low Resolution: Yes
Start Time: 2.65
Ions In Group: 83.90 85.90 81.90 77.90 79.90
[Real Time Plot Parameters]
Time Window: 10 min
Iconize Real Time Display: False
Plot 1 Type: Total ion
Scale Minimum: 100
Scale Maximum: 2000000
Plot 2 Type: No Plot

GC Temperature Information
[GC Zone Temperatures]
Inj. A: 200 C
Inj. B: 200 C
Det. A: 250 C
Det. B: 250 C
[Oven Parameters]
Oven Equib Time: 0.50 min
Oven Max: 250 C
Oven: On
Cryo: Off
[Oven Program]
Initial Temp.: 155 C
Initial Time: 5.00 min

Level	Rate (C/min)	Final Temp. (C)	Final Time (min)
1	0.00		

Next Run Time: 5.00 min

Injector Information
Injection Source: Manual
[Purge Information]

Purge A/B	Init. Value	On Time	Off Time
A	On	0.00	0.00
B	On	0.00	0.00

DATA ANALYSIS PARAMETERS

Method Name: C:\HPCHEM\1\METHODS\DEFAULT.M

Percent Report Settings
Sort By: Retention Time
Output Destination
Screen: Yes
Printer: No
File: No
Integration Events: AutoIntegrate
Generate Report During Run Method: Yes
Signal Correlation Window: 0.020

Qualitative Report Settings

Peak Location of Unknown: Apex
Library to Search Minimum Quality

Report Type: Summary
Output Destination
Screen: No
Printer: Yes
File: No
Generate Report During Run Method: No

Quantitative Report Settings
Report Type: Summary
Output Destination
Screen: Yes
Printer: No
File: No
Generate Report During Run Method: No
Calibration Last Updated:
Reference Window: 10.00 Percent
Non-reference Window: 5.00 Percent
Correlation Window: 0.02 minutes
Default Multiplier: 1.00
Default Sample Concentration: 0.00

Table A2. Method used to program HP Chemstation software to run HP5890 GC and ECD

Method Information

Method for the analysis of SF_6 using no cryo cooling.
Isothermal at 32 C.

Method Change History

-

Run Time Checklist

Pre-Run Cmd/Macro: Off
Data Acquisition: On
Standard Data Analysis: On
Customized Data Analysis: Off
Save GLP Data: Off
Post-Run Cmd/Macro: Off
Save Method With Data: Off

Injection Source and Location

Injection Source: Manual
Injection Location: Front

7673 Injector

Front Injector: No Parameters Specified
Back Injector:
not configured, use these parameters if it becomes configured

Sample Washes		0
Sample Pumps		0
Injection Volume		1 microliters
Syringe Size		10 microliters
On Column		Off
Nanoliter Adapter		Off
PostInj Solvent A Washes	0	
PostInj Solvent B Washes	0	
Viscosity Delay		0
Plunger Speed		Fast

Oven\Det

Runtime (min): 7.1
Zone Temperatures:

	State	Setpoint
Inl. A	On	200 C.
Inl. B	On	250 C.
Det. A	On	300 C.
Det. B	On	300 C.
Aux.	Off	50 C.

Oven Zone:

Oven max	325 C.
Equib Time	0.5 min.
Oven State	On

Cryo State Off
Ambient 25C.
Cryo Blast Off
Oven Program:

	Setpoint	
Initial Temp.:	200	C.
Initial Time:	2.0	min.

Level	Rate (C/min)	Final Temp (C)	Final Time (min)
1	0.00	0	0.00

Inlet A Pressure Program Information
Constant Flow: On
Pressure: 10.8 psi
Temperature: 0 C
Pressure Program:

	Setpoint	
Initial Pres.:	0.00	psi
Initial Time:	650.00	min

Level	Rate (psi/min)	Final Pres. (psi)	Final Time (min)
1	0.00	0.0	0.00
2 (A)	0.00	0.0	0.00
3 (B)	0.00	0.0	0.00

Total Program Time: 650.00
Pressure Units: psi
Entered Values:
Column Length: 30.00 m.
Column Diameter: 0.250 mm.
Gas: He
Vacuum Comp: Off

Inlet B Pressure Program Information
Constant Flow: On
Pressure: 10.8 psi
Temperature: 0 C
Pressure Program:

	Setpoint	
Initial Pres.:	0.00	psi
Initial Time:	650.00	min

Level	Rate (psi/min)	Final Pres. (psi)	Final Time (min)
1	0.00	0.0	0.00
2 (A)	0.00	0.0	0.00
3 (B)	0.00	0.0	0.00

Total Program Time: 650.00
Pressure Units: psi
Entered Values:
Column Length: 30.00 m.
Column Diameter: 0.250 mm.
Gas: He
Vacuum Comp: Off

Purge Valve Settings

Purge A/B	Init Value	On Time (Min.)	Off Time (Min.)
A (Valve 3)	Off	0.05	0.00
B (Valve 4)	Off	0.00	0.00

A-Splitless Injection: Yes
B-Splitless Injection: Yes

Valves/Relays Information
Initial Setpoints:
5890 Valves:
Valve 1: Off
Valve 2: Off
Valve 3 (Purge A): Off
Valve 4 (Purge B): Off

Detector Information
Detector A:
Type: FID
State: On
Detector A:
Type: ECD
State: On
Save Data: Signal 2
Signal 1:
Signal: Det. A
Data rate: 5.000 Hz.
Peakwidth: 0.053 min.
Start Time: 0.00 min.
Stop Time: 650.00 min.
Signal: Det. B
Data rate: 5.000 Hz.
Peakwidth: 0.053 min.
Start Time: 0.00 min.
Stop Time: 650.00 min.

APPENDIX B

CALIBRATION CURVE DATA

Table B1. Krypton calibration data*
Equation for Curve: y=1.24x+15.37
R^2: 0.9984

g inj	log g inj	peak area	log p.a.
3.42E-09	-8.47	7.05E+04	4.85
3.42E-09	-8.47	5.61E+04	4.75
1.71E-08	-7.77	8.44E+05	5.93
1.71E-08	-7.77	7.49E+05	5.87
3.43E-08	-7.47	1.32E+06	6.12
3.43E-08	-7.47	1.28E+06	6.11
1.72E-07	-6.76	1.13E+07	7.05
1.72E-07	-6.76	1.17E+07	7.07
3.44E-07	-6.46	1.82E+07	7.26
3.44E-07	-6.46	1.94E+07	7.29

*Direct Injection of known mass into GC.

Table B2. Krypton calibration data*
Equation for Curve: y=0.05x+0.41 Assumes: 1 atm pressure, 22°C, and K_H'~14.8
R^2: 0.9956

g Kr inj.	vial conc. (mg/L)	orig water conc. (mg/L)	Kr/Ar
3.46E-07	2.83E-02	0.06	n.d.
1.73E-06	1.42E-01	0.30	0.07
3.46E-06	2.83E-01	0.60	0.11
3.46E-05	2.83E+00	6.01	0.22
8.65E-05	7.08E+00	15.03	0.39
1.73E-04	1.42E+01	30.06	0.88
2.59E-04	2.12E+01	45.09	1.71
3.46E-04	2.83E+01	60.12	2.33
4.32E-04	3.54E+01	75.16	3.19
5.19E-04	4.25E+01	90.19	3.55
6.05E-04	4.96E+01	105.22	4.83
6.92E-04	5.66E+01	120.25	5.32
7.78E-04	6.37E+01	135.28	6.42
8.65E-04	7.08E+01	150.31	7.44
9.51E-04	7.79E+01	165.34	8.27
1.04E-03	8.50E+01	180.37	8.85
1.12E-03	9.21E+01	195.41	9.68
1.21E-03	9.91E+01	210.44	10.58
1.30E-03	1.06E+02	225.47	11.19
1.38E-03	1.13E+02	240.50	11.90
1.47E-03	1.20E+02	255.53	12.70

*Known mass injected into vial and related to a hypothetical 4 mL water sample by Henry's Law.

Table B3. Sulfur hexafluoride calibration data Assumes: 1 atm pressure, 23°C

Equation for Curve: $y=0.15x^2+2.88x+17.80$

R^2: 0.9931

mol gas injected	g SF6 inj	peak area
8.23E-07	1.23E-07	8.89E+04
8.23E-07	1.23E-07	8.22E+04
8.23E-07	1.23E-07	7.94E+04
1.65E-06	2.47E-07	1.83E+05
2.47E-06	3.70E-07	3.01E+05
3.29E-06	4.93E-07	4.50E+05
4.12E-06	6.17E-07	5.34E+05
8.23E-07	1.26E-09	1.01E+04
8.23E-07	1.26E-09	1.02E+04
8.23E-07	1.26E-09	1.01E+04
1.65E-06	2.52E-09	1.16E+04
2.47E-06	3.79E-09	1.25E+04
4.12E-06	6.31E-09	1.63E+04
8.23E-07	1.24E-07	9.91E+04
8.23E-07	1.24E-07	1.04E+05
8.23E-07	1.24E-07	1.06E+05
1.65E-06	2.48E-07	1.97E+05
2.47E-06	3.72E-07	3.43E+05
3.29E-06	4.96E-07	5.11E+05
4.12E-06	6.20E-07	6.23E+05
8.23E-07	1.26E-06	9.82E+05
8.23E-07	1.26E-06	1.07E+06
8.23E-07	1.26E-06	9.84E+05
1.65E-06	2.52E-06	2.01E+06
2.47E-06	3.79E-06	3.15E+06
3.29E-06	5.05E-06	4.58E+06
4.12E-06	6.31E-06	5.39E+06
8.23E-07	1.25E-08	2.04E+04
8.23E-07	1.25E-08	1.68E+04
8.23E-07	1.25E-08	1.75E+04
1.65E-06	2.50E-08	2.88E+04
2.47E-06	3.75E-08	3.65E+04
3.29E-06	5.00E-08	4.47E+04
4.12E-06	6.25E-08	-
0.00	0.00	9.77E+03
0.00	0.00	9.35E+03
0.00	0.00	9.66E+03

Table B4. Bromide calibration data
Equation for Curve: $y=8.86x^2+3.59x+30.12$
R^2: 0.9873

mg/L KBr	log mg/L	mev
10000	4.0	171.4
5000	3.7	169.8
2500	3.4	150.7
1250	3.1	134.9
625	2.8	113.3
1000	3.0	126.9
500	2.7	102.5
250	2.4	86.1
125	2.1	72.8
100	2.0	69.1
50	1.7	59.9
25	1.4	52.4
10	1.0	39.1
5	0.7	34.4
1	0.0	33.5
0.5	-0.3	32.9
0.25	-0.6	30.1

Table B5. Tritium calibration data*
Equation for Curve: $y=7996.2x+26.37$
R^2: 0.9995

$^3H_20$	CPMA
0.0	6.8
0.5	4226.8
1.0	8136.1
1.5	12229.4
2.0	16423.8
2.5	20345.4
3.0	24471.8
3.5	28347.2
4.0	31690.8

All samples were a total of 4 mL in vol. (non-tritiated water made up balance)
*Due to lack of a standard, not quantified for actual value, calibration was performed to check linearity.

APPENDIX C

KRYPTON LOSS FROM OPEN CONTAINERS

DATA FOR KRYPTON LOSS VIA DIFFUSION

Table C1. Loss from open 30 gallon barrel
Data from Jones (1996)
equation: y=33.51e(-0.0157)(x)
(minutes)
where, y=concentration and x=time (hours)

time (hrs)	**water conc. (mg/l)**
0.00	33.51
0.25	33.37
0.50	33.24
0.75	33.11
1.00	32.98
1.25	32.85
1.50	32.73
1.75	32.60
2.00	32.47
2.25	32.34
2.50	32.22

Table C2. Loss from open 10 mL vials
equation: y=47.89e(-0.0039)(x)
where, y=concentration and x=time

time (min)	**water conc. (mg/l)**
0	43.05
5	48.34
10	42.07
15	46.77
20	42.47
25	44.42
30	41.29
35	43.64
40	43.05
45	40.12
50	47.36
55	41.49
60	32.49
90	36.79
120	31.31
150	23.87

APPENDIX D

LOSSES ATTRIBUTED TO PERISTATIC PUMP

Table D1. Estimated Losses due to peristaltic pump

Experiment	**2/16/2000**		
	Tritium	Krypton	SF_6
Avg C_o from Carboy	30981	4.19	3.19E+07
C_o after pump	30970	1.92	2.48E+07
% loss to pump	0.03	54.30	22.26

Experiment	**2/26/2000**		
	Tritium	Krypton	SF_6
Avg C_o from Carboy	31210.3	5.04	2.07E+07
C_o after pump	30267	3.94	1.21E+07
% loss to pump	3.02	21.75	41.64

Experiment	**3/21/2000**		
	Tritium	Krypton	SF_6
Avg C_o from Carboy	10993	2.43	1.31E+07
C_o after pump	10913	2.16	1.01E+07
% loss to pump	0.72	11.10	22.94

Experiment	**3/23/2000**		
	Tritium	Krypton	SF_6
Avg C_o from Carboy	18836	1.05	1.31E+07
C_o after pump	18606	0.96	7.89E+06
% loss to pump	1.22	8.67	39.80

Experiment	**4/3/2000**		
	Tritium	Krypton	SF_6
Avg C_o from Carboy	30497	3.55	1.99E+07
C_o after pump	31074	3.54	1.86E+07
% loss to pump	-1.89	0.29	6.69

Table D1. (cont'd)

Experiment	**5/5/2000**		
	Tritium	Krypton	SF_6
Avg C_o from Carboy	9608	5.09	6.41E+06
C_o after pump	9632	4.19	5.51E+06
% loss to pump	-0.25	17.73	14.04

Experiment	**5/11/2000**		
	Tritium	Krypton	SF_6
Avg C_o from Carboy	3717	3.24	3.02E+07
C_o after pump	3742	2.64	2.49E+07
% loss to pump	-0.67	18.72	17.46

APPENDIX E

FOUR MILE CREEK WELL INFORMATION

Table E1. 4 Mile Creek well location and elevation information.

Location ID	Installation Date	UTM North	UTM East
GSW130R	10/7/97	3681611.96	441977.85
GSW130Y	10/7/97	3681611.96	441977.85
GSW133R	9/30/97	3681619.55	441973.44
GSW133Y	9/30/97	3681619.55	441973.44
GSW161R	1/19/98	3681610.06	441968.64
GSW163R	9/30/97	3681615.06	441965.4
GSW163Y	9/30/97	3681615.06	441965.4
GSW163G	9/30/97	3681615.06	441965.4
GSW214R	1/21/98	3681625.49	441977.07
GSW214Y	1/21/98	3681625.49	441977.07
GSW214G	1/21/98	3681625.49	441977.07
GSW244R	1/20/98	3681620.65	441969.32
GSW244Y	1/20/98	3681620.65	441969.32
GSW274R	1/21/98	3681615.94	441961.57
GSW274Y	1/21/98	3681615.94	441961.57
GSW274G	1/21/98	3681615.94	441961.57
GSW317R	1/20/98	3681633.16	441972.88
GSW317Y	1/20/98	3681633.16	441972.88
GSW335R	9/29/97	3681624.88	441970.27
GSW335Y	9/29/97	3681624.88	441970.27
GSW337R	1/20/98	3681629.83	441967.35
GSW337Y	1/20/98	3681629.83	441967.35
GSW337G	1/20/98	3681629.83	441967.35
GSW345R	9/24/97	3681623.19	441967.92
GSW345Y	9/24/97	3681623.19	441967.92
GSW356R	1/19/98	3681624.02	441963.81
GSW356Y	1/19/98	3681624.02	441963.81
GSW365R	10/1/97	3681620.04	441962.71
GSW365Y	10/1/97	3681620.04	441962.71

Table E1. (cont'd)

Location ID	Ground Elev. (msl)	Top of Pipe Elevation (msl)	Depth to Screen Top (ft)	Depth to Screen Bottom (ft)
GSW130R	248.80	252.78	3.00	6.00
GSW130Y	248.80	252.76	8.00	9.00
GSW133R	246.90	251.26	0.50	3.50
GSW133Y	246.90	251.23	8.00	9.00
GSW161R	247.60	251.11	2.00	5.00
GSW163R	247.80	251.79	0.67	3.67
GSW163Y	247.80	251.78	5.58	6.58
GSW163G	247.80	251.77	9.50	10.50
GSW214R	245.20	251.68	-0.30	0.70
GSW214Y	245.20	251.67	2.10	3.10
GSW214G	245.20	251.67	7.00	8.00
GSW244R	246.00	251.29	-0.40	2.60
GSW244Y	246.00	251.32	7.00	8.00
GSW274R	245.70	251.30	-0.30	2.70
GSW274Y	245.70	251.23	3.60	4.60
GSW274G	245.70	251.24	7.00	8.00
GSW317R	247.70	251.96	2.00	3.00
GSW317Y	247.70	251.93	9.00	10.00
GSW335R	247.80	251.85	1.50	4.50
GSW335Y	247.80	251.85	9.00	10.00
GSW337R	247.60	252.02	2.60	3.60
GSW337Y	247.60	252.02	5.00	6.00
GSW337G	247.60	252.02	10.00	11.00
GSW345R	247.50	251.37	1.80	4.80
GSW345Y	247.50	251.34	6.30	7.30
GSW356R	247.70	251.10	2.00	5.00
GSW356Y	247.70	251.25	10.40	11.40
GSW365R	247.40	251.66	1.00	4.00
GSW365Y	247.40	251.67	8.50	9.50

Fig. E1. Lithology of well 335 (Dunn et al. 1998)

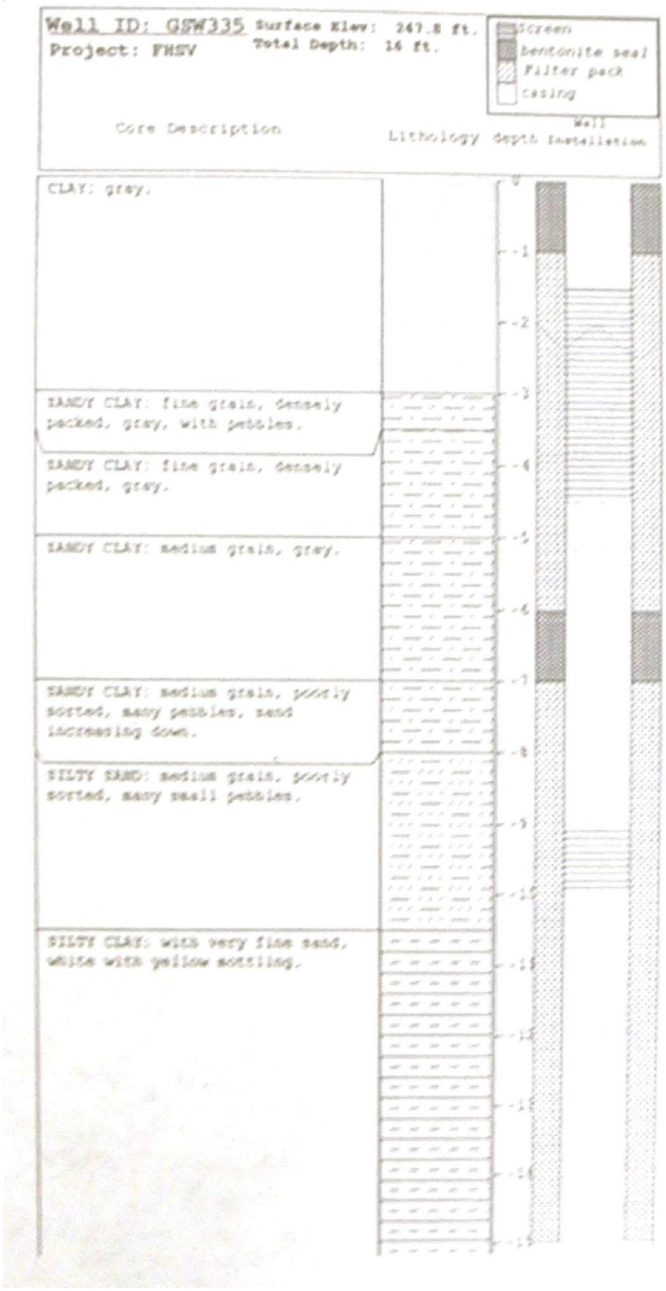

Fig. E2. Lithology of well 356 (Dunn et al. 1998)

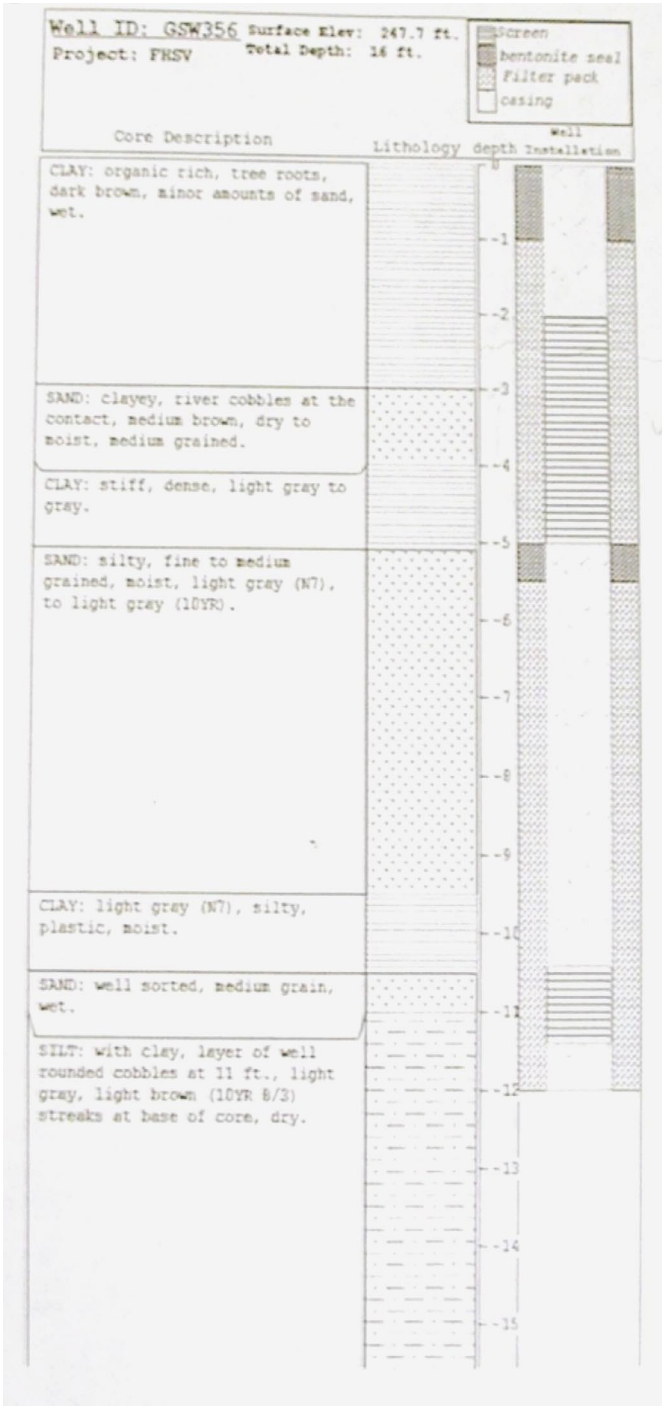

APPENDIX F

LABORATORY COLUMN DATA

Table F1. EXPERIMENT: M-1

Column Data

Flow rate=	4	mL/min	Porosity =	0.39		PV=Pore Volumes
Column ID =	2.5	cm	Sat. Pore Volume =	57.7	g	
Column length =	30	cm	Unsat Pore Volume=	NA	g	C/C_o=rel. conc.
Column Volume =	147.19	cm^3	After Exp Pore Volume=	NA	g	
Mass of porous media =	256.27	g	Pre-exp θ_g/θ_{aq}=	NA		C/C_o=rel. conc.
Bulk Density =	1.58	g/cm^3	Post exp θ_g/θ_{aq}=	NA		(modeled)

TRITIUM DATA			**KRYPTON DATA**			**SF_6 DATA**		
PV	C/C_o	C/C_o	PV	C/C_o	C/C_o	PV	C/C_o	C/C_o
0.06	0.00	0.00	0.82	0.00	0.01	0.13	0.00	0.00
0.13	0.00	0.00	0.95	0.17	0.24	0.25	0.00	0.00
0.19	0.00	0.00	1.08	0.68	0.79	0.38	0.00	0.00
0.25	0.00	0.00	1.20	0.95	0.93	0.51	0.00	0.00
0.32	0.00	0.00	1.33	1.22	0.95	0.63	0.00	0.00
0.38	0.00	0.00	1.58	0.98	0.96	0.76	0.00	0.00
0.44	0.00	0.00	1.84	0.91	0.97	0.89	0.04	0.03
0.51	0.00	0.00	2.09	0.66	0.82	1.01	0.27	0.24
0.57	0.00	0.00	2.34	0.14	0.06	1.14	0.42	0.43
0.63	0.00	0.00	2.59	0.07	0.03	1.27	0.46	0.48
0.70	0.00	0.00	2.85	0.04	0.02	1.39	0.55	0.51
0.76	0.00	0.00	3.10	0.02	0.02	1.52	0.56	0.54
0.82	0.00	0.01				1.65	0.57	0.57
0.89	0.05	0.07				1.77	0.58	0.60
0.95	0.25	0.25				1.90	0.65	0.63
1.01	0.53	0.55				2.03	0.52	0.64
1.08	0.82	0.84				2.15	0.52	0.48
1.14	0.96	0.96				2.28	0.33	0.29
1.20	0.95	0.99				2.41	0.27	0.25
1.27	0.94	1.00				2.53	0.25	0.23
1.33	1.00	1.00				2.66	0.19	0.22
1.39	1.03	1.00				2.78	0.20	0.21
1.46	0.98	1.00				2.91	0.16	0.19
1.52	0.99	1.00				3.04	0.16	0.18
1.58	0.99	1.00				3.42	0.12	0.15
1.65	0.99	1.00				3.80	0.11	0.12
1.71	1.01	1.00				4.18	0.08	0.10
1.77	1.02	1.00				4.56	0.07	0.08
1.84	0.97	1.00				4.94	0.05	0.06
1.90	1.01	1.00						
1.96	1.00	1.00						
2.03	0.97	0.96						
2.09	0.83	0.82						
2.15	0.53	0.54						
2.22	0.23	0.22						
2.28	0.05	0.07						
2.34	0.01	0.02						
2.41	0.00	0.00						
2.47	0.00	0.00						
2.53	0.00	0.00						
2.59	0.00	0.00						
2.66	0.00	0.00						

Table F2. EXPERIMENT: M-2

Column Data

Flow rate=	2 mL/min	Porosity =	0.40	PV=Pore Volumes
Column ID =	2.5 cm	Sat. Pore Volume =	58.9 g	
Column length =	30 cm	Unsat Pore Volume=	NA g	C/C_o=rel. conc.
Column Volume =	147.19 cm^3	After Exp Pore Volume=	NA g	
Mass of porous media =	254.71 g	Pre-exp θ_g/θ_{aq}=	NA	C/C_o=rel. conc.
Bulk Density =	1.73 g/cm^3	Post exp θ_g/θ_{aq}=	NA	(modeled)

TRITIUM DATA			**KRYPTON DATA**			**SF_6 DATA**		
PV	C/C_o	C/C_o	PV	C/C_o	C/C_o	PV	C/C_o	C/C_o
0.26	0.00	0.00	0.85	0.00	0.00	0.13	0.00	0.00
0.33	0.00	0.00	0.98	0.00	0.20	0.26	0.00	0.00
0.39	0.00	0.00	1.11	0.39	0.52	0.39	0.00	0.00
0.46	0.00	0.00	1.24	0.58	0.61	0.52	0.00	0.00
0.52	0.00	0.00	1.37	0.65	0.67	0.65	0.00	0.00
0.59	0.00	0.00	1.50	0.71	0.72	0.78	0.00	0.00
0.65	0.00	0.00	1.63	0.77	0.76	0.91	0.00	0.05
0.72	0.00	0.00	1.76	0.81	0.80	1.04	0.16	0.46
0.78	0.00	0.00	1.89	0.81	0.82	1.17	0.63	0.64
0.85	0.00	0.01	2.02	0.64	0.59	1.31	0.74	0.67
0.91	0.06	0.07	2.15	0.28	0.34	1.44	0.71	0.69
0.98	0.36	0.38	2.28	0.20	0.28	1.57	0.73	0.71
1.04	0.74	0.73	2.41	0.12	0.24	1.70	0.68	0.72
1.11	0.91	0.95	2.54	0.10	0.20	1.83	0.76	0.74
1.17	0.99	0.99	2.81	0.08	0.14	1.96	0.76	0.65
1.24	0.95	1.00	2.94	0.07	0.12	2.09	0.27	0.23
1.31	0.97	1.00	3.07	0.05	0.10	2.22	0.09	0.14
1.37	0.97	1.00	3.20	0.04	0.09	2.35	0.08	0.13
1.44	1.00	1.00				2.48	0.07	0.12
1.50	0.98	1.00				2.61	0.07	0.11
1.57	1.00	1.00				2.74	0.08	0.11
1.63	1.00	1.00				2.87	0.06	0.10
1.70	0.96	1.00				3.00	0.06	0.09
1.76	0.98	1.00				3.13	0.06	0.09
1.83	0.98	1.00				3.26	0.07	0.08
1.89	1.00	0.99						
1.96	0.85	0.84						
2.02	0.51	0.52						
2.09	0.17	0.16						
2.15	0.03	0.03						

Table F3. EXPERIMENT: M-3

Column Data

Flow rate=	2 mL/min	Porosity =	0.38	PV=Pore Volumes
Column ID =	2.5 cm	Sat. Pore Volume =	55.2 g	
Column length =	30 cm	Unsat Pore Volume=	NA g	C/C_o=rel. conc.
Column Volume =	147.19 cm^3	After Exp Pore Volume=	NA g	
Mass of porous media =	252.6 g	Pre-exp θ_g/θ_{aq}=	NA	C/C_o=rel. conc.
Bulk Density =	1.72 g/cm^3	Post exp θ_g/θ_{aq}=	NA	(modeled)

TRITIUM DATA			**KRYPTON DATA**			**SF_6 DATA**		
PV	C/C_o	C/C_o	PV	C/C_o	C/C_o	PV	C/C_o	C/C_o
0.45	0.00	0.00	0.8511	0.00	0.00	No data for SF_6		
0.51	0.00	0.00	0.9645	0.47	0.20			
0.57	0.00	0.00	1.078	0.74	0.87			
0.62	0.00	0.00	1.1915	0.90	0.93			
0.68	0.00	0.00	1.305	0.86	0.93			
0.74	0.00	0.00	1.4184	0.92	0.93			
0.79	0.00	0.00	1.5319	1.00	0.93			
0.85	0.00	0.00	1.6454	0.96	0.93			
0.91	0.04	0.03	1.7589	0.82	0.86			
0.96	0.25	0.21	1.8723	0.24	0.22			
1.02	0.68	0.65						
1.08	0.92	0.93						
1.13	0.95	0.99						
1.19	0.95	1.00						
1.25	0.98	1.00						
1.30	0.96	1.00						
1.36	0.99	1.00						
1.42	0.98	1.00						
1.48	0.98	1.00						
1.53	0.99	1.00						
1.59	0.98	1.00						
1.65	1.00	1.00						
1.70	1.00	1.00						
1.76	0.95	0.92						
1.82	0.57	0.57						
1.87	0.19	0.22						
1.93	0.05	0.03						
1.99	0.00	0.00						
2.04	0.00	0.00						
2.10	0.00	0.00						
2.16	0.00	0.00						
2.21	0.00	0.00						
2.27	0.00	0.00						
2.33	0.00	0.00						
2.38	0.00	0.00						

Table F4. EXPERIMENT: M-5

Column Data

Flow rate=	4 mL/min	Porosity =	0.37	PV=Pore Volumes
Column ID =	2.5 cm	Sat. Pore Volume =	54.08 g	
Column length =	30 cm	Unsat Pore Volume=	51.14 g	C/C_o=rel. conc.
Column Volume =	147.19 cm^3	After Exp Pore Volume=	NA g	
Mass of porous media =	246.73 g	Pre-exp θ_g/θ_{aq}=	0.054	C/C_o=rel. conc.
Bulk Density =	1.68 g/cm^3	Post exp θ_g/θ_{aq}=	NA	(modeled)

TRITIUM DATA			**KRYPTON DATA**			**SF_6 DATA**		
PV	C/C_o	C/C_o	PV	C/C_o	C/C_o	PV	C/C_o	C/C_o
0.61	0.00	0.00	0.55	0.00	0.00	0.45	0.00	0.00
0.67	0.00	0.00	0.67	0.00	0.00	0.57	0.00	0.00
0.73	0.00	0.00	0.79	0.00	0.00	0.68	0.00	0.00
0.79	0.00	0.00	0.91	0.00	0.01	0.79	0.00	0.00
0.85	0.01	0.01	1.03	0.02	0.07	0.91	0.01	0.00
0.91	0.10	0.09	1.15	0.14	0.15	1.02	0.03	0.02
0.97	0.38	0.33	1.27	0.20	0.21	1.13	0.03	0.03
1.03	0.69	0.67	1.40	0.33	0.29	1.25	0.03	0.03
1.09	0.92	0.89	1.52	0.46	0.36	1.36	0.05	0.04
1.15	0.99	0.98	1.64	0.47	0.42	1.47	0.05	0.04
1.21	0.99	1.00	1.76	0.57	0.48	1.59	0.06	0.04
1.27	0.97	1.00	1.88	0.54	0.54	1.70	0.06	0.05
1.33	0.97	1.00	2.00	0.53	0.60	1.81	0.06	0.05
1.40	0.99	1.00	2.12	0.55	0.64	1.93	0.04	0.06
1.46	1.07	1.00	2.25	0.55	0.64	2.04	0.06	0.06
1.52	1.01	1.00	2.37	0.56	0.60	2.15	0.05	0.07
1.58	0.98	1.00	2.49	0.57	0.57	2.27	0.05	0.06
1.64	0.99	1.00	2.61	0.59	0.54	2.38	0.04	0.05
1.70	0.98	1.00	2.73	0.60	0.50	2.49	0.03	0.05
1.76	1.02	1.00	2.85	0.49	0.45	2.61	0.05	0.05
1.82	1.05	1.00	2.97	0.46	0.41	2.72	0.05	0.06
1.88	0.98	1.00	3.09	0.36	0.37	2.83	0.05	0.06
1.94	1.00	1.00	3.22	0.27	0.33	2.94	0.05	0.06
2.00	1.02	1.00	3.34	0.25	0.29	3.06	0.06	0.06
2.06	1.00	0.97	3.46	0.24	0.26	3.17	0.05	0.06
2.12	0.81	0.82	3.58	0.23	0.23	3.28	0.06	0.06
2.18	0.51	0.51	3.70	0.21	0.20	3.40	0.06	0.06
2.25	0.18	0.17	3.82	0.20	0.17	3.51	0.07	0.06
2.31	0.03	0.04	3.94	0.16	0.15	3.62	0.09	0.07
2.37	0.00	0.01	4.07	0.13	0.13	3.74	0.05	0.07
2.43	0.00	0.00	4.19	0.10	0.11	3.85	0.08	0.07
			4.31	0.09	0.09	3.96	0.07	0.07
			4.43	0.07	0.08	4.08	0.08	0.07
			4.55	0.06	0.07	4.19	0.07	0.07
			4.67	0.05	0.06	4.30	0.08	0.07
			4.79	0.04	0.05	4.42	0.08	0.07
			4.92	0.04	0.04	4.53	0.08	0.07
			5.04	0.03	0.03	4.64	0.08	0.07
			5.16	0.03	0.03	4.76	0.07	0.07
			5.28	0.00	0.02	4.87	0.08	0.07
			5.40	0.00	0.02	4.98	0.05	0.07
						5.10	0.08	0.08

Table F5. EXPERIMENT: M-6

Column Data

Flow rate=	4 mL/min	Porosity =	0.38	PV=Pore Volumes
Column ID =	2.5 cm	Sat. Pore Volume =	56.14 g	
Column length =	30 cm	Unsat Pore Volume=	NA g	C/C_o=rel. conc.
Column Volume =	147.19 cm^3	After Exp Pore Volume=	NA g	
Mass of porous media =	241.28 g	Pre-exp θ_g/θ_{aq}=	~0	C/C_o=rel. conc.
Bulk Density =	1.64 g/cm^3	Post exp θ_g/θ_{aq}=	NA	(modeled)

TRITIUM DATA			**KRYPTON DATA**			**SF_6 DATA**		
PV	C/C_o	C/C_o	PV	C/C_o	C/C_o	PV	C/C_o	C/C_o
0.45	0.00	0.00	0.54	0.00	0.00	0.45	0.00	0.00
0.51	0.00	0.00	0.67	0.00	0.00	0.56	0.00	0.00
0.56	0.00	0.00	0.79	0.00	0.00	0.68	0.00	0.00
0.62	0.00	0.00	0.91	0.00	0.01	0.79	0.01	0.00
0.68	0.00	0.00	1.03	0.20	0.21	0.90	0.10	0.04
0.73	0.00	0.00	1.15	0.62	0.57	1.02	0.55	0.49
0.79	0.00	0.00	1.27	0.73	0.83	1.13	0.78	0.78
0.85	0.00	0.01	1.39	0.94	0.94	1.24	0.83	0.83
0.90	0.05	0.05	1.51	0.84	0.98	1.35	0.84	0.85
0.96	0.24	0.26	1.63	0.92	1.00	1.47	0.83	0.87
1.02	0.59	0.62	1.75	1.05	0.99	1.58	0.91	0.88
1.07	0.88	0.85	1.88	0.88	0.79	1.69	0.88	0.89
1.13	0.91	0.97	2.00	0.37	0.43	1.81	0.63	0.64
1.19	0.98	1.00	2.12	0.10	0.17	1.92	0.24	0.21
1.24	1.00	1.00	2.24	0.05	0.06	2.03	0.12	0.12
1.30	1.04	1.00	2.36	0.02	0.02	2.15	0.14	0.10
1.35	0.98	1.00	2.48	0.01	0.00	2.26	0.09	0.09
1.41	0.95	1.00				2.37	0.06	0.08
1.47	1.00	1.00						
1.52	1.00	1.00						
1.58	0.98	1.00						
1.64	1.02	1.00						
1.69	1.02	0.99						
1.75	0.88	0.90						
1.81	0.62	0.62						
1.86	0.32	0.32						
1.92	0.09	0.09						
1.98	0.00	0.02						

Table F6. EXPERIMENT: M-7

Column Data

Flow rate=	4 mL/min	Porosity =	0.38	PV=Pore Volumes
Column ID =	2.5 cm	Sat. Pore Volume =	56.14 g	
Column length =	30 cm	Unsat Pore Volume=	55.04 g	C/C_o=rel. conc.
Column Volume =	147.19 cm^3	After Exp Pore Volume=	NA g	
Mass of porous media =	231.84 g	Pre-exp θ_g/θ_{aq}=	0.107	C/C_o=rel. conc.
Bulk Density =	1.58 g/cm^3	Post exp θ_g/θ_{aq}=	NA	(modeled)

TRITIUM DATA			**KRYPTON DATA**			**SF_6 DATA**		
PV	C/C_o	C/C_o	PV	C/C_o	C/C_o	PV	C/C_o	C/C_o
0.73	0.00	0.00	0.77	0.01	0.00	0.83	0.01	NA
0.79	0.00	0.00	0.89	0.00	0.02	0.94	0.18	
0.85	0.00	0.01	1.00	0.06	0.24	1.06	0.87	
0.91	0.02	0.07	1.12	0.64	0.52	1.18	0.53	
0.97	0.16	0.32	1.24	0.70	0.63	1.30	0.70	
1.03	0.52	0.68	1.36	0.68	0.71	1.42	0.70	
1.09	0.84	0.91	1.48	0.78	0.77	1.54	0.77	
1.15	0.95	0.99	1.59	0.99	0.82	1.65	0.75	
1.21	1.01	1.00	1.71	0.80	0.86	1.77	0.75	
1.27	1.04	1.00	1.83	0.67	0.84	1.89	0.43	
1.33	1.02	1.00	1.95	0.63	0.55	2.01	0.17	
1.40	0.99	1.00	2.07	0.30	0.37	2.13	0.15	
1.46	0.99	1.00	2.19	0.35	0.29	2.24	0.13	
1.52	0.98	1.00	2.30	0.26	0.23	2.36	0.12	
1.58	1.01	1.00	2.42	0.25	0.18	2.48	0.16	
1.64	1.01	1.00	2.54	0.16	0.14	2.60	0.15	
1.70	0.99	1.00	2.66	0.11	0.11	2.72	0.16	
1.76	0.99	1.00	2.78	0.09	0.09	2.83	0.15	
1.82	0.98	0.97	2.89	0.06	0.07	2.95	0.04	
1.88	0.82	0.82	3.01	0.06	0.05	3.07	0.14	
1.94	0.48	0.47	3.13	0.04	0.04	3.19	0.13	
2.00	0.15	0.16	3.25	0.04	0.03	3.31	0.11	
2.06	0.00	0.03	3.37	0.03	0.02	3.43	0.13	
2.12	0.00	0.00	3.48	0.01	0.02	3.54	0.13	
			3.60	0.01	0.01	3.66	0.13	
						3.78	0.12	
						3.90	0.11	
						4.02	0.10	
						4.13	0.10	
						4.25	0.09	
						4.37	0.09	
						4.49	0.08	
						4.61	0.08	
						4.72	0.12	
						4.84	0.12	
						4.96	0.12	
						5.08	0.12	
						5.20	0.10	
						5.31	0.11	

Table F7. EXPERIMENT:SI-3

Column Data

Flow rate=	4 mL/min	Porosity =	0.36	PV=Pore Volumes
Column ID =	2.5 cm	Sat. Pore Volume =	53.55 g	
Column length =	30 cm	Unsat Pore Volume=	52.59 g	C/C_o=rel. conc.
Column Volume =	147.19 cm^3	After Exp Pore Volume=	51.38 g	
Mass of porous media =	262.31 g	Pre-exp θ_g/θ_{aq}=	0.018	C/C_o=rel. conc.
Bulk Density =	1.78 g/cm^3	Post exp θ_g/θ_{aq}=	0.041	(modeled)

TRITIUM DATA			**KRYPTON DATA**			**SF_6 DATA**		
PV	C/C_o	C/C_o	PV	C/C_o	C/C_o	PV	C/C_o	C/C_o
0.82	0.00	0.00	0.89	0.00	0.03	0.89	0.00	0.03
0.89	0.00	0.05	1.12	0.51	0.59	1.12	0.36	0.50
0.97	0.10	0.34	1.34	0.59	0.66	1.34	0.47	0.55
1.04	0.47	0.71	1.56	0.70	0.70	1.56	0.53	0.57
1.12	0.85	0.94	1.79	0.70	0.73	1.79	0.54	0.59
1.19	0.98	0.99	2.01	0.63	0.76	2.01	0.59	0.61
1.27	1.00	1.00	2.23	0.67	0.79	2.23	0.74	0.63
1.34	0.99	1.00	2.46	0.71	0.81	2.46	0.65	0.65
1.41	1.00	1.00	2.68	0.65	0.83	2.68	0.59	0.66
1.49	1.00	1.00	2.90	0.76	0.85	2.90	0.64	0.68
1.56	1.01	1.00	3.13	0.81	0.87	3.13	0.64	0.70
1.64	1.01	1.00	3.35	0.81	0.88	3.35	0.71	0.71
1.71	1.01	1.00	3.57	0.81	0.90	3.57	0.71	0.72
1.79	1.00	1.00	3.80	0.86	0.91	3.80	0.68	0.74
1.86	1.01	1.00	4.02	0.91	0.92	4.02	0.75	0.75
1.93	1.01	1.00	4.24	0.85	0.93	4.24	0.68	0.76
2.01	0.99	0.98	4.47	0.87	0.94	4.47	0.81	0.78
2.08	0.85	0.83	4.69	0.85	0.94	4.69	0.94	0.79
2.16	0.43	0.42	4.91	0.87	0.95	4.91	0.74	0.80
2.23	0.09	0.13	5.13	0.89	0.96	5.13	0.62	0.81
2.31	0.01	0.02	5.36	0.94	0.96	5.36	0.89	0.82
			5.58	0.94	0.97	5.58	0.87	0.83
			5.80	0.93	0.97	5.80	0.91	0.83
			6.03	0.92	0.97	6.03	0.73	0.84
			6.25	0.89	0.88	6.25	0.79	0.72
			6.47	0.54	0.37	6.47	0.47	0.34
			6.70	0.24	0.31	6.70	0.31	0.31
			6.92	0.14	0.28	6.92	0.28	0.30
			7.14	0.08	0.25	7.14	0.27	0.29
			7.37	0.05	0.22	7.37	0.25	0.27
			7.59	0.03	0.20	7.59	0.21	0.26
			7.81	0.03	0.17	7.81	0.18	0.25
			8.04	0.02	0.15	8.04	0.18	0.23
			8.26	0.01	0.14	8.26	0.09	0.22
			8.48	0.01	0.12	8.48	0.15	0.21
			8.71	0.01	0.11	8.71	0.13	0.20
			8.93	0.00	0.10	8.93	0.13	0.19
			9.15	0.00	0.09	9.15	0.12	0.18
			9.38	0.00	0.08	9.38	0.10	0.17
			9.60	0.00	0.07	9.60	0.10	0.17
			9.82	0.00	0.06	9.82	0.10	0.16
			10.05	0.00	0.05	10.05	0.10	0.15
			10.49	0.00	0.04	10.49	0.08	0.14
			10.72	0.00	0.04	10.72	0.09	0.13
			11.16	0.00	0.03	11.16	0.07	0.12

Table F8. EXPERIMENT:SI-4

Column Data

Flow rate=	4 mL/min	Porosity =	0.36	PV=Pore Volumes
Column ID =	2.5 cm	Sat. Pore Volume =	53.11 g	
Column length =	30 cm	Unsat Pore Volume=	51.05 g	C/C_o=rel. conc.
Column Volume =	147.19 cm^3	After Exp Pore Volume=	49.76 g	
Mass of porous media =	262.72 g	Pre-exp θ_g/θ_{aq}=	0.039	C/C_o=rel. conc.
Bulk Density =	1.78 g/cm^3	Post exp θ_g/θ_{aq}=	0.063	(modeled)

TRITIUM DATA			**KRYPTON DATA**			**SF_6 DATA**		
PV	C/C_o	C/C_o	PV	C/C_o	C/C_o	PV	C/C_o	C/C_o
0.65	0.00	0.00	0.87	0.00	0.00	0.65	0.00	0.00
0.73	0.00	0.00	1.09	0.11	0.10	1.09	0.12	0.05
0.80	0.00	0.00	1.31	0.21	0.19	1.53	0.08	0.07
0.87	0.00	0.01	1.53	0.35	0.27	1.96	0.09	0.09
0.95	0.00	0.17	1.75	0.42	0.36	2.40	0.11	0.11
1.02	0.61	0.64	1.96	0.45	0.44	2.84	0.11	0.13
1.09	0.90	0.95	2.18	0.55	0.52	3.27	0.12	0.16
1.16	0.98	1.00	2.40	0.61	0.59	3.71	0.14	0.18
1.24	0.98	1.00	2.62	0.64	0.66	4.15	0.14	0.20
1.31	1.00	1.00	2.84	0.70	0.71	4.58	0.18	0.22
1.38	1.01	1.00	3.05	0.76	0.76	5.02	0.19	0.24
1.45	1.00	1.00	3.27	0.73	0.80	5.45	0.34	0.27
1.53	1.00	1.00	3.49	0.76	0.84	5.89	0.34	0.29
1.60	1.01	1.00	3.71	0.85	0.87	6.33	0.34	0.25
1.67	1.00	1.00	3.93	0.94	0.89	6.76	0.29	0.25
1.75	1.01	1.00	4.15	0.76	0.92	7.20	0.27	0.26
1.82	1.01	1.00	4.36	0.83	0.93	7.64	0.25	0.26
1.89	1.00	1.00	4.58	0.91	0.95	8.07	0.27	0.26
1.96	0.99	1.00	4.80	0.91	0.96	8.51	0.26	0.26
2.04	0.81	0.87	5.02	0.99	0.97	8.95	0.25	0.26
2.11	0.43	0.42	5.24	0.87	0.97	9.38	0.25	0.26
2.18	0.13	0.07	5.45	0.97	0.98	9.82	0.25	0.25
2.25	0.02	0.00	5.67	1.05	0.98	10.25	0.21	0.25
			5.89	1.01	0.99	10.69	0.16	0.25
			6.11	0.83	0.91			
			6.33	0.94	0.82			
			6.55	0.81	0.74			
			6.76	0.74	0.65			
			6.98	0.56	0.57			
			7.20	0.49	0.49			
			7.42	0.43	0.42			
			7.64	0.33	0.35			
			7.85	0.26	0.30			
			8.07	0.22	0.25			
			8.29	0.18	0.20			
			8.51	0.12	0.17			
			8.73	0.09	0.14			
			8.95	0.06	0.11			
			9.16	0.05	0.09			
			9.38	0.03	0.07			
			9.60	0.03	0.06			
			9.82	0.02	0.05			
			10.04	0.02	0.04			
			10.25	0.01	0.03			
			10.91	0.00	0.01			

Table F9. EXPERIMENT:SI-5

Column Data

Flow rate=	4 mL/min	Porosity =	0.37	PV=Pore Volumes
Column ID =	2.5 cm	Sat. Pore Volume =	54.93 g	
Column length =	30 cm	Unsat Pore Volume=	50.47 g	C/C_o=rel. conc.
Column Volume =	147.19 cm^3	After Exp Pore Volume=	50.08 g	
Mass of porous media =	244.48 g	Pre-exp θ_g/θ_{aq}=	0.081	C/C_o=rel. conc.
Bulk Density =	1.66 g/cm^3	Post exp θ_g/θ_{aq}=	0.088	(modeled)

TRITIUM DATA			**KRYPTON DATA**			**SF_6 DATA**		
PV	C/C_o	C/C_o	PV	C/C_o	C/C_o	PV	C/C_o	C/C_o
0.77	0.00	0.00	0.69	0.00	0.00	0.69	0.00	0.00
0.85	0.01	0.01	0.92	0.00	0.00	1.15	0.00	0.00
0.92	0.09	0.12	1.15	0.01	0.01	1.62	0.01	0.01
1.00	0.49	0.50	1.38	0.04	0.03	2.08	0.01	0.01
1.08	0.82	0.86	1.62	0.07	0.06	2.54	0.02	0.02
1.15	0.99	0.98	1.85	0.11	0.11	3.00	0.03	0.02
1.23	1.04	1.00	2.08	0.17	0.17	3.46	0.01	0.03
1.31	0.99	1.00	2.31	0.25	0.23	3.92	0.06	0.05
1.38	1.02	1.00	2.54	0.33	0.30	4.38	0.03	0.06
1.46	1.02	1.00	2.77	0.41	0.38	4.85	0.09	0.07
1.54	1.02	1.00	3.00	0.46	0.45	6.08	0.12	0.12
1.62	1.04	1.00	3.23	0.56	0.53	6.54	0.14	0.14
1.69	0.95	1.00	3.46	0.56	0.59	7.00	0.16	0.16
1.77	1.03	1.00	3.69	0.66	0.66	7.46	0.18	0.18
1.85	1.00	1.00	3.92	0.69	0.71	7.92	0.19	0.20
1.92	0.97	1.00	4.15	0.76	0.76	8.38	0.23	0.22
2.00	1.03	1.00	4.38	0.84	0.81	8.85	0.28	0.24
2.08	1.02	0.99	4.85	0.80	0.88	9.31	0.26	0.26
2.15	0.87	0.89	5.08	0.83	0.90	9.77	0.30	0.28
2.23	0.54	0.52	6.08	0.81	0.97	10.23	0.29	0.29
2.31	0.14	0.15	6.31	0.86	0.97	10.69	0.30	0.30
2.38	0.02	0.03	6.54	0.93	0.98	11.15	0.21	0.32
2.46	0.00	0.00	6.77	0.81	0.99	11.62	0.35	0.33
2.54	0.00	0.00	7.00	0.96	0.98	12.08	0.36	0.33
			7.23	0.91	0.97	12.54	0.35	0.34
			7.46	1.00	0.94			
			7.69	0.83	0.90			
			7.92	0.88	0.84			
			8.15	0.74	0.78			
			8.38	0.84	0.71			
			8.62	0.68	0.63			
			8.85	0.60	0.55			
			9.08	0.44	0.48			
			9.31	0.42	0.41			
			9.54	0.34	0.35			
			9.77	0.29	0.29			
			10.00	0.18	0.24			
			10.23	0.14	0.20			
			10.46	0.13	0.16			
			10.69	0.08	0.13			
			10.92	0.06	0.10			
			11.15	0.03	0.08			
			11.38	0.04	0.06			
			11.62	0.03	0.05			
			11.85	0.02	0.04			

Table F10. EXPERIMENT:20 PV Column

Column Data

Flow rate=	8 mL/min	Porosity =	0.36	PV=Pore Volumes	
Column ID =	2.5 cm	Sat. Pore Volume =	52.55 g		
Column length =	30 cm	Unsat Pore Volume=	51.17 g	C/C_o=rel. conc.	
Column Volume =	147.19 cm^3	After Exp Pore Volume=	49.98 g		
Mass of porous media =	250.79 g	Pre-exp θ_g/θ_{aq}=	0.026	*C/Co*=rel. conc.	
Bulk Density =	1.70 g/cm^3	Post exp θ_g/θ_{aq}=	0.049	(modeled)	

TRITIUM DATA			**KRYPTON DATA**			**SF_6 DATA**		
PV	C/C_o	*C/Co*	PV	C/C_o	*C/Co*	PV	C/C_o	*C/Co*
0.23	0.00	0.00	0.78	0.00	0.00	0.86	0.00	0.00
0.94	0.02	0.02	1.56	0.57	0.54	1.64	0.33	0.36
1.72	1.02	1.00	2.35	0.75	0.79	2.42	0.46	0.40
4.85	1.02	1.00	3.13	0.88	0.91	3.21	0.51	0.45
7.82	1.00	1.00	3.91	1.00	0.96	3.99	0.49	0.49
11.02	1.01	1.00	4.69	1.05	0.98	4.77	0.58	0.53
14.15	0.98	1.00	5.47	1.20	0.99	5.55	0.59	0.56
15.71	0.99	1.00	6.25	1.06	1.00	6.33	0.63	0.60
18.84	1.00	1.00	7.04	1.19	1.00	7.11	0.61	0.63
20.40	0.98	1.00	7.82	1.07	1.00	7.90	0.61	0.66
21.18	0.00	0.00	8.60	1.08	1.00	8.68	0.59	0.69
21.97	0.00	0.00	9.38	1.10	1.00	9.46	0.68	0.71
22.75	0.00	0.00	10.16	1.13	1.00	10.24	0.71	0.74
23.53	0.00	0.00	10.94	1.15	1.00	11.02	0.71	0.76
			11.73	1.15	1.00	11.80	0.72	0.78
			12.51	1.19	1.00	12.59	0.82	0.80
			13.29	1.09	1.00	13.37	0.82	0.81
			14.07	0.98	1.00	14.15	0.88	0.83
			14.85	0.98	1.00	14.93	0.85	0.84
			15.63	0.86	1.00	15.71	0.85	0.86
			16.42	1.00	1.00	16.49	0.90	0.87
			17.20	0.95	1.00	17.28	0.87	0.88
			17.98	0.87	1.00	18.06	0.85	0.89
			18.76	1.03	1.00	18.84	0.87	0.90
			19.54	1.08	1.00	19.62	0.87	0.91
			20.32	1.14	1.00	20.40	0.95	0.92
			21.11	0.71	0.73	21.18	0.57	0.60
			21.89	0.41	0.36	21.97	0.61	0.56
			22.67	0.16	0.16	22.75	0.62	0.52
			23.45	0.06	0.07	23.53	0.48	0.48
			24.23	0.03	0.03	24.31	0.48	0.45
			25.01	0.01	0.01	25.09	0.46	0.41
						25.87	0.32	0.38
						26.66	0.37	0.35
						27.44	0.34	0.32
						28.22	0.26	0.30
						29.00	0.19	0.28
						29.78	0.14	0.25

Table F11. EXPERIMENT:High V_x column

Column Data

Flow rate=	8 mL/min	Porosity =	0.36	PV=Pore Volumes	
Column ID =	2.5 cm	Sat. Pore Volume =	52.55 g		
Column length =	30 cm	Unsat Pore Volume=	51.17 g	C/C_o=rel. conc.	
Column Volume =	147.19 cm^3	After Exp Pore Volume=	49.98 g		
Mass of porous media =	250.79 g	Pre-exp θ_g/θ_{aq}=	0.026	C/C_o=rel. conc.	
Bulk Density =	1.70 g/cm^3	Post exp θ_g/θ_{aq}=	0.049	(modeled)	

TRITIUM DATA			**KRYPTON DATA**			**SF_6 DATA**		
PV	C/C_o	C/C_o	PV	C/C_o	C/C_o	PV	C/C_o	C/C_o
0.53	0.00	0.00	0.53	0.00	0.00	0.53	0.03	0.00
1.05	0.69	0.69	1.05	0.33	0.34	1.05	0.32	0.35
1.58	1.00	1.00	1.58	0.66	0.66	1.58	0.49	0.51
2.11	1.00	1.00	2.11	0.80	0.79	2.11	0.54	0.54
6.32	1.01	1.00	2.63	0.86	0.87	2.63	0.57	0.56
10.00	1.01	1.00	3.16	0.92	0.92	3.16	0.60	0.58
14.21	1.01	1.00	3.68	0.97	0.95	3.68	0.64	0.60
17.89	1.01	1.00	4.21	0.97	0.97	4.21	0.60	0.63
19.47	0.99	1.00	4.74	0.99	0.98	4.74	0.67	0.64
20.00	0.06	0.08	5.26	0.89	0.99	5.26	0.70	0.66
20.53	0.00	0.00	5.79	1.01	1.00	6.32	0.74	0.70
21.05	0.00	0.00	6.32	1.03	1.00	7.37	0.78	0.73
24.21	0.00	0.00	6.84	1.01	1.00	8.42	0.69	0.76
28.42	0.00	0.00	7.37	1.02	1.00	9.47	0.81	0.78
			7.89	1.04	1.00	10.53	0.75	0.80
			8.42	0.98	1.00	11.58	0.83	0.82
			8.95	0.95	1.00	12.63	0.85	0.84
			10.53	0.99	1.00	13.68	0.86	0.86
			12.11	0.92	1.00	14.74	0.89	0.87
			13.68	0.96	1.00	15.79	0.90	0.89
			15.26	0.94	1.00	16.84	0.89	0.90
			16.84	0.94	1.00	17.89	0.88	0.91
			18.42	1.03	1.00	18.95	0.80	0.92
			20.00	0.43	0.42	20.00	0.47	0.47
			20.53	0.24	0.26	20.53	0.42	0.41
			21.05	0.16	0.16	21.05	0.42	0.39
			21.58	0.10	0.10	21.58	0.39	0.37
			22.11	0.06	0.06	22.11	0.38	0.36
			22.63	0.05	0.03	23.16	0.31	0.32
			23.16	0.02	0.02	24.21	0.28	0.29
			24.74	0.01	0.00	25.26	0.25	0.26
			26.32	0.01	0.00	26.32	0.23	0.23
						27.37	0.21	0.21
						28.42	0.19	0.19

Table F12. EXPERIMENT: LT1

Column Data

Flow rate=	1 mL/min	Porosity =	0.36	PV=Pore Volumes
Column ID =	2.5 cm	Sat. Pore Volume =	53.20 g	
Column length =	30 cm	Unsat Pore Volume=	52.68 g	C/C_o=rel. conc.
Column Volume =	147.19 cm^3	After Exp Pore Volume=	51.54 g	
Mass of porous media =	262.93 g	Pre-exp θ_g/θ_{aq}=	0.010	C/C_o=rel. conc.
Bulk Density =	1.79 g/cm^3	Post exp θ_g/θ_{aq}=	0.031	(modeled)

TRITIUM DATA			**KRYPTON DATA**			**SF_6 DATA**		
PV	C/C_o	C/C_o	PV	C/C_o	C/C_o	PV	C/C_o	C/C_o
0.86	0.00	0.04	0.86	0.01	0.01	1.15	0.09	0.22
1.15	0.92	0.95	1.15	0.28	0.36	1.99	0.30	0.29
1.43	1.00	1.00	1.43	0.63	0.65	2.84	0.37	0.36
1.71	0.95	1.00	1.71	0.90	0.82	3.68	0.45	0.41
1.99	0.96	1.00	1.99	1.06	0.91	4.53	0.48	0.47
4.53	0.99	1.00	2.27	1.04	0.96	5.38	0.62	0.52
7.35	1.00	1.00	2.56	1.06	0.98	6.22	0.68	0.56
12.42	0.98	1.00	2.84	1.05	0.99	7.35	0.73	0.62
18.06	0.97	1.00	3.12	1.01	1.00	9.04	0.78	0.69
24.83	0.99	1.00	3.40	1.00	1.00	11.30	0.79	0.77
25.68	1.01	1.00	4.25	1.05	1.00	12.99	0.85	0.82
25.96	0.18	0.18	5.66	1.13	1.00	14.68	0.81	0.86
26.24	0.00	0.00	7.35	1.12	1.00	16.37	0.85	0.89
26.52	0.00	0.00	10.17	0.89	1.00	18.06	0.80	0.91
26.80	0.00	0.00	12.42	0.92	1.00	19.76	0.85	0.93
27.09	0.00	0.00	15.81	0.88	1.00	21.45	0.90	0.95
27.37	0.00	0.00	18.63	0.91	1.00	23.14	0.88	0.96
27.65	0.00	0.00	21.45	0.94	1.00	24.83	0.81	0.97
			24.27	0.94	1.00	25.96	0.79	0.97
			25.96	0.80	1.00	26.80	0.79	0.81
			26.24	0.64	0.75	27.65	0.74	0.69
			26.52	0.43	0.42	28.50	0.69	0.63
			26.80	0.30	0.22	29.91	0.62	0.54
			27.09	0.21	0.10	31.60	0.49	0.45
			27.37	0.11	0.05			
			27.65	0.07	0.02			
			27.93	0.05	0.01			
			28.21	0.03	0.00			

Table F13. EXPERIMENT: LT2

Column Data

Flow rate=	2 mL/min	Porosity =	0.36	PV=Pore Volumes
Column ID =	2.5 cm	Sat. Pore Volume =	52.90 g	
Column length =	30 cm	Unsat Pore Volume=	51.74 g	C/C_o=rel. conc.
Column Volume =	147.19 cm^3	After Exp Pore Volume=	51.07 g	
Mass of porous media =	263.69 g	Pre-exp θ_g/θ_{aq}=	0.022	C/C_o=rel. conc.
Bulk Density =	1.79 g/cm^3	Post exp θ_g/θ_{aq}=	0.035	(modeled)

TRITIUM DATA			**KRYPTON DATA**			**SF_6 DATA**		
PV	C/C_o	C/C_o	PV	C/C_o	C/C_o	PV	C/C_o	C/C_o
0.58	0.00	0.00	0.87	0.01	0.01	0.87	0.01	0.01
0.87	0.00	0.03	1.16	0.56	0.58	1.16	0.19	0.48
1.16	0.95	0.98	1.45	0.81	0.78	1.45	0.26	0.50
1.45	0.98	1.00	1.74	0.98	0.89	1.74	0.40	0.51
1.74	0.98	1.00	2.03	1.01	0.94	2.03	0.51	0.53
3.19	1.00	1.00	2.32	0.97	0.97	2.32	0.59	0.54
5.22	0.99	1.00	2.61	1.00	0.99	2.61	0.63	0.55
8.12	1.01	1.00	2.90	1.07	0.99	2.90	0.75	0.56
11.02	1.00	1.00	3.19	1.02	1.00	3.19	0.75	0.57
13.92	0.98	1.00	3.77	1.08	1.00	3.48	0.66	0.58
16.81	0.99	1.00	4.06	0.95	1.00	4.64	0.94	0.63
19.71	1.00	1.00	4.64	0.97	1.00	6.38	0.90	0.68
19.83	0.99	1.00	5.22	1.02	1.00	8.12	0.89	0.73
19.95	0.99	1.00	7.54	0.95	1.00	9.86	0.92	0.77
20.06	0.98	1.00	9.86	1.01	1.00	11.60	0.89	0.81
20.18	0.98	1.00	12.18	0.85	1.00	13.34	0.92	0.84
20.29	0.98	1.00	14.50	0.91	1.00	15.08	0.81	0.86
20.41	0.98	0.98	16.81	1.01	1.00	16.24	0.80	0.88
			19.13	0.95	1.00	18.55	0.71	0.90
			19.95	1.04	1.00	19.71	0.77	0.91
			20.18	1.07	1.00	19.83	0.78	0.91
			20.41	1.10	1.00	20.06	0.72	0.91
			20.64	1.07	1.00	20.29	0.74	0.92
			20.87	1.08	1.00	20.53	0.78	0.92
			21.11	0.87	1.00	20.64	0.73	0.92
			21.34	0.66	0.74	20.99	0.77	0.92
			21.57	0.40	0.36	21.22	0.87	0.92
			21.80	0.27	0.21	21.45	0.95	0.93
			22.03	0.16	0.13	21.69	0.97	0.93
			22.50	0.09	0.04	21.92	1.02	0.93
			22.96	0.05	0.01	22.27	1.01	0.93
			23.42	0.03	0.00	22.73	0.93	0.93
			23.89	0.02	0.00	23.19	0.84	0.94
			24.35	0.02	0.00	23.66	0.70	0.71
						24.12	0.55	0.44
						24.93	0.53	0.41
						26.09	0.42	0.37
						27.25	0.34	0.33
						28.41	0.28	0.30

APPENDIX G

FIELD DATA

Table G1. EXPERIMENT: 1/06/00
Well: 274
Experiment type: 5 L push-pull
Injection rate: ~0.65 L/min
Withdrawal rate: ~ 0.57 L/min
Sampling interval (green): 5 min (continuous pumping)
Sampling interval (yellow): 20 min (intermittent pumping)

Time (min)	Cuml. Vol (L)	TRITIUM C/C_0 (green)	TRITIUM C/C_0 (yellow)	BROMIDE C/C_0 (green)	BROMIDE C/C_0 (yellow)	SF_6 C/C_0 (green)	SF_6 C/C_0 (yellow)
0.0	0.00	1.00	-	1.00	-	1.00	-
5.0	2.85	0.58	-	0.65	-	0.65	-
10.0	5.70	0.27	-	0.33	-	0.36	-
15.0	8.55	0.13	-	0.17	-	0.10	-
20.0	11.40	0.07	-	0.08	-	0.02	-
24.0	13.68	-	-	-	0.01	-	-
25.0	14.25	0.05	-	0.04	-	0.01	-
30.0	17.10	0.03	-	0.03	-	0.01	-
35.0	19.95	0.02	-	0.02	-	0.00	-
38.0	21.66	-	0.00	-	0.01	-	0.60
40.0	22.80	0.02	-	0.02	-	0.00	-
45.0	25.65	0.01	-	0.02	-	-	-
50.0	28.50	0.01	-	0.01	-	0.00	-
52.5	29.93	-	0.00	-	0.01	-	0.51
55.0	31.35	0.01	-	0.01	-	-	-
60.0	34.20	0.01	-	0.01	-	-	-
65.0	37.05	0.01	-	0.01	-	-	-
68.0	38.76	-	0.00	-	0.00	-	0.28
70.0	39.90	0.01	-	0.01	-	-	-
75.0	42.75	0.00	-	0.01	-	0.00	-
80.0	45.60	0.00	-	0.00	-	-	-
83.0	47.31	-	0.00	-	0.00	-	-
85.0	48.45	0.00	-	0.00	-	-	-
90.0	51.30	0.00	-	0.00	-	-	-
95.0	54.15	0.00	-	0.00	-	-	-
97.5	55.58	-	0.00	-	0.01	-	0.06
100.0	57.00	0.00	-	0.00	-	0.00	-
110.0	62.70	0.00	-	0.00	-	-	-
112.0	63.84	-	0.00	-	0.00	-	-
120.0	68.40	0.00	-	0.00	-	-	-
125.0	71.25	0.00	-	0.00	-	0.00	-
129.0	73.53	-	0.00	-	0.00	-	0.04
130.0	74.10	0.00	-	0.00	-	-	-
140.0	79.80	0.00	-	0.00	-	-	-
143.0	81.51	-	0.00	-	0.00	-	-
145.0	82.65	0.00	-	0.00	-	-	-
150.0	85.50	0.00	-	0.00	-	0.00	-

Table G1. EXPERIMENT 01/06/00 (cont'd)

Time (min)	Cuml. Vol (L)	C/C_0 (green)	C/C_0 (yellow)	C/C_0 (green)	C/C_0 (yellow)	C/C_0 (green)	C/C_0 (yellow)
156.5	89.21	-	0.00	-	0.00	-	0.03
160.0	91.20	0.00	-	0.00	-	-	-
170.0	96.90	0.00	-	0.00	-	-	-
171.0	97.47	-	0.00	-	0.00	-	-
175.0	99.75	0.00	-	0.00	-	0.00	-
180.0	102.60	0.00	-	0.00	-	-	-
186.0	106.02	-	0.00	-	0.00	-	0.02
190.0	108.30	-	-	0.00	-	-	-

Table G2. EXPERIMENT: 2/16/00
Well: 274
Experiment type: 5 L push-pull
Injection rate: ~0.80 L/min
Withdrawal rate (green): ~ 0.89 L/min
Withdrawal rate (yellow): ~ 0.085 L/min
Sampling interval (green): 5 min
Sampling interval (yellow): variable

	TRITIUM	TRITIUM	BROMIDE	BROMIDE	Kr	Kr
Time (min)	C/C_0 (green)	C/C_0 (yellow)	C/C_0 (green)	C/C_0 (yellow)	C/C_0 (green)	C/C_0 (yellow)
0.5	1.00	-	1.00	-	1.00	-
5.0	0.39	0.00	0.40	-	0.25	0.53
10.0	0.12	0.03	0.12	0.01	0.07	0.12
15.0	0.05	0.03	0.04	0.02	0.03	0.08
20.0	0.03	-	0.03	0.02	0.01	-
25.0	0.02	-	0.02	-	-	-
30.0	0.01	-	0.01	-	-	-
35.0	0.01	0.01	0.01	-	-	-
40.0	0.01	-	0.01	0.01	-	-
45.0	0.01	-	0.01	-	-	-
50.0	0.00	-	0.00	-	-	-
55.0	0.00	0.00	0.00	-	-	-
60.0	0.00	-	0.00	0.00	-	-
65.0	0.00	-	0.00	-	-	-
70.0	0.00	-	0.00	-	-	-
75.0	0.00	0.00	0.00	-	-	-
80.0	0.00	-	0.00	0.00	-	-
85.0	0.00	-	0.00	-	-	-
90.0	0.00	-	0.00	-	-	-
95.0	0.00	0.01	0.00	-	-	-
100.0	0.00	-	0.00	0.00	-	-
105.0	0.00	-	0.00	-	-	-
110.0	0.00	-	0.00	-	-	-
115.0	0.00	0.00	0.00	-	-	-
120.0	0.00	-	0.00	0.00	-	-
125.0	0.00	-	0.00	-	-	-

Table G3. EXPERIMENT: 2/26/00
Well: 274
Experiment type: 5 L push-pull
Injection rate: ~0.93 L/min
Withdrawal rate (green): ~ 0.91 L/min
Withdrawal rate (yellow): ~ 0.094 L/min
Sampling interval (green): variable
Sampling interval (yellow): variable

	TRITIUM	TRITIUM	Kr	Kr	SF_6	SF_6
Time (min)	C/C_0 (green)	C/C_0 (yellow)	C/C_0 (green)	C/C_0 (yellow)	C/C_0 (green)	C/C_0 (yellow)
0.5	1.00	0.00	0.5	1.00	1.00	0.00
5.0	0.34	0.05	5	0.38	0.35	0.09
10.0	0.10	0.04	10	0.10	0.11	0.06
15.0	0.04	0.02	15	0.05	0.07	0.03
20.0	0.02	0.01	20	0.03	0.03	0.01
25.0	0.01	0.01	25	0.02	0.03	0.01
30.0	0.01	0.01	30	0.01	0.02	0.01
40.0	0.01	0.00	-	-	0.01	0.00
50.0	0.00	0.00	-	-	0.01	0.00
60.0	0.00	0.00	-	-	0.01	0.00
70.0	0.00	0.00	-	-	-	-
80.0	0.00	0.00	-	-	-	-
90.0	0.00	0.00	-	-	-	-

Table G4. EXPERIMENT: 3/21/00
Well: 335
Experiment type: 4.55 L push-pull
Injection rate: ~0.91 L/min
Withdrawal rate (red): ~ 0.91 L/min
Sampling interval (red): variable

	TRITIUM	Kr	SF_6
Time (min)	**C/C_0 (green)**	**C/C_0 (green)**	**C/C_0 (green)**
0.25	1.00	1.00	1.00
5.00	0.36	0.36	0.34
10.00	0.08	0.10	0.11
15.00	0.03	0.05	0.07
20.00	0.01	0.03	0.04
25.00	0.01	0.02	0.03
30.00	0.01	0.01	0.03
35.00	0.00	0.01	0.03
40.00	0.00	0.01	0.02
45.00	0.00	0.01	0.02
50.00	0.00	0.01	0.02
55.00	0.00	-	0.02
60.00	0.00	-	0.02

Table G5. EXPERIMENT: 3/21/00
Well: 356
Experiment type: 4.99 L push-pull
Injection rate: ~0.87 L/min
Withdrawal rate (red): ~ 0.92 L/min
Sampling interval (red): variable

	TRITIUM	**Kr**	**SF_6**
Time (min)	**C/C_0 (green)**	**C/C_0 (green)**	**C/C_0 (green)**
0.33	1.00	1.00	1.00
2.50	0.64	0.60	0.49
5.00	0.32	0.32	0.26
7.50	0.16	0.19	0.14
10.00	0.10	0.12	0.11
15.00	0.04	0.06	0.09
20.00	0.02	0.03	0.07
25.00	0.02	0.02	0.04
30.00	0.01	0.02	0.03
35.00	0.01	0.01	0.03
40.00	0.01	0.01	0.02
45.00	0.01	-	0.01
50.00	0.01	-	0.01
55.00	0.00	-	0.01
60.00	0.00	-	0.01

Table G6. EXPERIMENT: 4/03/00
Well: 356
Experiment type: 4.95 L push-pull
Injection rate: ~0.90 L/min
Withdrawal rate (red): ~ 0.85 L/min
Sampling interval (red): variable

	TRITIUM	**Kr**	**SF_6**
Time (min)	**C/C_0 (green)**	**C/C_0 (green)**	**C/C_0 (green)**
0.33	1.00	1.00	1.00
2.5	0.60	0.57	0.62
5	0.32	0.29	0.28
7.5	0.17	0.16	0.15
10	0.12	0.11	0.11
15	0.07	0.07	0.08
20	0.05	0.04	0.05
25	0.02	0.02	0.04

Table G7. EXPERIMENT: 5/05/00
Well: 335
Experiment type: 20 L (dosed) followed by 30 L (unntreated) push-pull
Injection rate: ~0.87 L/min
Withdrawal rate (red): ~ 0.80 L/min
Sampling interval (red): variable

	TRITIUM	Kr	SF_6
Time (min)	**C/C_0 (green)**	**C/C_0 (green)**	**C/C_0 (green)**
0	0.04	0.00	0.01
5	-	0.02	-
10	-	0.02	-
15	0.08	0.02	0.01
30	0.11	0.01	0.01
45	0.12	0.01	0.00
60	0.11	0.00	0.00
75	0.10	0.00	0.00
90	0.10	0.00	0.00
105	0.09	0.00	0.00
120	0.08	0.00	0.00

Table G8. EXPERIMENT: 5/11/00
Well: 274
Experiment type:~17.1 L (dosed) followed by ~25.6 L (unntreated) push-pull
Injection rate: ~0.89 L/min
Withdrawal rate (green): ~ 0.87 L/min
Sampling interval (green): variable

	TRITIUM	Kr	SF_6
Time (min)	**C/C_0 (green)**	**C/C_0 (green)**	**C/C_0 (green)**
0	0.04	0.04	-
5	0.07	0.07	-
10	0.13	0.13	-
15	0.18	0.14	-
20	0.22	0.17	0.22
25	0.25	0.20	0.24
30	0.26	0.20	0.22
35	0.25	0.20	0.19
40	0.24	0.19	0.17
45	0.22	0.18	0.17
50	0.20	0.16	0.14
55	0.18	0.15	0.13
60	0.16	0.13	0.10
65	0.15	0.12	0.09
70	0.13	0.10	0.08
75	0.11	0.10	0.07
80	0.11	0.08	0.07
85	0.10	0.08	0.05
90	0.09	0.07	0.06
95	0.08	0.06	0.05
100	0.07	0.06	0.05
105	0.07	0.05	0.04
110	0.06	0.05	0.04
115	0.06	0.04	0.04
120	0.05	0.04	0.04
125	0.05	0.04	0.03

APPENDIX H

SALT COLUMN DATA

Table H1. 4 mL/min salt column

Column Data

Flow rate=	4	mL/min
Column ID =	2.5	cm
Column length =	30	cm
Column Volume =	147.19	cm^3
Mass of porous media =	262.20	g
Bulk Density =	1.78	g/cm^3

PV=Pore Volumes
C/C_o=rel. conc.

TRITIUM DATA		KRYPTON DATA			SF_6 DATA		
PV	**C/C_o**	**PV**	**no salt C/C_o**	**w.salt C/C_o**	**PV**	**no salt C/C_o**	**w.salt C/C_o**
0.84	0.01	0.53	0.00	0.00	0.53	0.00	0.00
0.94	0.14	0.63	0.00	0.01	0.63	0.00	0.00
1.04	0.67	0.74	0.00	0.01	0.74	0.00	0.00
1.15	0.96	0.84	0.01	0.02	0.84	0.00	0.01
1.25	0.99	0.94	0.12	0.19	0.94	0.13	0.20
1.35	1.00	1.04	0.62	0.89	1.04	0.52	0.80
1.45	1.00	1.15	0.97	0.92	1.15	0.88	0.79
1.56	0.99	1.25	0.95	0.90	1.25	0.87	0.83
1.66	1.01	1.45	0.93	0.83	1.35	0.89	0.93
1.76	0.99	1.66	0.97	0.94	1.45	0.83	0.77
1.86	1.01	1.86	0.93	0.87	1.56	0.84	0.92
1.97	0.88	1.97	0.84	0.88	1.66	0.92	0.91
2.07	0.39	2.07	0.37	0.33	1.76	0.90	1.01
2.17	0.05	2.17	0.11	0.10	1.86	0.89	0.86
					1.97	0.78	0.76
					2.07	0.37	0.36
					2.17	0.12	0.14

Table H2. 8 mL/min salt column

Column Data

Flow rate= 8 mL/min

Column ID = 2.5 cm

Column length = 30 cm

Column Volume = 147.19 cm^3

Mass of porous media = 263.03 g

Bulk Density = 1.79 g/cm^3

PV=Pore Volumes

C/C_o=rel. conc.

TRITIUM DATA		KRYPTON DATA			SF_6 DATA		
PV	**C/C_o**	**PV**	**no salt C/C_o***	**w.salt C/C_o***	**PV**	**no salt C/C_o***	**w.salt C/C_o***
0.75	0.00	0.75	0.01	0.00	0.75	0.00	0.00
0.91	0.09	0.91	0.10	0.17	0.91	0.16	0.16
1.07	0.78	1.07	0.68	0.82	1.07	0.68	0.75
1.23	0.94	1.23	0.96	0.87	1.23	0.81	0.81
1.39	1.02	1.39	0.93	0.99	1.39	0.85	0.86
1.54	1.01	1.54	0.96	0.98	1.54	0.86	0.82
1.70	0.97	1.70	0.95	0.47	1.70	0.87	0.35
1.86	0.37	1.86	0.45	0.17	1.86	0.37	0.08
2.02	0.02	2.02	0.11	0.08	2.02	0.10	0.06
2.18	0.00	2.18	0.03	0.03	2.18	0.08	0.04
2.34	0.00	2.34	0.03	0.02	2.34	0.07	0.04
2.50	0.00	2.50	0.02	0.02	2.50	0.06	0.04

*-Injection volumes are not equal sizes for high ionic strength pulse and low ionic strength pulse.

REFERENCES

Air Products, 1995, Physical Properties of Gases, Air Products catalog.

Barry, D. A. and Li, L., 1994 Physical basis of nonequilibrium solute transport in soil, *Transactions*, 15th World Congress of Soil Science, Acapulco, Mexico, v. 2a: pp. 86-105

Bear, J., 1972, *Dynamics of fluids in porous media,* Dover Publications, New York. 764 pp.

Bench, H. L., Elliot, W. P., Dietz, R. N., Barr, S., Kern, C. D., Turkevich, A.L., 1978, Heavy methane-SF_6 tracer test conducted at the Savannah River Plant, December 10, 1975, DuPont Savannah River Laboratory, Report no. DP-1469.

Butler, J. H., Battle, M., Bender, M. L., Montzka, S. A., Clarke, A. D. Saltzman, E. S., Sucher, C. M., Sevringhaus, J. P., and Elkins, J. W., 1999, A record of atmospheric halocarbons during the twentieth century from polar firn air, *Nature*, v. 399, pp. 749-755.

Carter, R. C., Kaufman, W. F., Orlob, G. T., and Todd, D. K., 1959, Helium as a ground-water tracer, *Journal of Geophysical Research*, v. 64, pp. 2433-2439.

Colt, J., 1984, *Computation of Dissolved Gas Concentrations in Water as Functions of Temperature, Salinity and Pressure*: American Fisheries Society Special Publication, no. 14, pp. 154.

Cook, P. G., Solomon, D. K. , Plummer, L. N., Busenberg, E., Schiff, S. L., 1995, Chlorofluorocarbons as tracers of groundwater transport processes in a shallow, silty sand aquifer, *Water Resources Research*, v. 31, pp. 425-434.

Chemical Rubber Company, 1994/95, *CRC handbook of chemistry and physics*, CRC Press: Cleveland, OH, 75th ed.

Davis, S. N., Campbell, D. J., Bentley, H. W., and Flynn, T. J., 1985, *Ground-water tracers*, National Well Water Association, 200 pp.

Domenico, P. A. and Schwartz, F. W., 1990, *Physical and Chemical Hydrogeology*, John Wiley and Sons, New York, NY. 678 pp.

Donaldson, J. H., Istok, J. D., Humphrey, M. D., O' Reilly, K. T., Hawelka, C. A., and Mohr, D. H., 1996, Development and testing of a kinetic model for oxygen transport in porous media in the presence of trapped gas, *GroundWater*, v. 35, pp. 270-278.

Donaldson, J. H., Istok, J. D., and O' Reilly, 1998, Development and testing of a kinetic model for oxygen transport in porous media in the presence of trapped gas, *GroundWater*, v. 36, pp. 133-142.

Dunkle, S. A., Plummer, L. N., Busenberg, E., Phillips, P. J., Denver, J. M., and Hamilton, P. 1993, Chlorofluorocarbons CCl_3F and CCl_2F_2 as dating tools and hydrologic tracers in shallow groundwater of the Delmarva Peninsula, Atlantic Coastal Plain, United States, *Water Resources Research,* v. 29, pp. 3837-3860.

Dunn, D. L., Dixon, K. L., and Nichols, R. L., 1998, *Using Vibracoring and Multilevel Wells to Examine the Hyporheic Zone within a Riparian Wetland*, Westinghouse Savannah River Corporation, Report no. WSRC-MS-98-00319X.

Dyck, W., and Da Silva, F. G., 1981, The use of ping-pong balls and latex tubing for sampling the helium content of lake sediments, *Journal of Geochemical Exploration*, v. 14, pp. 41-48.

Fetter, C. W., 1994, *Applied hydrogeology*: third edition, Merrill Publishing Co., Columbus, OH. 592 pp.

Fetter, C. W., 1993 *Contaminant Hydrogeology*: first edition Macmillan Publishing Co., New York NY, 458 pp.

Fry, V. A., Istok, J. D., Lewis, S., O'Reilly, K.T., and Buscheck, T. E., 1995, Retardation of dissolved oxygen due to trapped gas phase in porous media, *GroundWater*, v.33, pp. 391-398.

Fry, V. A., Istok, J. D., and O'Reilly, K.T., 1996, Effect of trapped gas on dissolved oxygen transport-implications for *in situ* bioremediation, *GroundWater*, v.34, pp. 200-210.

Gaspar, E., and Oncescu, M., 1972, *Developments in Hydrology I: Radioactive Tracers in Hydrology*.

Gupta, S. K., Lau, L. S., and Moravcik, P. S., 1994, Ground-water tracing with injected helium, *Ground Water*, v. 32, pp. 96-102.

Haggerty, R., Schroth, M. H., and Istok, J. D., 1998, Simplified method of "push-pull" test data analysis for determining *in situ* reaction rate coefficients, *Ground Water*, v. 36, pp. 314-323.

Hibbs, D. E., Parkhill, K. L., and Gulliver, J. S., 1998, Sulfur Hexafluoride gas tracer studies in streams, *Journal of Environmental Engineering*, v. 124, pp. 752-760.

Holbeck-Pelham, S.A., Rasmussen, T.C. and Fowler, L.A., 2000, Regulation of injected ground water tracers, *Ground Water*, v. 38, pp. 541-549.

Jardine, P. M., Sanford, W. E., Gwo, J. P., Reedy, O. C., Hicks, D. S., Riggs, J. S., and Bailey, W. B., 1999, Quantifying diffusive mass transfer in fractured shale bed rock, *Water Resources Research*, v. 35, pp. 2015-2030.

Jones, B., 1996, Dissolved krypton gas as a tracer for groundwater flow: its use in fractured crystalline bedrock and unconfined sands of Georgia; M. S. thesis; The University of Georgia.

Jury, W. A., Gardner, W. R., and Gardner, W. H., 1991, *Soil Physics*: fifth edition, John Wiley and Sons, Inc., New York, NY. 328 pp.

Mazor, E., 1991, *Applied Chemical and Isotopic Groundwater Hydrology*: Halsted Press, New York, NY, 274 pp.

Miller, J. M., 1987, *Chromotography: Concepts and Contrasts*: John Wiley and Sons, Inc., New York, NY. 297 pp.

National Council of the Paper Industry for Air and Stream Improvement, 1991, Development of a gas chromatographic protocol for the measurement of krypton gas in water and demonstration of its use in stream reaeration measurements, Tech. Bull. no. 614.

Pang, L., and Close, M. E., Non-equilibrium transport of Cd in alluvial gravels, 1999, *Journal of Contaminant Hydrology*, v. 36, pp. 185-206.

Petrucci, R. H., 1989, *General Chemistry: Principles and Applications*: fifth edition, Macmillan Publishing Co., New York, NY. 1042 pp.

Pickens J. F., Jackson R. E., Inch K. J., and Merritt W. F., 1981, Measurement of distribution coefficients using a radial injection dual-tracer test, *Water Resources Research*, v. 17, 529-544 pp.

Sander, R., 1996, Compilation of Henry's law constants for inorganic and organic species of potential importance in environmental chemistry, http://www.science.york.ca/cac/people/sander/res/henry.html, version 2.

Sanford, W. E., Shopshire, R. G., and Solomon, D. K., 1996, Dissolved gas tracers in groundwater: simplified injection, sampling, and analysis, *Water Resources Research* v. 32, pp. 1635-1642.

Sanford, W. E., Solomon, D. K., 1998, Site characterization and containment assessment with dissolved gases, *Journal of Environmental Engineering*, v. 124, pp. 572-574.

Schwarzenbach, R. P., Gschwend, P. M., and Imboden, D. M., 1993, *Environmental Organic Chemistry*, John Wiley and Sons, New York, NY.681 pp.

Seaman, J.C., 1998, Retardation of fluorobenzoate tracers in highly weathered soils and sediments, *Journal of the Soil Science Society of America*, v. 62, pp. 354-361.

Syracuse Research Corporation, Physical Properties of chemicals, http://esc.syrres.com/interkow/database.htm.

Solomon, D. K., P. G. Cook, and W. E. Sanford, 1999, *Chapter 10: Dissolved gases in subsurface hydrology: In: Isotope Tracers in Catchment Hydrology*, C. Kendall and J. J. McDonnell, editors, Elsevier Publishing Co., Amsterdam, The Netherlands.

Sugisaki R., Takeda H., Kawabe I., and Miyazaki H. 1982 Simplified gas chromatographic analysis of H_2, He, Ne, Ar, N_2 and CH_4 in subsurface gases for seismo-geochemical studies**.** Chemical Geology, v. 36, pp. 217-226.

Szabo, Z., Rice, D. E., Plummer, L. N., Busenberg, E., Michel, R. L., 1996, Age dating of shallow groundwater with chlorofluorocarbons, tritium/helium 3, and flow path

analysis, southern New Jersey coastal plain, *Water Resources Research*, v. 32, 1023-1038.

Thene, J. R., and Gulliver, J. S., 1990, Gas-transfer measurements using headspace analysis of propane, *Journal of Environmental Engineering,* v. 116, pp. 1107-1124.

Toride, N., Leij, F. J., and van Genuchten, M. T., 1995, The CXTFIT code for estimating transport parameters from laboratory or field tracer experiments, Research Report 137, U. S. Dept. of Agriculture, U. S. Salinity Laboratory.

Triola, M., 1995, *Elementary Statistics*: sixth edition, Addison-Wesley Publishing Co., New York, NY.

Upstill-Goodard, R. C., Wilkins, C. S., 1995, The potential of SF_6 as a geothermal tracer, *Water Resources Research*, v. 29, pp. 1065-1068.

van Genuchten, M. T., 1981, Non-equilibrium transport parameters from miscible displacement experiments, Research Report 119, U. S. Dept. of Agriculture, U. S. Salinity Laboratory.

Wanninkhof, R., Ledwell, J. R., Broecker, W. S., 1985, Gas exchange-wind speed relationship measured with sulfur hexafluoride on a lake, *Science*, v. 227, pp. 1224-1226.

Wanninkhof, R., Mulholland, P. J., and Elwood, J. W., 1990, Gas exchange rates for a first-order stream determined with deliberate and natural tracers, *Water Resources Research*, v. 26 pp. 1621-1630.

Wilson, R. D., and Mackay, D. M., 1993, The use of sulphur hexafluoride as a conservative tracer in saturated sandy media, *Ground Water*, v. 31, pp. 719-724.

Wilson, R. D., and Mackay, D. M., 1996, SF_6 as a conservative tracer in saturated media with high intragranular porosity or high organic carbon content, *Ground Water*, v. 34, pp. 241-249.